THE INTESTINAL MESODERM:

INVESTIGATION OF ITS DEVELOPMENT AND POTENTIAL

By

REBECCA TAYLOR THOMASON

Dissertation

Submitted to the Faculty of the

Graduate School of Vanderbilt University

in partial fulfillment of the requirements

for the degree of

DOCTOR OF PHILOSOPHY

in

Cell and Developmental Biology

December, 2012

Nashville, Tennessee

Approved:

Associate Professor E. Michelle Southard-Smith

Associate Professor Lawrence S. Prince

Assistant Professor Andries Zijlstra

Professor David M. Bader

I dedicate this dissertation to my mother, Nancy F. Thomason

For supporting me through all of my science endeavors and

always reminding me to “keep it simple”

ACKNOWLEDGEMENTS

There are many important people who have been vital to my success in graduate school at Vanderbilt University. First and foremost, I would like to acknowledge my financial support throughout graduate school from the National Institutes of Health, the Vanderbilt Digestive Disease Research Grant, and the Vanderbilt Cell Imaging Shared Resource Core grants. Next, I would like to thank my mentor, Dr. David Bader. I chose David's lab because I wanted to utilize classical developmental biology techniques to answer basic scientific questions, and he allowed me to pursue this goal. Little did I know that I would gain great insight into the scientific process, learn project independence, and become a critically thinking scientist under his tutelage. David is incredibly generous and always available to chat about anything from science to the meaning of life. Another group of scientists that I would like to give a big thanks to is my thesis committee. Thank you Drs.Trish Labosky, Michelle Southard-Smith, Lance Prince, Lila Solnica-Kretzel, and Andries Zijlstra. You all have challenged me in so many ways and provided me with excellent guidance with my project. I would also like to thank Trenis Palmer, my "eggman," Dave Huss, my "quailman," Jennifer and Clark at Ozark Quail Farm, and Sean Scheffer, all who have been integral in providing reagents and support in all of my scientific experiments. Other great support has come from Kim Kane (PDB), Elaine Caine (CDB), Jeff Shenton (Writing Studio), and Christy Carey (PCC). I also want to acknowledge my former mentors Dr. Barbara Lom (Davidson) and Dr. Dave McClay (Duke).

These mentors took me under their wing and encouraged me to work towards this goal. Thank you all for everything.

I am extremely grateful for the encouragement and friendship I have received throughout this experience. I want to thank the (original) Bader Babes, Hillary Hager Carter, Kt Moynihan Gray, Emily Cross Benesh, and Niki Winters. I don't think anyone could have as wonderful friends as these ladies. I will always remember swimming with Hills before lab, fun after-lab activities with Kt, enjoying happy hour with Em, and Burgers & Bones with Niki. I would like to give a huge thanks to the members of the Bader Lab past and present including Elise Pfaltzgraff, Sam Reddy, Cheryl Seneff, Annabelle Williams, Paul Miller, Ryan Roberts, Pierre Hunt, Alexis Schiable, and Michelle Robinson. I would like to thank my other graduate school friends who have been tremendously supportive throughout this academic endeavor, including Lindsay Marjoram, Abby Hardaway, Jess Mazerik, Rachel Skelton, and EA Durham. And thank you to the wonderful staff at G'house and RDE for making me feel like the glass is half full.

I don't think I could have made it through this graduate work without support from my family. Thank you Dad, Bud, and Piper for always being there for me, helping me out when I needed it, and just for being so damn funny. Bud, the Lolcats always put a smile on my face. Mom, I cannot begin to thank you for your encouragement and always being there for me. Man, back when I was doing science fair, I never thought I would actually grow up to be a scientist. Thanks for making me follow through with my commitments and be a good person.

And lastly, I would like to thank my boyfriend, Drew. You have been so understanding and compassionate through this whole process. I also thank you for leaving your kittehs with me, Sam and Leo have kept me sane during the writing process. I don't think I could have asked for a better man in my life. I never thought I would date another scientist, especially someone in the same field, but I am thankful everyday that I do. I am grateful everyday for your friendship, humor, intellect, and love.

TABLE OF CONTENTS

LIST OF TABLES

Table Page

LIST OF FIGURES

LIST OF ABBREVIATIONS

A	Artery
α-SMA	alpha Smooth Muscle Actin
A-P	Anterior-Posterior
AV/IC	Atrioventricular Region/Inner Curvature
β-gal	beta-Galactosidase
BMP	Bone Morphogenic Protein
BSA	Bovine Serum Albumin
BV	Blood Vessels
BW	Body Wall
C	Caeca
CC	Coelomic Cavity
Cfc	Cripto
Cyto	Cytokeratin
DA	Dorsal Aorta
DAPI	4',6-diamidino-2-phenylindole
DM	Dorsal Mesentery
DMEM	Dulbecco's Modified Eagle Medium
DNA	Deoxyribonucleic Acid
E	Embryonic Day
E	Endoderm (Chapter 3)
EC	Endocardium
ECP	Endocardial Progenitors
Ect	Ectoderm
En	Endoderm
ENS	Enteric Nervous System
EGF	Epithelial Growth Factor
EMT	Epithelial-to-Mesenchymal Transition
EP	Endothelial Plexus
EPCD	Epicardial-Derived Cells
Ep/Epi	Epicardium
eYFP	Enhanced Yellow Fluorescent Protein
F	Fibroblast
FBS	Fetal Bovine Serum
FGF	Fibroblast Growth Factor
FL	Forelimb
Foxf1	Forkhead Box Protein 1
G	Graft-derived Gut Tube
γ-SMA	gamma Smooth Muscle Actin
GFP	Green Fluorescent Protein
GIST	Gastrointestinal Stromal Tumors
GM	Gut Mesothelium
GN	Glass Needle
GT	Gut Tube

H	Head
H	Host (Chapter 3)
He	Heart
HFH-8	Hepatocyte nuclear factor-8
HH	Hamburger Hamilton Stage
Hh	Hedgehog
HL	Hindlimb
IC	Inner Circular Muscle Layer
Ihh	Indian Hedgehog
IHC	Immunohistochemistry
IL	Inner Longitudinal Muscle Layer
IM	Intermediate Mesoderm
IntMes	Intestinal Mesothelium
ISH	*In situ* Hybridization
L	Lumen
LC	Lateral Cavity
LP	Lamina Propria
LP	Lateral Plate (Chapter 3)
LPM	Lateral Plate Mesoderm
L-R	Left-Right
L	Lumen
M	Mesenchyme
M	Mesothelium (Chapter 3)
ME	Muscularis Externa
Me	Mesenchyme (Chapter 3)
Mes	Mesothelium
Mes	Mesentery (Chapter 3)
MET	Mesenchymal-to-Epithelial Transition
MF20	Myosin Heavy Chain (Clone MF20)
MI	Myocardial Infarction
Mu	Mucosa
Myo	Myocardium
N	Notochord
Nf1	Neurofibromin
NT	Neural Tube
OC	Outer Circular Muscle Layer
OCT	Optical Cutting Temperature compound
OE	Outer Epithelium
OFT	Outflow Tract
OL	Outer Longitudinal Muscle Layer
PAS	Periodic Schiff Staining
PBS	Phosphate Buffered Saline solution
PCR	Polymerase Chain Reaction
PD	Peritoneal Dialysis
PDGF	Platelet Derived Growth Factor
PE	Proepicardium

PGP9.5	Neuron Cytoplasmic Protein 9.5
QCPN	Quail not-Chicken Perinuclear
QH1	Quail specific endothelial
RA	Retinoic Acid
Raldh2	Retinaldehyde dehydrogenase 2
RT-PCR	Reverse Transcription PCR
S	Somite(s)
Scx	Scleraxis
Se	Serosa
SEM	Scanning Electron Microscopy
Sema3D	Semaphorin 3D
Shh	Sonic Hedgehog
SI	Small Intestine
SM	Submucosa
Sp	Splanchnic Mesoderm (Chapter 3)
SpM	Splanchnic Mesoderm
So	Somatic Mesoderm (Chapter 3)
SoM	Somatic Mesoderm
SuEp	Subepicardium
Tβ4	Thymosin β4
Tbx18	T-box Transcription Factor 18
Tcf21	Transcription Factor 21
TEM	Transmission Election Microscopy
TGFβ	Transforming Growth Factor beta
Tie1	Tyrosine kinase with immunoglobulin-like and EGF-like domains 1
TOPRO-3	Carbocyanine Monomer Nucleic Acid Stain
UR	Urogenital Ridges
V	Villi
VA	Vitelline Artery
VCAM-1	Vascular Cell Adhesion Molecule 1
Ve	Vein
Ven	Ventriculus
viSM	Visceral Smooth Muscle
VV	Vitelline Vein
W	Wing
Wt1	Wilms' tumor protein 1
Xgal	5-bromo-4-chloro-3-indolyl- beta-D-galactopyranoside
8F3	Chicken not-Quail Cytoplasmic Marker

CHAPTER I

INTRODUCTION

The mesoderm is a primary germ layer that gives rise to connective tissue, muscle, bone, blood vessels, and mesothelium in the embryo. Particularly, the development of the intestinal mesoderm, in large part is understudied. Our laboratory is predominantly interested in the development of a mesodermal component, the mesothelium. A mesothelium is a simple squamous epithelial sheet of cells that lines all coelomic cavities and organs, providing a non-adhesive surface for which organs can freely move within the body cavity. Both heart and intestinal mesothelia share conserved characteristics that include: initially both organs lack a mesothelium, then mesothelia cover the organs, and cells from the mesothelium undergo epithelial-to-mesenchymal (EMT) transition, and contribute cells to the vasculature of the organ (Dettman et al., 1998; Gittenberger-de Groot et al., 1998; Männer, 1999; Mikawa and Gourdie, 1996; Wilm et al., 2005). The purpose of this dissertation is to investigate the development of the mesoderm in a spatiotemporal context, and more specifically the origin and plasticity of mesothelial cells in the developing intestine. In this introduction, I will cover what is currently understood pertaining to intestinal mesoderm and mesothelial development.

Development of the Lateral Plate Mesoderm and Coelomic Cavities

Proper specification and differentiation of the lateral plate mesoderm (LPM) is required for the formation of the coelomic organs in the developing vertebrate embryo. During avian gastrulation, epiblast cells converge and ingress (migrating inward and then moving laterally) along the primitive streak to form the mesodermal layer just below the epiblast (future ectoderm) and above the hypoblast (future endoderm). Once gastrulation is complete, the mesodermal layer is specified as the chordamesoderm at the midline, and moving laterally from the midline: the paraxial or somitic mesoderm, the intermediate mesoderm, and the LPM (Figure 1.1 A). Studies have demonstrated that regulation of bone morphogenic protein (BMP) signaling is involved in specification of each region in the mesoderm (Funayama et al., 1999; Tonegawa et al., 1997; Tonegawa and Takahashi, 1998). At this stage, the avian embryo is flat and all three germ layers are extending and developing concurrently.

The LPM will eventually give rise to the body wall, coelomic cavities, and organs within the cavities. The LPM divides into two layers, the somatic mesoderm and the splanchnic mesoderm (Figure 1.1 A). The somatic mesoderm is located dorsally and associates with the ectoderm to form the somatopluere. The splanchnic mesoderm is ventral and unites with the endoderm, now referred to as the splanchnopleure (Figure 1.1 A, B). In the mouse, hepatocyte nuclear factor-2/*forkhead* homologue-8 (*HFH-8*/*Foxf1*) is involved in formation of mesodermally derived tissues, including the lung and intestine

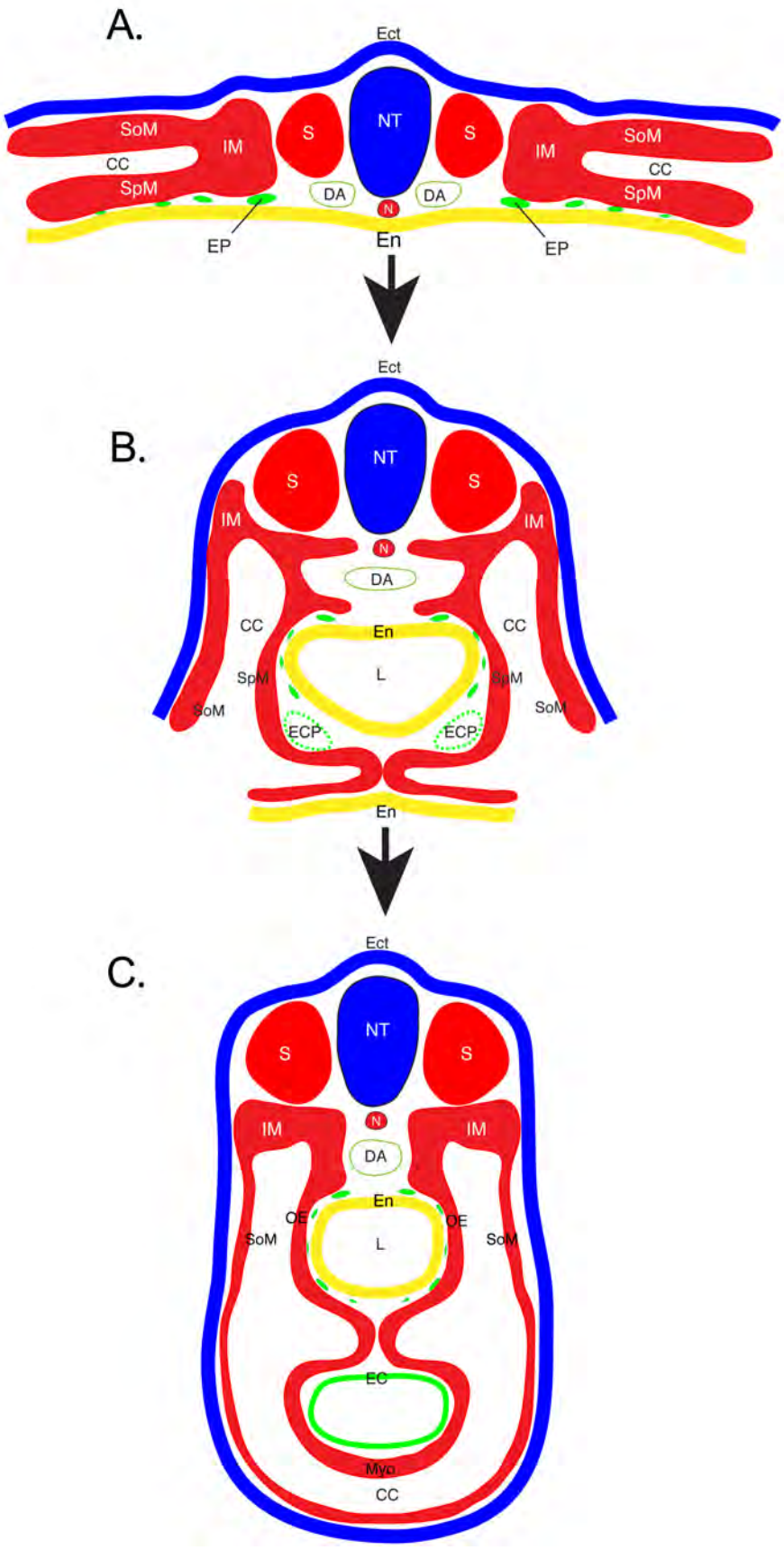
A.
Ect
SoM
IM
S
NT
S
IM
SoM
CC
CC
SpM
SpM
DA
DA
N
EP
En
EP
B.
Ect
NT
S
S
IM
IM
N
DA
CC
En
CC
SpM
L
SpM
SoM
SoM
ECP
ECP
En
C.
Ect
NT
S
S
IM
IM
N
DA
En
OE
OE
SoM
L
SoM
EC
Myo
CC

Figure 1.1 Mesoderm organization leads to tubular organ development and coelom formation. A: Schematic of post-gastrulation events in an avian embryo. The embryo develops flat and all three germ layers are organized. Ectoderm (Ec) in blue, mesoderm in red, and endoderm (En) in yellow. The mesoderm contains four regions: chordamesoderm (nc), paraxial (S), intermediate (IM), and the lateral plate, the somatic and splanchnic mesoderm (SoM and SpM). At this time, the lateral plate mesoderm has split to form a coelomic cavity (CC) between the SoM and SpM. A thin endothelial plexus (EP) is located between the SpM and En. Endothelial cells are green. **B**: The SpM and En together form the splanchnopleure. The splanchnopleure fuses ventrally to form the primitive gut tube. The endocardial primordia (ECP) form ventral to the gut tube. **C**: In the most ventral region of the embryo, the heart tube forms. At this stage, the heart tube is comprised of myocardium (Myo), derived from the SpM, and endocardium (EC) formed via fusion of the ECP. Upon organ tube formation, the left and right coeloms (CC) merge to create one large cavity. Figures are transverse cross-sections and are not drawn to scale. CC, coelomic cavity; DA, dorsal aorta; EC, endocardium; Ect, ectoderm; En, endoderm; EP, endothelial plexus; EPC, endocardial progenitors; IM, intermediate mesoderm; L, lumen; Myo, myocardium; N, notochord; NT, neural tube; OE, outer epithelium; S, somite; SoM, somatic mesoderm; SpM, splanchnic mesoderm.

(Peterson et al., 1997), specifically during vasculogenesis and development of extraembryonic membranes (Mahlapuu et al., 2000). Next, the LPM splits to generate an open cavity, known as a coelom, between the somatopluere and splanchnopleure. The epithelial histology of the mesodermal layers facing the lumen of the coelom reflects one another in an apical-apical manner (personal observations). The split of the LPM and formation of a coelom initiates the process of organogenesis in the embryo (Funayama et al., 1999).

Organogenesis of the viscera begins essentially as the formation of a tube. This process is defined by the embryo folding ventrally toward its midline, which fuses and forms the primitive gut tube in the anterior region of the embryo (Figure 1.1 B). The gut tube is composed of endoderm, splanchnic mesoderm, and a thin space between containing an endothelial plexus (Meier, 1980). Ventral to the gut tube is the forming primitive heart tube (Figure 1.1 C). The heart tube does not contain embryonic endoderm, but instead two endocardial primordia fuse to form the endocardium in the ventral-most region of the embryo. The heart tissue is now comprised of two layers, the endocardium and myocardium, and is attached to both the dorsal and ventral body wall. Eventually, the heart tube detaches from the ventral aspect. After the organ tubes have formed, the left and right somatopleure adhere at the midline, and the left and right coelomic cavities fuse to form the pericardial cavity (the space around the heart), pleural cavity (the space around the lungs), and the peritoneal cavity (the space around the gut) (Figure 1.1 C). The coelom provides a fluid filled cavity for organs, a space in which organs can separate from the body wall to become free-form entities,

which creates space for other organs to expand and develop (Funayama et al., 1999). Coelom formation is intimately involved with LPM specification and separation, all fundamental to organogenesis. The next section will focus on the development of the small intestine.

Intestinal Development

All gastrointestinal organs are important for proper digestion and nutrition in an organism. This section focuses on the vertebrate midgut (small intestine) because it is conserved and similar in organization in most vertebrate species, including humans. Additionally, this section will describe morphogenesis of each intestinal layer, mesodermally- and endodermally-derived, all contributing to the final adult structure.

Embryonic structure and function of the intestinal layers

Upon generation of the gut primordium, the splanchnic mesoderm and endoderm are lined by two basement membranes with a small almost acellular space between. Meier utilized ultrastructural resolution techniques, including transmission electron microscopy (TEM) and scanning electron microscopy (SEM), to describe as an endothelial plexus that exists between the mesoderm and endoderm in the early gut anlage (Meier, 1980). An endothelial plexus is situated within the middle layer known as the mesenchyme. These data demonstrate that the gut primordium consists of three layers. However, the

developmental program and dynamic morphological changes of the three layers are not well characterized at this time.

The outer layer of the intestinal primordium, the splanchnic mesoderm, has not been a prominent focus in the literature. However, some studies have investigated the relationship between the mesoderm and endoderm. Early in development, the splanchnic mesoderm has been referred to as the “signaling center” for establishing left-right (L-R) asymmetry in the vertebrate (Burn and Hill, 2009; Green, 1967; Hecksher-Sørensen et al., 2004; Levin et al., 1995). These studies have shown that the splanchnic mesoderm signals to the endoderm on the left side of the body and is important for asymmetric positioning of the organs.

The most outer component of the intestine is the mesothelium. An important study in the mouse embryo demonstrated that the intestinal mesothelium was initially absent from the gut tube. Antibody labeling for mesothelial markers were observed covering the dorsal mesentery at E10.5 and over the entire intestine at E11.5 (Wilm et al., 2005). These studies also revealed the ability of intestinal mesothelial cells to undergo EMT, migrate into the organ and contribute cells to the vasculature of the organs (Mikawa and Gourdie, 1996; Poelmann et al., 1993; Wilm et al., 2005). While reports regarding intestinal mesothelial development have provided more detail in recent years, gaps in the field remain. Specifically, how does the outer epithelium morphologically change before a mesothelium arises? Does the outer basement membrane play a role in the EMT process? Further information is needed to assess the full developmental program and potential of the splanchnic mesoderm and gut mesothelium.

The mesenchymal layer of the gut tube is comprised of stromal cells (fibroblasts and myofibroblasts), muscle, endothelial, and nerve cells, along with connective tissue. Studies analyzing laminin, a component of basement membranes, investigated the formation of endoderm and mesenchyme through association with endodermal basement membrane dynamics (Lefebvre et al., 1999; Simon-Assmann et al., 1998). These data were supportive in characterizing organization and signaling in the developing intestine relative to endodermal development. However, investigation of the outer basement membrane lining the splanchnic mesoderm is required to fully understand formation of the mesenchyme and mesothelium.

Subjacent to the endoderm is the mesenchymally-derived lamina propria. This structure is well studied in the intestine in the context of the adult gastrointestinal tract. The lamina propria is composed of myofibroblasts and fibroblasts, bone marrow derived stromal stem cells, lymphocytes, smooth muscle, and blood vessels (Powell et al., 2011). Neural crest cells have been implicated in the formation of specialized myofibroblasts, called endoneural fibroblasts, and their composition of peripheral nerves (Joseph et al., 2004). It has also been suggested myofibroblasts and pericytes in the lamina propria may originate from gut mesothelium (Wilm et al., 2005). While much as been elucidated concerning the basic development of the lamina propria, the basic developmental timing and location of smooth muscle and vasculature have not been determined at this time.

In the adult, the mucosa is responsible for digestion and absorption of nutrients from luminal contents and barrier function, thus serving as the main focus of most gastrointestinal research. In the embryo, the mucosa is derived from the inner most layer of the small intestine, the endoderm. During intestinal development, the endoderm is initially organized as a pseudostratified layer, which undergoes remodeling and apical surface expansion to form a simple columnar epithelium (Grosse et al., 2011). The surface area expansion results in protruding tips and invaginations, known as the villi and crypts, respectively. During normal development, *Hh* signals emanate from the epithelium to signal the mesenchyme promoting expansion and elongation of the midgut tube (Bitgood and McMahon, 1995; Ramalho-Santos et al., 2000). Defects in *Hh* signaling can lead to aberrant myofibroblast localization, increased epithelial proliferation, reduced smooth muscle differentiation, defects in proper nutrient absorption, disruption in the muscularis mucosa and embryonic lethality (Kosinski et al., 2010; Madison et al., 2005; Mao et al., 2010; Zacharias et al., 2010). The signaling involved in endodermal-mesenchymal development has been well characterized, yet the field lacks a comprehensive study that compares and associates timing and formation of mesothelium and mesenchyme to the development of the villi.

Endothelial Development

The endothelial plexus is the vascular supply to the gut tube and develops early in the embryo. Preliminary ultrastructure studies in the chick embryo

proposed that a vascular plexus developed via recruitment of cells from the splanchnic mesoblast, situated between the endoderm and splanchnic mesoderm (Meier, 1980). Subsequently, chick-quail chimera transplant experiments revealed that endothelial cells developed via vasculogenesis in the splanchnopleure and angiogenesis in the somatopleure (Pardanaud et al., 1989). More recent studies employed transgenic quail embryos that express a nuclear fusion protein (H2B-eYFP) under control of the *Tie1* promoter, to identify endothelial cells and study vessel formation and dynamics (Poynter and Lansford, 2008). The avian model has excellent tools available to study vasculogenesis, all valuable to investigate the development of the endothelial plexus and major surface vessels of the intestine.

Enteric Nervous System Development

The enteric nervous system (ENS) is essential for coordination of gut movements including peristalsis, blood flow, and fluid exchange. In the intestinal field, the development of the ENS is amply described in the literature. Important studies in the 1970's utilized the novel chick-quail chimera to demonstrate that the majority of cells comprising the ENS are derived from vagal neural crest cells (Le Douarin and Teillet, 1973). The enteric neural crest-derived cells (ENCCs) migrate in a rostral to caudal fashion throughout the entire gut before differentiating into neurons and glial cells (reviewed in (Gershon, 2010; Heanue and Pachnis, 2007). Intriguingly, the patterning of the ENS is intimately associated with the development of the endothelial plexus in the intestine.

ENCCs are patterned along previously established concentric rings of endothelial cells (plexus) in the intestine (Nagy et al., 2009). These studies also determined that endothelial cells promote proliferation of ENCCs. Current models of ENCC development have utilized transgenic mouse models to perform precise, live imaging of cellular dynamics of ENCC cells within the intestine (Corpening et al., 2011). The development of the enteric nervous system is closely associated with other developmental processes in the gut, specifically muscle and vasculature formation, all of which warrant further investigation.

Visceral Smooth Muscle Organization

The muscularis externa is responsible for motility and movement, or peristalsis, of contents in the small intestinal tract. This muscle layer is comprised of the inner circular layer, which circumferentially extends around the intestine, and the external longitudinal layer, which runs length-wise through the intestine. In the embryo, early muscle cells are marked by α-smooth muscle actin and originate from early muscle progenitors in the loose mesenchyme (McLin et al., 2009). Studies in the mouse have demonstrated that smooth muscle differentiation occurs in a cranial to caudal manner (McHugh, 1995). The development of visceral smooth muscle in the avian embryo was reported as early as E8.5, the circular layer developing before the longitudinal layer (Gabella, 2002). Few studies have investigated earlier stages in the avian for the arrival of smooth muscle. Other than association with the ENS, there has been little

correlation of smooth muscle development with other morphogenic events during small intestine development.

Gut Mesothelial Characteristics

The intestinal mesothelium is a simple squamous epithelium that covers all organs in the peritoneal cavity. Organs within this cavity include the foregut (stomach, pancreas, liver, lungs), midgut (small intestine), and hindgut (colon) (Zorn and Wells, 2009). Our group is most interested with the development and potential of the intestinal mesothelium.

Development of the gut mesothelium

Studies in the mouse have only begun to elucidate the development and cellular contribution of the mesothelium to the embryonic intestine. Initially, at E9.5, there was no histological evidence of a mesothelium covering the gut tube, as evidenced by antibody labeling with Wilms' Tumor Protein 1 (Wt1) (Wilm et al., 2005). By E11.5, a mesothelium covered the entire intestine via cytokeratin and Wt1 labeling (Figure 1.2 B). Based on the location of Wt1-positive cells, it was suggested that the gut mesothelium developed in a dorsal to ventral manner. Thus, Wilm and colleagues proposed that gut mesothelium derived from a migratory population of cells

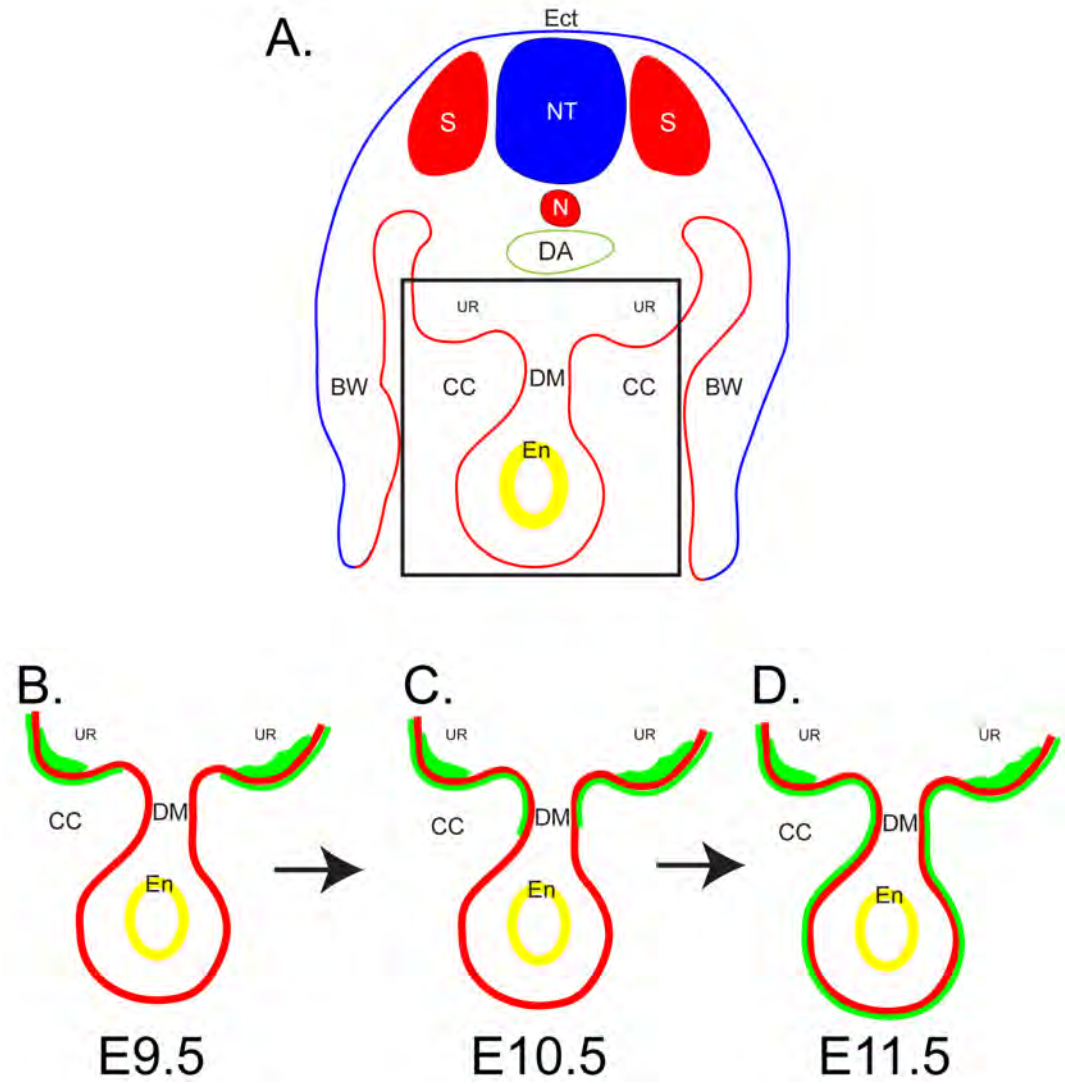

Figure 1.2 Development of gut mesothelium in the mouse embryo. A: Cross-section through the developing gut tube region. **B**: Antibody labeling for Wt1 (green), a mesothelial marker, is absent from the gut tube at E9.5, but staining for Wt1 is present in the urogenital ridges. **C**: Wt1 labeling is evident over the dorsal mesentery (DM) at E10.5, but not the gut tube. **D**: At E12.5, mesothelium, as verified by Wt1 labeling, is evident over the entire gut tube and DM. BW, body wall; CC, coelomic cavity; DA, dorsal aorta; Ec, ectoderm; En, endoderm; N, notochord; NT, neural tube S, somite; UR, urogenital ridges. Adapted from (Wilm et al., 2005).

located at the junction of the splanchnic and somatic mesodermal regions (Wilm et al., 2005). These data were among the first to describe the arrival and location of gut mesothelial cells in the mouse, but they did not provide specific evidence of an origin for gut mesothelium.

Similar to the epicardium, mesothelial cells undergo EMT and contribute cells to the vasculature of the intestine. To investigate this process, mesothelium of the gut tube labeled with a vital dye and then cultured. Cells from the mesothelium underwent EMT and migrated into the submesothelial space (Wilm et al., 2005). Employing genetic lineage tracing in the mouse, Wilm et al. established that the majority of vascular smooth muscle cells and a small portion of the endothelial cells in the major vessels in the small intestine were derived from *Wt1*-positive cells, which originally marked the mesothelial cells (Wilm et al., 2005). Subsequent studies observed similar results in the lung; mesothelial cells contributed smooth muscle cells to the vessels and mesenchyme (Que et al., 2008). Together, these studies demonstrate the significance of mesothelial development and mesothelial cell contribution to blood vessels. Importantly, elucidating the origin of the gut mesothelium would be the first step in understanding the development and potential of this important tissue.

Proepicardial and Epicardial Development

Of all mesothelial populations in the body, the heart mesothelium, a major component of the epicardium, is the best characterized. Studies have focused on

the development, signaling, and migration of the epicardial precursors, proepicardial (PE) cells. This section introduces the PE and epicardium: the history of its discovery, developmental processes, important signaling cascades involved, and cell types contributed to the heart.

History

In the late nineteenth century, researchers proposed that the epicardium arose from the myocardium; this structure was coined the “epimyocardium” (reviewed in (Männer et al., 2001)). Subsequently in 1909, Kirkowitz was the first to observe naked myoblastic cells with no mesothelial cells, suggesting that the epicardium developed independently from the myocardium (reviewed in (Männer et al., 2001). It was not until the use of TEM that the structure of the epicardium was identified (Manasek, 1969). Periodic Schiff Staining (PAS) labeling of the cytoplasmic accumulation of glycogen was only observed in myocytes and not epicardial cells, providing evidence that myocytes were not dedifferenting into epicardial cells. This work overturned a position held for over a century that the epicardium was independent from the myocardium. These data initiated a series of reports that were important for epicardial and heart development but required further investigation. Using mostly avian and mouse models and a variety of novel techniques, researchers began to elucidate the structure of epicardial cells (Ho and Shimada, 1978; Shimada et al., 1981; Virágh and Challice, 1973) and the origin and migratory properties of the epicardium and its anlage the PE (Hiruma and Hirakow, 1989; Männer, 1992; Virágh and Challice, 1981). These

seminal papers identified the epicardium as the thin, but essential third layer of the heart.

Structure and Function of PE cells

The PE is the 'extracardiac' population of progenitor cells that give rise to the mesothelium of the epicardium, which migrates over the heart as a sheet. The PE is described as a cluster of mesothelial cells with villus-like protrusions, analogous to a bunch of grapes (Figure 1.3 A, B). It initially develops bilaterally, on the sinus venosus, facing the dorsal aspect of the developing heart tube at Hamburger Hamilton (HH) stage 13-14 in the avian system (Männer, 1999; Poelmann et al., 1993), or over the septum transversum in the mouse at E9-9.5 (Ho and Shimada, 1978; Komiyama et al., 1987; Virágh and Challice, 1981). In chick, the PE is positioned on the right horn of the sinus venosus, whereas the mouse PE first forms on both right and left horns and subsequently merges at the midline before making contact with the heart (Schulte et al., 2007). Components of the PE cells include proteoglycans at the apical, basal, and luminal surfaces, with patchy staining for fibronectin and laminin at the basal surfaces (Kálmán et al., 1995; Nahirney et al., 2003). Although the origin of the epicardial anlage is not completely defined, reports suggest that the PE arises from the mesoderm of the developing liver bud and/or the precardiac mesoderm (Ishii et al., 2007; Männer, 1992; van Wijk et al., 2009). At this time in development, the PE is independent from the developing heart tube.

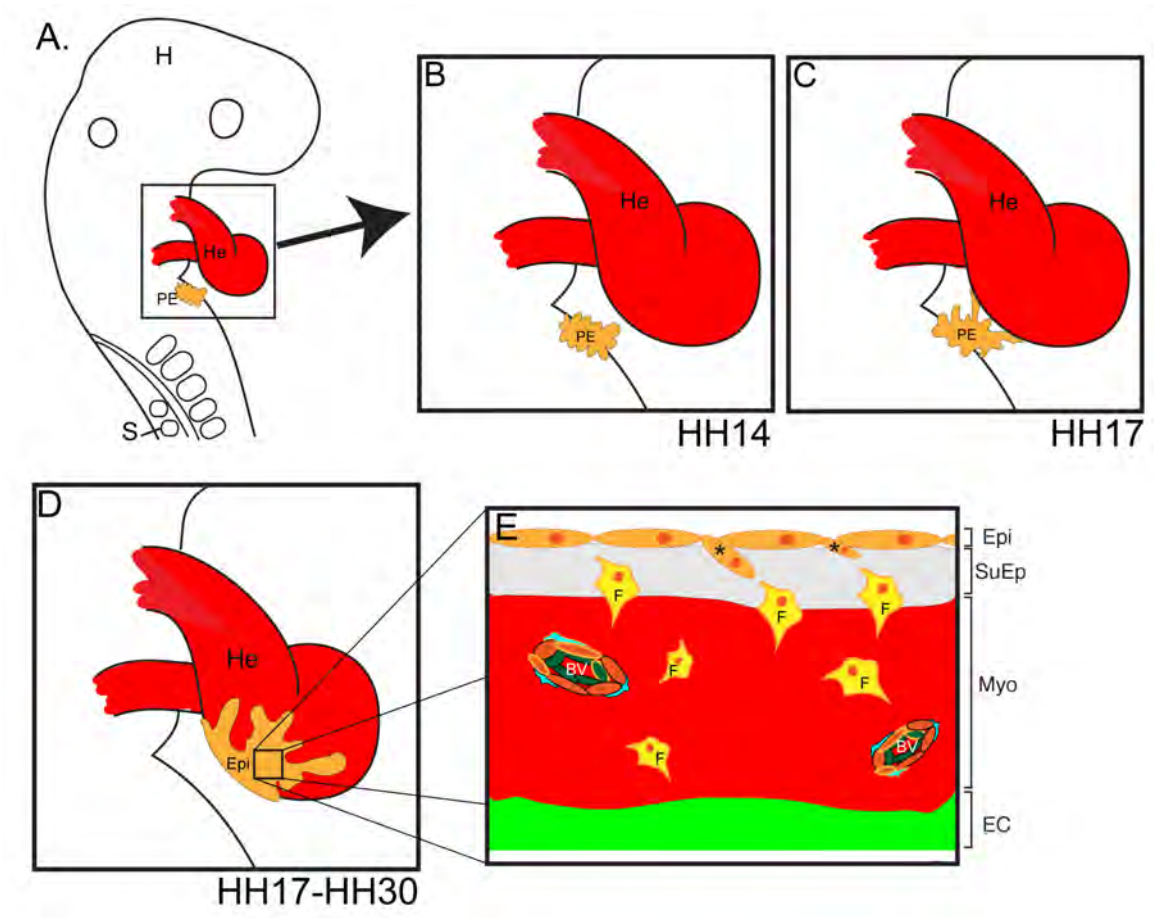

Figure 1.3 Development of the heart mesothelium in the avian. **A-B**: Schematic of an avian embryo at HH14. The proepicardium (PE), a mesothelial progenitor cell population, is located dorsal to the heart tube (He). At this time, the PE is separate from the heart tube. **C**: The PE makes contact with the heart tube in the atrioventricular groove. **D**: PE cells spread in a radial fashion over the heart. The covering is now referred to as the epicardium (Epi). **E**: Inset from D. A cross-section through the heart covered with epicardium reveals cells undergoing epithelial-to-mesenchymal transition (denoted by *). Epicardial cells differentiate into specific cell types in the myocardium (Myo) and heart vasculature (BV). Cell contribution to the myocardium includes fibroblasts (yellow, F), pericytes (teal cells around BVs), smooth muscle cells (red cells in BVs), and endothelial cells (green cells in BVs). Epicardial-derived cells are outlined in orange. Figures not drawn to scale. BV, blood vessel; EC, endocardium; Epi, epicardium; F, fibroblast; H, head; He, heart tube; Myo, myocardium; PE, proepicardium; S, somites; SuEp, subepicardium.

Signaling factors in PE recruitment to the heart

Cellular signaling involved PE and epicardial development has been well described in the literature. Studies from the past few decades have focused on cell autonomous signaling programs and more recent data are shedding light on paracrine factors involved in PE development and recruitment to the myocardium (Ishii et al., 2010). Two transcription factors, *Wt1* and *T-box transcription factor 18* (*Tbx18*) are strongly expressed in PE cells before and after contact with the heart (Carmona et al., 2001; Ishii et al., 2007; Kraus et al., 2001; Moore et al., 1999). These markers are not exclusive to epicardium, or mesothelium, both transcription factors are also involved in urogenital and kidney development (Armstrong et al., 1993). Thus, there are not any mesothelial-specific markers available at this time.

Wt1 and *Tbx18* also play important roles in PE and heart development. Multiple studies have shown that before PE cells are present, *Tbx18* expression is prominent over the right horn of the sinus venosus and in PE cells prior to making contact with the myocardium (Ishii et al., 2010; Schlueter et al., 2006). In functional studies of *Wt1*, mutant embryos died before birth, due to heart defects, mainly the absence of an epicardium (Moore et al., 1999). Additionally, these authors observed defects in proper development of the myocardium. This suggested that cellular communication between the epicardium and myocardium is essential for proper myocardial formation. Thus, *Tbx18* and *Wt1* are required for formation of an epicardium and embryonic survival.

Epicardial cell contribution to the heart

Epicardial cells also serve as an important supplier for other cell types in the heart. Once the epicardium migrates over the myocardium, cells begin to delaminate from the sheet and undergo EMT (Figure 1.3 E). This process results in cells migrating into the subepicardial space, then subsequently the myocardium. Studies throughout the years have shown that epicardial-derived cells (EPDCs) give rise to cells in coronary arteries including vascular smooth muscle cells, endothelial cells, and pericytes; heart fibroblasts or stromal cells; and some reports suggest they contribute cardiomyocytes (Cai et al., 2008; Dettman et al., 1998; Gittenberger-de Groot et al., 1998; Männer, 1999; Mikawa and Gourdie, 1996; Vrancken Peeters et al., 1999; Wessels and Pérez-Pomares, 2004; Zhou et al., 2008). Clarifying EPDC contribution to the heart has been the main emphasis in the field, especially in recent years, yet there is much that remains to be resolved.

To begin elucidating cell signaling, heart researchers studied the factors involved in initiation of the EMT process and specification of EPDCs. A major obstacle in deciphering the EMT process has been attempting to determine reciprocal signaling cascades between epicardium and myocardium. An important paracrine factor signaling to the epicardium from the myocardium is Transforming Growth Factor β (TGFβ). *TGFβ* is commonly associated with EMT processes in development and disease (Hay, 2005; Levayer and Lecuit, 2008; Shook and Keller, 2003). In the heart, TGFβ was originally shown to act as an antagonist, inhibiting EMT in cultured cells (Morabito et al., 2001). Later studies

demonstrated that TGFβ stimulates EMT in EPDCs (Compton et al., 2006; Cross et al., 2011; Olivey et al., 2006; Sanchez and Barnett, 2012; Sridurongrit et al., 2008). While most of these studies were conducted in culture using primary PE explants, primary epicardial cells, or immortalized epicardial cells lines from adult animals, few studies have been conducted *in vivo*. Other reports have revealed a role for *Wt1* signaling in EMT via binding with *Snail1*, and downregulating *E-cadherin* expression, thus inducing cells to delaminate from the epicardial sheet (Martínez-Estrada et al., 2010). These studies have demonstrated that cells from the epicardium must undergo EMT or the heart will not mature and the embryo is not viable (Kwee et al., 1995; Moore et al., 1999; Smith et al., 2011; Yang et al., 1995). Strides have been made to elucidate the signaling factors involved in EMT, but there is much to be uncovered in how these factors and molecules work together or independently in development.

EPDCs that have undergone EMT and migrated into the subepicardium or myocardium of the heart possess potential to differentiate into one of several cell types in the heart. The signals involved in this process are not completely understood at this time. Early studies utilized infection with a replication-incompetent retrovirus encoding *β-galactosidase* in PE and epicardial cells to determine that vascular smooth muscle cells, pericytes and endothelial cells of the coronaries all originated from EPDCs (Mikawa et al., 1992; Mikawa and Gourdie, 1996). Cardiac fibroblasts are also derived from EPDCs, although it should be noted that these cells comprise a heterogeneous population of cells (reviewed in (Pérez-Pomares and de la Pompa, 2011). Recent reports identified

candidate genes and signaling pathways involved in EPDC contribution to the heart. A study demonstrated that the levels of retinoic acid (RA) and *VEGF* signaling served as control mechanisms in differentiation of coronary smooth muscle cells after the formation of endothelial tubes (Azambuja et al., 2010). While these studies provide useful information regarding EPDC potential, it remains unclear whether EPDCs can differentiate into other, unidentified cell types, and how the signaling cascades work in concert to mediate these events.

The PE and epicardium are essential components necessary for heart development and function. Great strides have been made in the past 60 years that has expanded the field to vast proportions. This system is unique in that the PE develops independently from the heart, makes contact with the heart, covers the heart, and provides not only protection, but also cells that contribute to the vasculature and the stroma. The features of heart mesothelial development influenced the investigation of other coelomic mesothelial cell populations to determine if a similar processes occur in all organs.

Potential of Adult Mesothelial Cell Populations

A unique feature of embryonic mesothelium is that once it forms, it is sustained throughout adulthood. The dogma of the field rested on the fact that normal adult mesothelial cells are not renewable. However, due to the embryonic properties of mesothelial cells—cells undergo EMT and differentiate into numerous cell types—researchers began considering reprogramming of adult

mesothelial cells in potential repair models. To this end, elucidating the developmental processes of mesothelia may result in a better understanding of when processes go awry in adult mesothelial populations. This section provides a brief overview of disease and disorder in the adult mesothelium and current models of adult mesothelial regeneration and repair.

Epicardium in Disease, Regeneration, and Repair

In the United States, the Center for Disease Control reported that heart disease has consistently been a top five cause of mortality in a study assessing human health from 1935-2010 (Hoyert, 2012). A major complication in heart health is myocardial infarction (MI), or heart attack, commonly associated with an obstruction within coronary arteries. Since epicardium is the embryonic source of cells that comprise the coronaries, researchers have been hopeful that these cells hold the key for therapeutic treatments of MI. Amphibians and teleosts have served as excellent models because of their ability regenerate heart tissue (Bader and Oberpriller, 1978; Poss et al., 2002). In the adult fish, activation of *raldh2* and *Tbx18* was observed upon ablation of the cardiac apex, both genes normally downregulated in the adult, resulting in development of a new epicardial layer (Lepilina et al., 2006). Studies of heart regeneration in mammals have provided insight into changes in paracrine signaling involved between epicardial and myocardial tissues upon injury (reviewed in (Von Gise and Pu, 2012)). Promising experiments have involved *thymosin β4* Tβ4 “priming” of epicardial cells prior to injury resulting in cardiomyocytes differentiation upon MI (Smart et

al., 2011). While important contributions have been made in developing a better understanding for epicardial regeneration, much remains to be seen in terms of MI repair in the adult. It is clear that understanding the developmental structure, signaling, and potential of the PE and epicardium will contribute to advances in therapeutics for heart disease.

Gut Mesothelium in Disease and Regeneration

In adults, the mesothelium of the gut (also called the serosa), is important for organ function, providing a lubricated surface for organ locomotion, protection, and transport of required fluids from cavity to organ (Mutsaers, 2004). However, in some cases, developmental disorders and injury to the mesothelium can result in major medical complications. Developmentally, intestinal atresia is associated with the lack of blood flow causing occlusion or complete absence of regions of the intestine (Guzman et al., 2011; Louw and Barnard, 1955). In a rare but severe case of atresia, called apple peel bowel syndrome, the superior mesenteric artery does not supply blood to the intestine causing the tissue to twist around its only blood supply, the ileocolic artery, and absence of a dorsal mesentery (Festen et al., 2002). There has been speculation that this disorder could be linked to defects in embryonic mesothelium, specifically in its ability to undergo EMT and contribute to the vasculature (Wilm et al., 2005).

More commonly, the adult mesothelium is subject to injury. Peritoneal dialysis (PD), adhesion formation as a complication of surgery, and mesothelioma are maladies of mesothelium. PD is frequently implemented

among patients with end-stage renal failure, utilizing the abdominal cavity as a natural filter for blood. Complications arise with PD when patients develop peritonitis, or inflammation and fibrosis of the peritoneum, rendering the treatment ineffective and causing extreme pain and infection (reviewed in (Yung and Chan, 2012). *In vitro* studies have demonstrated that activation of the TGFβ pathway initiates and accounts for peritoneal fibrosis in PD treatment (Liu et al., 2008). Mesothelial cells are also implicated in the formation of peritoneal adhesions, commonly observed after injury to the mesothelium in the abdominal and pelvic regions. The etiology of adhesions are not completely understood, but studies have shown that upon inflammation or ischemia, the mesothelial cells release factors that cause fibrin build-up and adhesion of the serosa to the body wall (Brochhausen et al., 2011). Finally, cancer of the mesothelium, or mesothelioma, is linked to DNA damage in normal mesothelial cells (Izzi et al., 2012). Overall, the activation of signals, immune responses, and physical injuries account for most of these changes in the peritoneal mesothelium. Currently, relationships between gut mesothelial development and adult disorders are not well defined. Thus, if embryonic origins, functions, and mechanisms of gut mesothelial development are elucidated, associations may be drawn between embryo and adult, leading to useful therapeutics.

Adult mammalian mesothelial cells display plastic properties in culture (Cross et al., 2011; Kawaguchi et al., 2007; Yung et al., 2006). These properties have influenced studies that employ mesothelial cells in repair. Interestingly, the omentum, which is composed of two mesothelial sheets ensheathing adipose

tissue, has been utilized in surgeries for centuries called “omental transposition” to repair injured sites in the body (Cannaday, 1948; Shah et al., 2012). The transplanted omentum revascularizes the injured area and provides pluripotent cells, but the mechanisms are not well understood. In a mouse model, transplanted grafts treated with Tβ4 migrated to an injured carotid artery site and differentiated into vascular smooth muscle cells, essentially repairing the artery (Shelton et al., 2012). Currently, most studies focus on the potential of adult intestinal mesothelial cells, and few studies have investigated cell differentiation in the embryo. Understanding an embryonic potential may lead to a better understanding the mechanisms involved in adult repair.

Summary of Dissertation and Aims

Mesothelia are mesodermally derived, simple squamous epithelial cells that line all body cavities and the organs contained within these cavities. In the heart, the mesothelium arises from an external population of progenitor cells called the PE, which makes contact and migrates over the heart, forming the epicardium. In contrast, the origin of gut mesothelial cells is currently unknown. A study in the murine model demonstrated that gut mesothelial cells developed over intestine in a dorsal to ventral manner, suggesting migratory properties of gut mesothelia. Thus, we hypothesized that there would be an exogenous population of “PE-like” cells in the peritoneal cavity that give rise to the gut mesothelium, similar to the heart.

Collectively, it appears that similarities exist between the heart and gut mesothelial populations after they have covered their respective organs. Initially, both heart and gut tubes lack mesothelial cells. Once the organs are covered with a mesothelium, some cells undergo EMT and migrate into the myocardium of the heart and mesenchyme layer of the gut. Finally, both mesothelial populations contribute vascular cells to the major surface vessels over the organs. I hypothesized that the heart and gut mesothelium possess plastic properties and are capable of integrating into any coelomic organ. All studies presented in this dissertation were conducted in the avian embryo. I approached my hypotheses with the following specific aims:

Aim 1. Determine the timeline of gut mesodermal development

Using immunohistochemistry, transgenic quail embryos, and morphometric analysis, three intestinal compartments were identified and described in detail. Antibody labeling of the basement membranes revealed morphological changes in the outer epithelium before a mesothelium was identified at E6. Analysis of Tg(*tie1*:H2B-eYPF) embryonic revealed the timing of vascular organization within the mesenchymal space and the formation of major surface blood vessels over the gut. Finally, morphometric analysis provided insight into changes in the mesenchymal space. These data are described in Chapter II.

Aim 2. Identify the origin of the gut mesothelium

The progenitor population of the gut mesothelium was investigated utilizing direct lineage tracing techniques and an application of the chick-quail

chimera system. First, two direct-labeling techniques were employed to determine if mesothelial cells derived from the splanchnic mesoderm. Next, quail splanchnopleure transplanted into chick host revealed novel generation of a separate gut tube that developed an endogenous mesothelium. These three methods clearly demonstrated that the gut mesothelium originates from cells resident to the splanchnic mesoderm and not from an extrinsic source. These data are presented in Chapter III.

Aim 3. Investigate an interchangeable potential between heart and gut mesothelial populations

The potential of heart and gut mesothelial cells were further elucidated using *in vitro* and *in vivo* techniques. First, isolates from PE, epicardial, and gut mesothelium were analyzed using immunohistochemistry, RT-PCR, and cell culture. These methods provided data pertaining to cell types within the isolates at time zero (starting products) and revealed the potential for mesothelia to differentiate in culture. Next, quail PE and heart mesothelia were surgically placed into the peritoneal cavity of a chick host, and gut mesothelium was placed into the peritoneal cavity. Embryos were analyzed using markers specific to quail cells to identify the location of mesothelial tissues in their analogous cavities. Intestinal mesothelial cells exhibited plastic properties, whereas PE and epicardial cells did not share this potential. The results of these experiments are discussed in Chapter IV.

References

Armstrong, J. F., Pritchard-Jones, K., Bickmore, W. A., Hastie, N. D. and Bard, J. B. (1993). The expression of the Wilms' tumour gene, WT1, in the developing mammalian embryo. *Mech Dev* **40**, 85-97.

Azambuja, A. P., Portillo-Sánchez, V., Rodrigues, M. V., Omae, S. V., Schechtman, D., Strauss, B. E., Costanzi-Strauss, E., Krieger, J. E., Pérez-Pomares, J. M. and Xavier-Neto, J. (2010). Retinoic acid and VEGF delay smooth muscle relative to endothelial differentiation to coordinate inner and outer coronary vessel wall morphogenesis. *Circ Res* **107**, 204-216.

Bader, D. and Oberpriller, J. O. (1978). Repair and reorganization of minced cardiac muscle in the adult newt (Notophthalmus viridescens). *J Morphol* **155**, 349-357.

Bitgood, M. J. and Mcmahon, A. P. (1995). Hedgehog and Bmp genes are coexpressed at many diverse sites of cell-cell interaction in the mouse embryo. *Dev Biol* **172**, 126-138.

Brochhausen, C., Schmitt, V. H., Rajab, T. K., Planck, C. N. E., Krämer, B., Wallwiener, M., Hierlemann, H. and Kirkpatrick, C. J. (2011). Intraperitoneal adhesions-an ongoing challenge between biomedical engineering and the life sciences. *J Biomed Mater Res* **98A**, 143-156.

Burn, S. F. and Hill, R. E. (2009). Left-right asymmetry in gut development: what happens next? *Bioessays* **31**, 1026-1037.

Cai, C.-L., Martin, J. C., Sun, Y., Cui, L., Wang, L., Ouyang, K., Yang, L., Bu, L., Liang, X., Zhang, X., Stallcup, W. B., Denton, C. P., Mcculloch, A., Chen, J. and Evans, S. M. (2008). A myocardial lineage derives from Tbx18 epicardial cells. *Nature* **454**, 104-108.

Cannaday, J. E. (1948). Some uses of undetached omentum in surgery. *Am J Surg* **76**, 502-505.

Carmona, R., González-Iriarte, M., Pérez-Pomares, J. M. and Muñoz-Chápuli, R. (2001). Localization of the Wilm's tumour protein WT1 in avian embryos. *Cell Tissue Res* **303**, 173-186.

Compton, L. A., Potash, D. A., Mundell, N. A. and Barnett, J. V. (2006). Transforming growth factor-beta induces loss of epithelial character and smooth muscle cell differentiation in epicardial cells. *Dev Dyn* **235**, 82-93.

Corpening, J. C., Deal, K. K., Cantrell, V. A., Skelton, S. B., Buehler, D. P. and Southard-Smith, E. M. (2011). Isolation and live imaging of enteric progenitors based on Sox10-Histone2BVenus transgene expression. *Genesis* **49**, 599-618.

Cross, E. E., Thomason, R. T., Martinez, M., Hopkins, C. R., Hong, C. C. and Bader, D. M. (2011). Application of Small Organic Molecules Reveals Cooperative TGFβ and BMP Regulation of Mesothelial Cell Behaviors. *ACS Chem Biol* **6**, 952-961.

Dettman, R. W., Denetclaw, W., Ordahl, C. P. and Bristow, J. (1998). Common epicardial origin of coronary vascular smooth muscle, perivascular fibroblasts, and intermyocardial fibroblasts in the avian heart. *Dev Biol* **193**, 169-181.

Festen, S., Brevoord, J. C. D., Goldhoorn, G. A., Festen, C., Hazebroek, F. W. J., Van Heurn, L. W. E., De Langen, Z. J., Van Der Zee, D. C. and Aronson, D. C. (2002). Excellent long-term outcome for survivors of apple peel atresia. *J Pediatr Surg* **37**, 61-65.

Funayama, N., Sato, Y., Matsumoto, K., Ogura, T. and Takahashi, Y. (1999). Coelom formation: binary decision of the lateral plate mesoderm is controlled by the ectoderm. *Development* **126**, 4129-4138.

Gabella, G. (2002). Development of visceral smooth muscle. *Results Probl Cell Differ* **38**, 1-37.

Gershon, M. D. (2010). Developmental determinants of the independence and complexity of the enteric nervous system. *Trends Neurosci* **33**, 446-456.

Gittenberger-De Groot, A. C., Vrancken Peeters, M. P., Mentink, M. M., Gourdie, R. G. and Poelmann, R. E. (1998). Epicardium-derived cells contribute a novel population to the myocardial wall and the atrioventricular cushions. *Circ Res* **82**, 1043-1052.

Green, M. C. (1967). A defect of the splanchnic mesoderm caused by the mutant gene dominant hemimelia in the mouse. *Dev Biol* **15**, 62-89.

Grosse, A. S., Pressprich, M. F., Curley, L. B., Hamilton, K. L., Margolis, B., Hildebrand, J. D. and Gumucio, D. L. (2011). Cell dynamics in fetal intestinal epithelium: implications for intestinal growth and morphogenesis. *Development* **138**, 4423-4432.

Guzman, M. A., Prasad, R., Duke, D. S. and De Chadarévian, J.-P. (2011). Multiple intestinal atresias associated with angiodysplasia in a newborn. *J Pediatr Surg* **46**, 1445-1448.

Hay, E. D. (2005). The mesenchymal cell, its role in the embryo, and the remarkable signaling mechanisms that create it. *Dev Dyn* **233**, 706-720.

Heanue, T. A. and Pachnis, V. (2007). Enteric nervous system development and Hirschsprung's disease: advances in genetic and stem cell studies. *Nat Rev Neurosci* **8**, 466-479.

Hecksher-Sørensen, J., Watson, R. P., Lettice, L. A., Serup, P., Eley, L., De Angelis, C., Ahlgren, U. and Hill, R. E. (2004). The splanchnic mesodermal plate directs spleen and pancreatic laterality, and is regulated by Bapx1/Nkx3.2. *Development* **131**, 4665-4675.

Hiruma, T. and Hirakow, R. (1989). Epicardial formation in embryonic chick heart: computer-aided reconstruction, scanning, and transmission electron microscopic studies. *Am J Anat* **184**, 129-138.

Ho, E. and Shimada, Y. (1978). Formation of the epicardium studied with the scanning electron microscope. *Dev Biol* **66**, 579-585.

Hoyert, D. L. (2012). "75 Years of Mortality in the United States, 1935–2010." Retrieved 17 October 2012, from http://www.cdc.gov/nchs/data/databriefs/db88.htm.

Ishii, Y., Garriock, R. J., Navetta, A. M., Coughlin, L. E. and Mikawa, T. (2010). BMP signals promote proepicardial protrusion necessary for recruitment of coronary vessel and epicardial progenitors to the heart. *Dev Cell* **19**, 307-316.

Ishii, Y., Langberg, J. D., Hurtado, R., Lee, S. and Mikawa, T. (2007). Induction of proepicardial marker gene expression by the liver bud. *Development* **134**, 3627-3637.

Izzi, V., Masuelli, L., Tresoldi, I., Foti, C., Modesti, A. and Bei, R. (2012). Immunity and malignant mesothelioma: From mesothelial cell damage to tumor development and immune response-based therapies. *Cancer Letters* **322**, 18-34.

Joseph, N. M., Mukouyama, Y.-S., Mosher, J. T., Jaegle, M., Crone, S. A., Dormand, E.-L., Lee, K.-F., Meijer, D., Anderson, D. J. and Morrison, S. J. (2004). Neural crest stem cells undergo multilineage differentiation in developing peripheral nerves to generate endoneurial fibroblasts in addition to Schwann cells. *Development* **131**, 5599-5612.

Kálmán, F., Virágh, S. and Módis, L. (1995). Cell surface glycoconjugates and the extracellular matrix of the developing mouse embryo epicardium. *Anat Embryol* **191**, 451-464.

Kawaguchi, M., Bader, D. M. and Wilm, B. (2007). Serosal mesothelium retains vasculogenic potential. *Dev Dyn* **236**, 2973-2979.

Komiyama, M., Ito, K. and Shimada, Y. (1987). Origin and development of the epicardium in the mouse embryo. *Anat Embryol* **176**, 183-189.

Kosinski, C., Stange, D. E., Xu, C., Chan, A. S., Ho, C., Yuen, S. T., Mifflin, R. C., Powell, D. W., Clevers, H., Leung, S. Y. and Chen, X. (2010). Indian hedgehog regulates intestinal stem cell fate through epithelial-mesenchymal interactions during development. *Gastroenterology* **139**, 893-903.

Kraus, F., Haenig, B. and Kispert, A. (2001). Cloning and expression analysis of the mouse T-box gene Tbx18. *Mech Dev* **100**, 83-86.

Kuhn, H. J. and Liebherr, G. (1988). The early development of the epicardium in Tupaia belangeri. *Anat Embryol* **177**, 225-234.

Kwee, L., Baldwin, H. S., Shen, H. M., Stewart, C. L., Buck, C., Buck, C. A. and Labow, M. A. (1995). Defective development of the embryonic and extraembryonic circulatory systems in vascular cell adhesion molecule (VCAM-1) deficient mice. *Development* **121**, 489-503.

Le Douarin, N. M. and Teillet, M. A. (1973). The migration of neural crest cells to the wall of the digestive tract in avian embryo. *J Embryol Exp Morphol* **30**, 31-48.

Lefebvre, O., Sorokin, L., Kedinger, M. and Simon-Assmann, P. (1999). Developmental expression and cellular origin of the laminin alpha2, alpha4, and alpha5 chains in the intestine. *Dev Biol* **210**, 135-150.

Lepilina, A., Coon, A. N., Kikuchi, K., Holdway, J. E., Roberts, R. W., Burns, C. G. and Poss, K. D. (2006). A dynamic epicardial injury response supports progenitor cell activity during zebrafish heart regeneration. *Cell* **127**, 607-619.

Levayer, R. and Lecuit, T. (2008). Breaking down EMT. *Nature* **10**, 757-759.

Levin, M., Johnson, R. L., Stern, C. D., Kuehn, M. and Tabin, C. (1995). A molecular pathway determining left-right asymmetry in chick embryogenesis. *Cell* **82**, 803-814.

Liu, Q., Mao, H., Nie, J., Chen, W., Yang, Q., Dong, X. and Yu, X. (2008). Transforming growth factor β1 induces epithelial-mesenchymal transition by activating the JNK-Smad3 pathway in rat peritoneal mesothelial cells. *Perit Dial Int* **28 Suppl 3**, S88-95.

Louw, J. H. and Barnard, C. N. (1955). Congenital intestinal atresia; observations on its origin. *Lancet* **269**, 1065-1067.

Madison, B. B., Braunstein, K., Kuizon, E., Portman, K., Qiao, X. T. and Gumucio, D. L. (2005). Epithelial hedgehog signals pattern the intestinal crypt-villus axis. *Development* **132**, 279-289.

Mahlapuu, M., Ormestad, M., Enerbäck, S. and Carlsson, P. (2000). The forkhead transcription factor Foxf1 is required for differentiation of extra-embryonic and lateral plate mesoderm. *Development* **128**, 155-166.

Manasek, F. J. (1969). Embryonic development of the heart. II. Formation of the epicardium. *J Embryol Exp Morphol* **22**, 333-348.

Männer, J. (1992). The development of pericardial villi in the chick embryo. *Anat Embryol* **186**, 379-385.

Männer, J. (1999). Does the subepicardial mesenchyme contribute myocardioblasts to the myocardium of the chick embryo heart? A quail-chick chimera study tracing the fate of the epicardial primordium. *Anat Rec* **255**, 212-226.

Männer, J., Pérez-Pomares, J. M., Macías, D. and Muñoz-Chápuli, R. (2001). The origin, formation and developmental significance of the epicardium: a review. *Cells Tissues Organs* **169**, 89-103.

Mao, J., Kim, B.-M., Rajurkar, M., Shivdasani, R. A. and Mcmahon, A. P. (2010). Hedgehog signaling controls mesenchymal growth in the developing mammalian digestive tract. *Development* **137**, 1721-1729.

Martínez-Estrada, O. M., Lettice, L. A., Essafi, A., Guadix, J. A., Slight, J., Velecela, V., Hall, E., Reichmann, J., Devenney, P. S., Hohenstein, P., Hosen, N., Hill, R. E., Muñoz-Chápuli, R. and Hastie, N. D. (2010). Wt1 is required for cardiovascular progenitor cell formation through transcriptional control of Snail and E-cadherin. *Nat Genet* **42**, 89-93.

Mchugh, K. M. (1995). Molecular analysis of smooth muscle development in the mouse. *Dev Dyn* **204**, 278-290.

Mclin, V. A., Henning, S. J. and Jamrich, M. (2009). The role of the visceral mesoderm in the development of the gastrointestinal tract. *Gastroenterology* **136**, 2074-2091.

Meier, S. (1980). Development of the chick embryo mesoblast: pronephros, lateral plate, and early vasculature. *J Embryol Exp Morphol* **55**, 291-306.

Mikawa, T., Borisov, A., Brown, A. M. and Fischman, D. A. (1992). Clonal analysis of cardiac morphogenesis in the chicken embryo using a replication-defective retrovirus: I. Formation of the ventricular myocardium. *Dev Dyn* **193**, 11-23.

Mikawa, T. and Gourdie, R. G. (1996). Pericardial mesoderm generates a population of coronary smooth muscle cells migrating into the heart along with ingrowth of the epicardial organ. *Dev Biol* **174**, 221-232.

Moore, A. W., Mcinnes, L., Kreidberg, J., Hastie, N. D. and Schedl, A. (1999). YAC complementation shows a requirement for Wt1 in the development of epicardium, adrenal gland and throughout nephrogenesis. *Development* **126**, 1845-1857.

Morabito, C. J., Dettman, R. W., Kattan, J., Collier, J. M. and Bristow, J. (2001). Positive and negative regulation of epicardial-mesenchymal transformation during avian heart development. *Dev Biol* **234**, 204-215.

Mutsaers, S. E. (2004). The mesothelial cell. *Int J Biochem Cell Biol* **36**, 9-16.

Nagy, N., Mwizerwa, O., Yaniv, K., Carmel, L., Pieretti-Vanmarcke, R., Weinstein, B. M. and Goldstein, A. M. (2009). Endothelial cells promote migration and proliferation of enteric neural crest cells via beta1 integrin signaling. *Dev Biol* **330**, 263-272.

Nahirney, P. C., Mikawa, T. and Fischman, D. A. (2003). Evidence for an extracellular matrix bridge guiding proepicardial cell migration to the myocardium of chick embryos. *Dev Dyn* **227**, 511-523.

Nesbitt, T., Lemley, A., Davis, J., Yost, M. J., Goodwin, R. L. and Potts, J. D. (2006). Epicardial development in the rat: a new perspective. *Microsc Microanal* **12**, 390-398.

Olivey, H. E., Mundell, N. A., Austin, A. F. and Barnett, J. V. (2006). Transforming growth factor-beta stimulates epithelial-mesenchymal transformation in the proepicardium. *Dev Dyn* **235**, 50-59.

Pardanaud, L., Yassine, F. and Dieterlen-Lievre, F. (1989). Relationship between vasculogenesis, angiogenesis and haemopoiesis during avian ontogeny. *Development* **105**, 473-485.

Pérez-Pomares, J.-M. and De La Pompa, J. L. (2011). Signaling during epicardium and coronary vessel development. *Circ Res* **109**, 1429-1442.

Peterson, R. S., Lim, L., Ye, H., Zhou, H., Overdier, D. G. and Costa, R. H. (1997). The winged helix transcriptional activator HFH-8 is expressed in the mesoderm of the primitive streak stage of mouse embryos and its cellular derivatives. *Mech Dev* **69**, 53-69.

Poelmann, R. E., Gittenberger-De Groot, A. C., Mentink, M. M., Bökenkamp, R. and Hogers, B. (1993). Development of the cardiac coronary vascular endothelium, studied with antiendothelial antibodies, in chicken-quail chimeras. *Circ Res* **73**, 559-568.

Poss, K. D., Wilson, L. G. and Keating, M. T. (2002). Heart regeneration in zebrafish. *Science* **298**, 2188-2190.

Powell, D. W., Pinchuk, I. V., Saada, J. I., Chen, X. and Mifflin, R. C. (2011). Mesenchymal Cells of the Intestinal Lamina Propria. *Annu Rev Physiol* **73**, 213-237.

Poynter, G. and Lansford, R. (2008). Generating transgenic quail using lentiviruses. *Methods Cell Biol* **87**, 281-293.

Que, J., Wilm, B., Hasegawa, H., Wang, F., Bader, D. and Hogan, B. (2008). Mesothelium contributes to vascular smooth muscle and mesenchyme during lung development. *Proc Natl Acad Sci USA*.

Ramalho-Santos, M., Melton, D. A. and Mcmahon, A. P. (2000). Hedgehog signals regulate multiple aspects of gastrointestinal development. *Development* **127**, 2763-2772.

Sanchez, N. S. and Barnett, J. V. (2012). TGFβ and BMP-2 regulate epicardial cell invasion via TGFβR3 activation of the Par6/Smurf1/RhoA pathway. *Cell Signal* **24**, 539-548.

Schlueter, J., Männer, J. and Brand, T. (2006). BMP is an important regulator of proepicardial identity in the chick embryo. *Dev Biol* **295**, 546-558.

Schulte, I., Schlueter, J., Abu-Issa, R., Brand, T. and Männer, J. (2007). Morphological and molecular left-right asymmetries in the development of the proepicardium: a comparative analysis on mouse and chick embryos. *Dev Dyn* **236**, 684-695.

Shah, S., Lowery, E., Braun, R. K., Martin, A., Huang, N., Medina, M., Sethupathi, P., Seki, Y., Takami, M., Byrne, K., Wigfield, C., Love, R. B. and Iwashima, M. (2012). Cellular basis of tissue regeneration by omentum. *PLoS ONE* **7**, e38368.

Shelton, E. L., Poole, S. D., Reese, J. and Bader, D. M. (2012). Omental grafting: a cell-based therapy for blood vessel repair. *J Tissue Eng Regen Med* doi: 10.1002/term.1528.

Shimada, Y., Ho, E. and Toyota, N. (1981). Epicardial covering over myocardial wall in the chicken embryo as seen with the scanning electron microscope. *Scan Electron Microsc* 275-280.

Shook, D. and Keller, R. (2003). Mechanisms, mechanics and function of epithelial-mesenchymal transitions in early development. *Mech Dev* **120**, 1351-1383.

Simon-Assmann, P., Lefebvre, O., Bellissent-Waydelich, A., Olsen, J., Orian-Rousseau, V. and De Arcangelis, A. (1998). The laminins: role in intestinal morphogenesis and differentiation. *Ann N Y Acad Sci* **859**, 46-64.

Smart, N., Bollini, S., Dubé, K. N., Vieira, J. M., Zhou, B., Davidson, S., Yellon, D., Riegler, J., Price, A. N., Lythgoe, M. F., Pu, W. T. and Riley, P. R. (2011). De novo cardiomyocytes from within the activated adult heart after injury. *Nature* **474**, 640-644.

Smith, C. L., Baek, S. T., Sung, C. Y. and Tallquist, M. D. (2011). Epicardial-derived cell epithelial-to-mesenchymal transition and fate specification require PDGF receptor signaling. *Circ Res* **108**, e15-26.

Sridurongrit, S., Larsson, J., Schwartz, R., Ruiz-Lozano, P. and Kaartinen, V. (2008). Signaling via the Tgf-beta type I receptor Alk5 in heart development. *Dev Biol*.

Tonegawa, A., Funayama, N., Ueno, N. and Takahashi, Y. (1997). Mesodermal subdivision along the mediolateral axis in chicken controlled by different concentrations of BMP-4. *Development* **124**, 1975-1984.

Tonegawa, A. and Takahashi, Y. (1998). Somitogenesis controlled by Noggin. *Dev Biol* **202**, 172-182.

Van Wijk, B., Van Den Berg, G., Abu-Issa, R., Barnett, P., Van Der Velden, S., Schmidt, M., Ruijter, J. M., Kirby, M. L., Moorman, A. F. M. and Van Den Hoff, M. J. B. (2009). Epicardium and myocardium separate from a common precursor pool by crosstalk between bone morphogenetic protein- and fibroblast growth factor-signaling pathways. *Circ Res* **105**, 431-441.

Virágh, S. and Challice, C. E. (1973). Origin and differentiation of cardiac muscle cells in the mouse. *J Ultrastruct Res* **42**, 1-24.

Virágh, S. and Challice, C. E. (1981). The origin of the epicardium and the embryonic myocardial circulation in the mouse. *Anat Rec* **201**, 157-168.

Von Gise, A. and Pu, W. T. (2012). Endocardial and epicardial epithelial to mesenchymal transitions in heart development and disease. *Circ Res* **110**, 1628-1645.

Vrancken Peeters, M. P., Gittenberger-De Groot, A. C., Mentink, M. M. and Poelmann, R. E. (1999). Smooth muscle cells and fibroblasts of the coronary arteries derive from epithelial-mesenchymal transformation of the epicardium. *Anat Embryol* **199**, 367-378.

Wessels, A. and Pérez-Pomares, J. M. (2004). The epicardium and epicardially derived cells (EPDCs) as cardiac stem cells. *Anat Rec* **276**, 43-57.

Wilm, B., Ipenberg, A., Hastie, N. D., Burch, J. B. E. and Bader, D. M. (2005). The serosal mesothelium is a major source of smooth muscle cells of the gut vasculature. *Development* **132**, 5317-5328.

Yang, J. T., Rayburn, H. and Hynes, R. O. (1995). Cell adhesion events mediated by alpha 4 integrins are essential in placental and cardiac development. *Development* **121**, 549-560.

Yung, S. and Chan, T. M. (2012). Pathophysiological Changes to the Peritoneal Membrane during PD-Related Peritonitis: The Role of Mesothelial Cells. *Mediators Inflamm* **2012**, 1-21.

Yung, S., Li, F. K. and Chan, T. M. (2006). Peritoneal mesothelial cell culture and biology. *Perit Dial Int* **26**, 162-173.

Zacharias, W. J., Li, X., Madison, B. B., Kretovich, K., Kao, J. Y., Merchant, J. L. and Gumucio, D. L. (2010). Hedgehog is an anti-inflammatory epithelial signal for the intestinal lamina propria. *Gastroenterology* **138**, 2368-2377-2377.e2361-2364.

Zhou, B., Ma, Q., Rajagopal, S., Wu, S. M., Domian, I., Rivera-Feliciano, J., Jiang, D., Von Gise, A., Ikeda, S., Chien, K. R. and Pu, W. T. (2008). Epicardial progenitors contribute to the cardiomyocyte lineage in the developing heart. *Nature* **454**, 109-113.

Zorn, A. M. and Wells, J. M. (2009). Vertebrate endoderm development and organ formation. *Annu Rev Cell Dev Biol* **25**, 221-251.

CHAPTER II

COMPREHENSIVE TIMELINE OF MESODERMAL DEVELOPMENT IN THE QUAIL SMALL INTESTINE

This chapter was accepted to *Developmental Dynamics* on 10 August 2012 under the same title by the following authors:

Rebecca T. Thomason, David M. Bader, Nichelle I. Winters

Abstract

Background: To generate the mature intestine, splanchnic mesoderm diversifies into six different tissue layers each with multiple cell types through concurrent and complex morphogenetic events. Hindering the progress of research in the field is the lack of a detailed description of the fundamental morphological changes that constitute development of the intestinal mesoderm. Results: We utilized immunofluorescence and morphometric analyses of wild type and Tg(*tie1*:H2B-eYFP) quail embryos to establish a comprehensive timeline of mesodermal development in the avian intestine. The following landmark features were analyzed from appearance of the intestinal primordium through generation of the definitive structure: radial compartment formation, basement membrane dynamics, mesothelial differentiation, mesenchymal expansion and growth patterns, smooth muscle differentiation, and maturation of the vasculature. In this way, structural relationships between mesodermal

components were identified over time. Conclusions: This integrated analysis presents a roadmap for investigators and clinicians to evaluate diverse experimental data obtained at individual stages of intestinal development within the longitudinal context of intestinal morphogenesis.

Introduction

Intestinal disorders affect a large number of individuals in both pediatric and adult settings. Many of these conditions including intestinal atresia, motility disorders, Hirschprung's disease, and gastrointestinal stromal tumors (GIST) have multiple and incompletely understood etiologies (Appelman, 2011; Guzman et al., 2011; Heanue and Pachnis, 2007; Hirota et al., 1998; Louw and Barnard, 1955; Mazur and Clark, 1983; Newgreen and Young, 2002; Sanders, 1996; Streutker et al., 2007). One of the difficulties in deciphering the mechanisms underlying these diseases is the lack of information available on the development of a major component of the gut tube—the intestinal mesoderm. Understanding development of the mesoderm is essential for a complete picture of the mechanisms leading to congenital as well as adult intestinal disorders.

A description of the structure of the adult intestine reveals the complexity of the mesodermal tissues generated in the embryo. The innermost layer, the mucosal epithelium, is comprised primarily of columnar epithelial cells resting on a basement membrane. Supporting the mucosal epithelium is a mesenchymal core called the lamina propria, which is composed of a capillary plexus, lymphatic

vessels, nerves, myofibroblasts and fibroblasts. The lamina propria and mucosal epithelium are arranged into fingerlike projections, called villi, protruding into the lumen of the intestine. External to the mucosal epithelium, minor variations in structure are observed between the avian and mammalian intestine. The adult chick intestine lacks a submucosal connective tissue layer and muscularis mucosa. Instead, there are four concentric visceral smooth muscle cell layers that begin just subjacent to the lamina propria and are positioned outwardly in the following order: inner longitudinal, inner circular, outer circular and outer longitudinal (Gabella, 1985; Yamamoto, 1996). The inner longitudinal muscle layer of the avian is analogous to the mammalian muscularis mucosa. The circular muscle layer of mammals including mice and humans can also be divided into two layers due to structural differences though is often referred to singularly (Eddinger, 2009). Thus, the most significant variation between the mammalian and avian intestine is the presence or absence of a submucosal connective tissue layer. The large blood vessels of the chick intestine reside within or just deep to the thin outer longitudinal visceral smooth muscle cell layer and extend circumferentially. Vascular branches dive deep into the intestinal layers to eventually supply the endothelial plexus of the villi (Jacobson and Noer, 1952). The enteric neuronal network is divided into two main regions: the first adjacent to the large blood vessels described above that reside near the surface and the second between the inner circular and inner longitudinal smooth muscle layers (Gabella, 1985). Finally, at the coelomic surface is a serosal membrane

composed of a flat sheet of epithelial cells called mesothelium with an underlying basement membrane and thin connective tissue layer (Figure 2.1).

On first examination, the embryonic intestinal primordium offers only hints of its eventual elaborate structure. After gastrulation in the avian embryo, the lateral plate mesoderm splits into splanchnic and somatic mesoderm bilaterally generating a right and left coelomic cavity between the two layers. The splanchnic mesoderm, underlying endoderm, and an intervening endothelial plexus compose the intestinal anlage and are initially organized as a flat sheet (Figure 2.1 A, (Meier, 1980; Pardanaud et al., 1989)). This anlage folds laterally and from the anterior and posterior ends to meet at the ventral midline giving rise to a tube and uniting the right and left lateral cavities into a common coelom (Figure 2.1 B, (Wells and Melton, 1999; Zorn and Wells, 2009)). The epithelial endoderm gives rise to the mucosa that lines the villi and intestinal crypts (Coulombre and Coulombre, 1958; Dauça et al., 2007; Grosse et al., 2011; Madison et al., 2005; Mitjans et al., 1997; Spence et al., 2011). The splanchnic mesoderm diversifies to generate the connective tissue, vasculature, smooth muscle and serosal layers (Drake et al., 1997; Hashimoto et al., 1999; Kim et al., 2007; McHugh, 1995; Milgrom-Hoffman et al., 2011; Powell et al., 2011; Wilm et al., 2005; Winters et al., 2012). Migratory neural crest cells invade to form the enteric nervous system and the vascular system organizes from incompletely identified progenitors (Burns et al., 2009; Nagy et al., 2009; Young et al., 2004; Young and Newgreen, 2001). Throughout these processes, the intestine must undergo a dramatic increase in length and diameter herniating outside of the

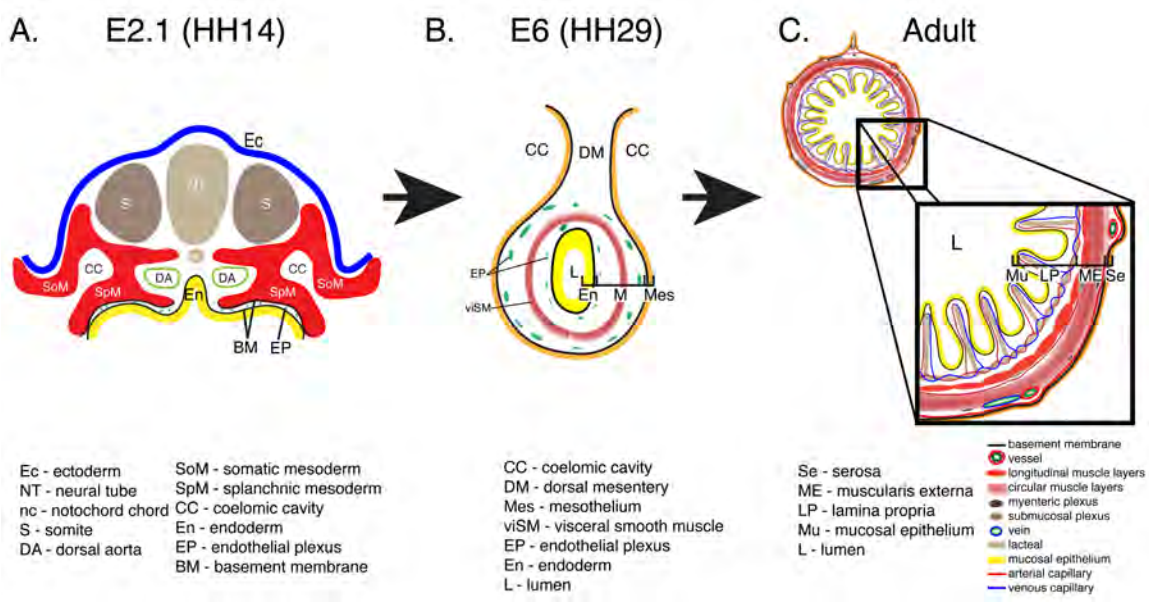

Figure 2.1 Schematic depicting the intestinal primordium, primitive intestinal tube and adult intestine. A: Transverse section through an embryonic day (E) 2.1 quail embryo equivalent to Hamburger and Hamilton (HH) stage 14. At this stage, the intestinal primordium is open and comprised of the splanchnic mesoderm (red; SpM), endoderm (yellow; En) and an intervening endothelial plexus (green; EP). **B**: At E6, the intestine is completely closed and composed of a mesothelium (orange; Mes), a two layered endothelial plexus (green; EP), a visceral smooth muscle layer (red; viSM), and endoderm (yellow; En). **C**: In the adult intestine, villi are lined with a mucosal epithelium (yellow; Mu) and contain a lamina propria (LP) composed of capillaries, a lymphatic lacteal, and connective tissue. A four-layered muscularis externa (ME) surrounds the lamina propria. A serosal membrane (Se) lines the coelomic surface.

body cavity to accommodate its tremendous growth (Savin et al., 2011). Thus, cells of all three germ layers must coordinate invasion, migration, differentiation, growth, and tissue morphogenesis to generate the mature intestinal structure.

Despite comprising the majority of the adult intestine, development of the mesoderm is poorly described relative to the more extensively studied endodermal and neuronal components. Within the mesoderm, multiple cellular types and tissue layers develop in concert. Most studies are focused on the differentiation of a specific cell type during a narrow developmental window. Furthermore, studies utilize a variety of model organisms. Thus, assembling the available data distributed within the literature into a basic timeline of the major morphological changes that occur during intestinal development is extremely difficult. Knowledge of the temporal and spatial relationships of developmental events in the intestine is essential to design experiments and interpret data.

We sought to establish a comprehensive timeline of the major events in intestinal mesoderm development from the first appearance of the intestinal anlage to formation of the definitive structure in a single species. Quail embryos were selected due to their availability in large quantities, emerging transgenic models, and the ability to easily time their development with precision (Huss et al., 2008). Additionally, small intestine development has not been described in the quail (Coulombre and Coulombre, 1958; Gabella, 1985; Grey, 1972; Hashimoto et al., 1999; Hiramatsu and Yasugi, 2004; Kim et al., 2007; Mao et al., 2010; Yamamoto, 1996). Importantly, the major structural features of the avian intestine, with the above noted variations, correspond with the mammalian intestine and

thus the information obtained from studies of the avian embryo is widely applicable. We describe landmark features of intestinal mesoderm formation throughout embryogenesis that if analyzed at any single stage, provide an inclusive snapshot of the status of mesodermal development. Furthermore, through this integrated approach, we identified pivotal developmental time points at which key processes occur simultaneously. These data provide the field with the fundamental developmental and morphological guideposts in intestinal mesoderm development upon which variation in organogenesis caused by genetic, experimental and surgical intervention can be compared and further analyzed.

Materials and Methods

Embryos

Quail embryos (*Coturnix coturnix japonicia*) were obtained from Ozark Egg Farm (Stover, Missouri). Tg(*tie1*:H2B-eYFP) quail embryos were a generous gift from Dr. Rusty Lansford (Caltech, Pasadena, CA). All eggs were incubated at 37°C in humidity and staged according to the Japanese quail and the Hamburger Hamilton staging chart (Ainsworth et al., 2010; Hamburger and Hamilton, 1992). Adult intestines were isolated from mature four-month-old wild type quail.

Immunofluorescence

All embryos and tissue were fixed in 4% formaldehyde (Sigma F1635) in PBS (pH 7.4) at room temperature or 4°C depending on tissue size. The samples were washed with PBS (pH 7.4), cryoprotected in 30% sucrose, embedded in OCT (TissueTek 4583) and transversely sectioned (unless otherwise noted) at 5μm. Sections were rehydrated, washed with PBS, and permeabilized with 0.2% Triton-X 100 (Sigma T9284) in PBS for ten minutes, washed with PBS, and blocked in 10% goat serum (Invitrogen 16210-072) + 1% BSA (Sigma A2153) in PBS. Samples were then treated with primary antibodies (see below) overnight at 4°C. Slides were then washed with PBS and incubated with secondary antibodies (see below) for 60 min. at room temperature. Slides were washed and mounted with ProLong Gold mounting agent (Invitrogen P36930).

Antibodies

Primary antibodies: laminin (Abcam ab11575; 1:200), cytokeratin (Abcam ab9377; 1:200), laminin (DSHB, 3H11 and 31 or 31-1; 1:25 (each)), anti-GFP (Invitrogen, A11122; 1:200), anti-αSMA Clone 1A4 (Sigma A2547; 1:200), αSMA (Abcam ab5694; 1:200), γSMA (MP Biomedicals 69133; 1:600). Secondaries: Alexa 488 and 568 (Invitrogen A11001, A11004; 1:500), TOPRO-3 (Invitrogen T3605; 1:1000), DAPI (Invitrogen D3571; 1:10,000).

Microscopy

Immunofluorescence was imaged using an Olympus Fluo-View1000 confocal microscope (Vanderbilt CISR Core). Images were taken in Z-stack format and analyzed using FV-1000, Metamorph and Photoshop software. Images in Figure 7 A-B were taken in Z-stack format on a Zeiss LSM 510 confocal microscope and analyzed in the LSM software. Brightness and contrast of all images were adjusted for visual representation in Photoshop.

Morphometric Analysis

Small intestine sections were stained with laminin antibody and imaged on an EVOS microscope (Joe Roland, Goldenring Lab, Vanderbilt). ImageJ software was used to measure the distance between the outer and endodermal basement membranes of intestines aged E1.9 through E6 (eight to twenty samples analyzed at each stage). The distances were averaged and the standard deviation and standard error of the mean were calculated in Excel. To determine the area of the mesenchymal space, six to ten samples were analyzed for each intestinal region (posterior, middle posterior, middle anterior, anterior) of each intestinal stage including: E8, E10, E12, E14, E16. Metamorph software (Vanderbilt CISR) was utilized to specify the mesenchymal region (area between outer and endodermal basement membranes). Average, standard deviation, and standard error of mean were calculated in Excel. To determine the total length of the intestines, samples were dissected from quail embryos and the mesentery and vessels completely removed. Four to ten samples were measured for each

stage including E6, E8, E10, E12, E14, E16. Averages, standard deviation, and standard error of mean were calculated in Excel.

Results

Establishment and maturation of the major intestinal compartments

As described above, the adult avian intestine has seven concentric tissue layers, six of which are derived from the splanchnic mesoderm. However, there are only two continuous basement membranes within the intestine (one below the mucosal epithelium and the other subjacent to the outer serosal mesothelium) that divide the seven layers into three compartments: the mucosa, the middle connective and muscular tissue (largest component), and the outer serosa (Lefebvre et al., 1999; Simon-Assmann et al., 1995). The intestinal primordium, similar to the adult structure, is divided by two basement membranes (black lines) into three compartments: endoderm (En), mesenchyme/mesenchymal space, and mesoderm/outer epithelium (SpM) (Figure 2.1 A). While subsequent morphogenetic events will greatly increase the complexity of cell and tissue relationships, the arrangement of these basement membranes represent one of the few histological similarities between the embryonic and adult intestine (Figure 2.1).

To determine whether this basic structural relationship is maintained throughout development into adult life, we examined laminin staining throughout development. Laminin is an integral component of basement membranes. At

embryonic day 1.9 (E1.9, equivalent to HH12) in the quail embryo, two basement membranes with solid, uninterrupted laminin staining were identified below the endoderm and the splanchnic mesoderm, respectively (Figure 2.2 A-B, arrowheads). The basement membranes were distinctly separated along the majority of the medial-lateral axis though they did appear to contact one another at discrete points (Figure 2.2 B, arrows). The mesenchymal space was very narrow and sparsely populated with cells (Figure 2.2 B, asterisk). At E2.1 (HH14), laminin staining of the outer basement membrane appeared slightly fragmented (white arrowheads) and in limited, sporadic regions, the mesenchymal space contained a single layer of cells (Figure 2.2 C-D, asterisks). At E2.2 (HH16) and E3 (HH18), the basement membrane underlying the outer epithelium was well dispersed evidenced by discontinuous laminin staining (Figure 2.2 E-F, white arrowheads; data not shown). There were also multiple cell layers within the mesenchyme (Figure 2.2 F, asterisks). At E3.5 (HH21), the anterior and posterior portions of the intestine had folded into a tube while the middle portion remained open ventrally. In both the open and closed regions, the outer epithelial basement membrane had returned to an unbroken configuration (arrowheads) without the large gaps observed in earlier stages (Figure 2.2 G-J). Though continuous, the outer basement membrane was still rough in appearance suggesting E3.5 was a transition point to the smooth, unbroken basement membrane observed at E4 (compare Figure 2.2 G-J to Figure 2.4 E-F).

Between E5 and E6 the gut tube completed ventral closure. At E5 (HH27), the outer epithelial basement membrane was again dispersed (Figure 2.3 A-B,

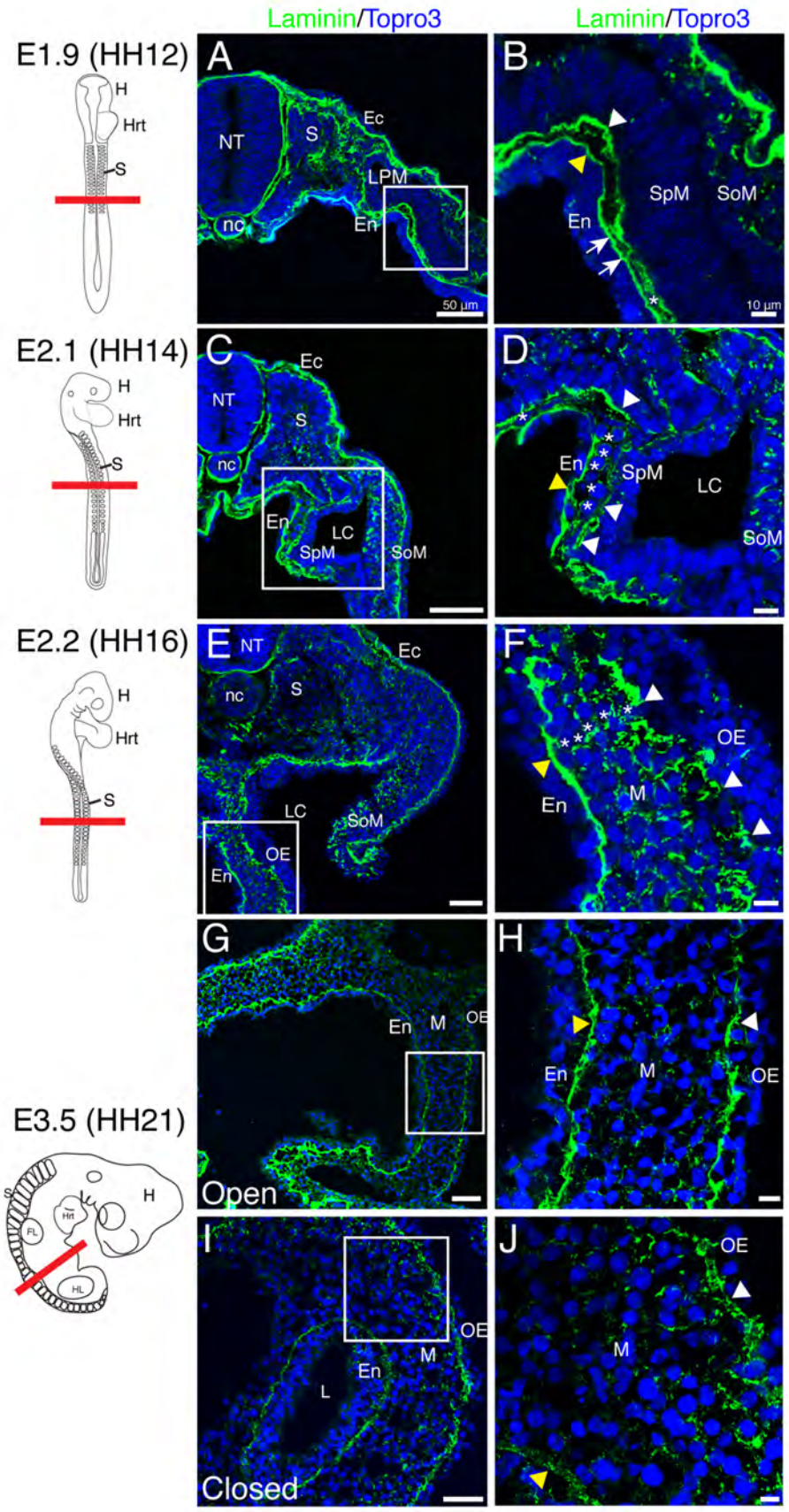
Laminin/Topro3
Laminin/Topro3
E1.9 (HH12)
H
Hrt
S
A
NT
S
Ec
LPM
nc
En
50 µm
B
SpM
SoM
En
10 µm
E2.1 (HH14)
H
Hrt
S
C
Ec
NT
S
nc
En
LC
SpM
SoM
D
En
SpM
LC
SoM
E2.2 (HH16)
H
Hrt
S
E
NT
Ec
nc
S
LC
SoM
OE
En
F
OE
M
En
E3.5 (HH21)
S
H
Hrt
FL
HL
G
En
M
OE
Open
H
En
M
OE
I
OE
M
En
L
Closed
J
OE
M

Figure 2.2 Early basement membrane dynamics in generation of the mesenchymal compartment. Schematics in left column depict quail embryos at the stage isolated and the red line denotes the plane of section. **A-B**: At E1.9, continuous basement membranes (arrowheads) lined the splanchnic mesoderm and endoderm with multiple apparent points of contact (arrows). Asterisk denotes a rare mesenchymal cell. **C-D:** The outer basement membrane (white arrowheads) began to break down at E2.1 and mesenchymal cells were more common (asterisks). The endodermal basement membrane (yellow arrowhead) remained solid. **E-F**: At E2.2, there were multiple mesenchymal cell layers (asterisks) and the outer basement membrane was dispersed (white arrowheads). Yellow arrowhead denotes the endodermal basement membrane. **G-J**: At E3.5, both the outer epithelial (white arrowhead) and endodermal (yellow arrowhead) basement membranes were continuous in the open and closed intestinal regions. Scale bars: 50μm (A, C, E, G, I) and 10μm (B, D, F, H, J). Ec, ectoderm; En, endoderm; FL, forelimb; H, head; Hrt, heart; HL, hindlimb; L, lumen; LC, lateral cavity; LPM, lateral plate mesoderm; M, mesenchyme; nc, notochord; NT, neural tube; OE, outer epithelium; S, somites; SoM, somatic mesoderm; SpM, splanchnic mesoderm.

white arrowhead) but quickly returned to a continuous configuration by E6 (HH29) (Figure 2.3 C-D, white arrowhead). Once solidified at E6, no further changes in the outer epithelial basement membrane were observed through E16. However, the mesenchymal layer underwent dynamic changes over these stages including contributing to villus formation at E10 (Figure 2.3 E-F) and mesenchymal compaction and differentiation (Figure 2.3 G-H). Additionally at E16, laminin staining in the endodermal basement membrane appeared diffuse (Figure 2.3 G-H, yellow arrowhead). Thus, though the outer basement membrane oscillates between discontinuous and continuous states, both basement membranes observed in the intestinal primordium were readily identified throughout development defining the three basic tissue compartments of the intestine.

Development of the outer epithelium

In the adult, the outer epithelium is a simple squamous cell layer, termed mesothelium, that is important for protection of coelomic organs and providing a non-adhesive surface for movement (Mutsaers, 2002; Mutsaers, 2004; Yung and Chan, 2007). We next sought to determine if the periodic dissociation of the outer basement membrane was correlated with differentiation of the outer epithelium into mesothelium. In the embryo and adult, the mesothelium expresses the intermediate filament protein cytokeratin and resides upon a continuous, laminin-enriched basement membrane. A recent lineage tracing study from our laboratory demonstrated that cells within the splanchnic mesoderm of the

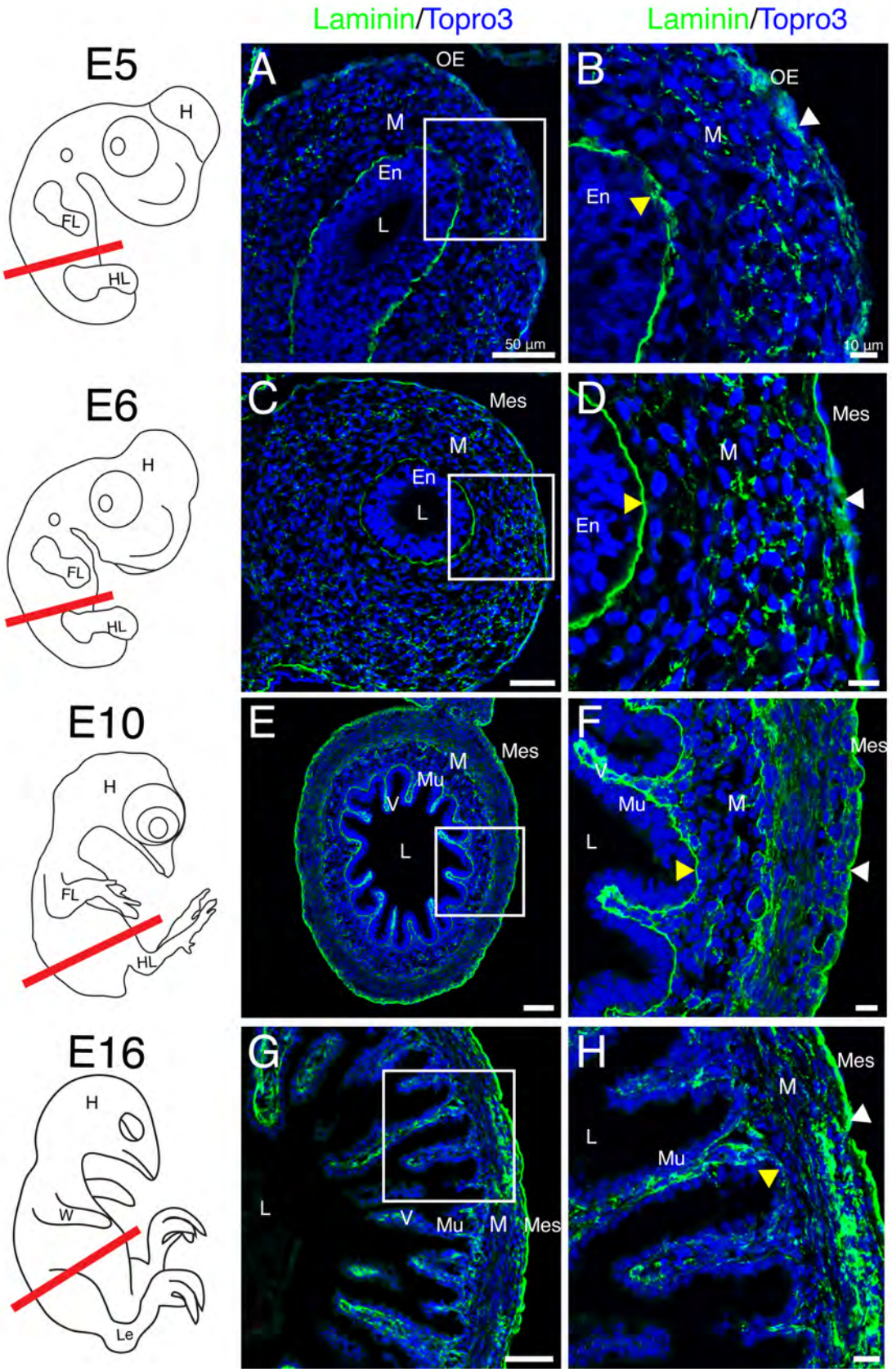
Laminin/Topro3
Laminin/Topro3
E5
E6
E10
E16
H
FL
HL
W
Le
A
B
C
D
E
F
G
H
OE
M
En
L
Mes
Mu
V
50 µm
10 µm

Figure 2.3 Basement membrane dynamics throughout gut tube closure and mesenchymal differentiation. Schematics in left column depict quail embryos at the stage isolated and the red line denotes the plane of section. **A-B**: At E5, the outer epithelial basement membrane appeared dispersed (white arrowhead). Yellow arrowhead denotes the endodermal basement membrane. **C-D**: At E6, both the outer (white arrowhead) and endodermal (yellow arrowhead) basement membranes were unbroken. **E-F**: At E10, villi (V) were present and both basement membranes were continuous (arrowheads). **G-H**: At E16, the mesenchyme was condensed (compare F and H). The outer basement membrane was robust and unbroken (white arrowhead) while the mucosal basement membrane weakly stained with laminin (yellow arrowhead). Scale bars: 50μm (A, C, E, G,) and 10μm (B, D, F, H). En, endoderm; FL, forelimb; H, head; HL, hindlimb; L, lumen; Le, leg; M, mesenchyme; Mes, mesothelium; Mu, mucosa; OE, outer epithelium; V, villi; W, wing.

developing gut tube eventually give rise to the intestinal mesothelium (Winters et al., 2012).

To investigate the development of the outer epithelium, we stained serial sections of quail midgut with antibodies for the epithelial markers cytokeratin and laminin. As described above, the outer epithelium and mesenchyme first appeared as distinct cellular layers at E2.1 (HH14). At this time, the outer epithelium was stratified and the underlying basement membrane was fragmented (see above, Figure 2.2 D). At E3.5 (HH21), the outer epithelium remained stratified and was cytokeratin-negative. Laminin staining in the outer basement membrane (arrows) had returned to an unbroken configuration (Figure 2.4 A-C). Twelve hours later, at E4 (HH24), the outer epithelium was, for the first time, a single cell layer thick (arrowheads) with very faint staining for cytokeratin (Figure 2.4 D-F). At E5 (HH27), we observed more prevalent cytokeratin staining within the outer epithelium despite dispersed laminin staining in the basement membrane (Figure 2.4 G-I, arrowheads). Finally, at E6 (HH29) a simple squamous epithelium with robust cytokeratin staining and a continuous basement membrane (arrows) characteristic of the adult mesothelial structure was present throughout the midgut (Figure 2.4 J-L). This mature mesothelial configuration was observed throughout the remainder of development. Thus, the transition of the basement membrane to an unbroken conformation at E3.5 was followed shortly by conversion of the outer epithelium from a stratified to simple layer. The subsequent breakdown and solidification of the outer basement membrane at

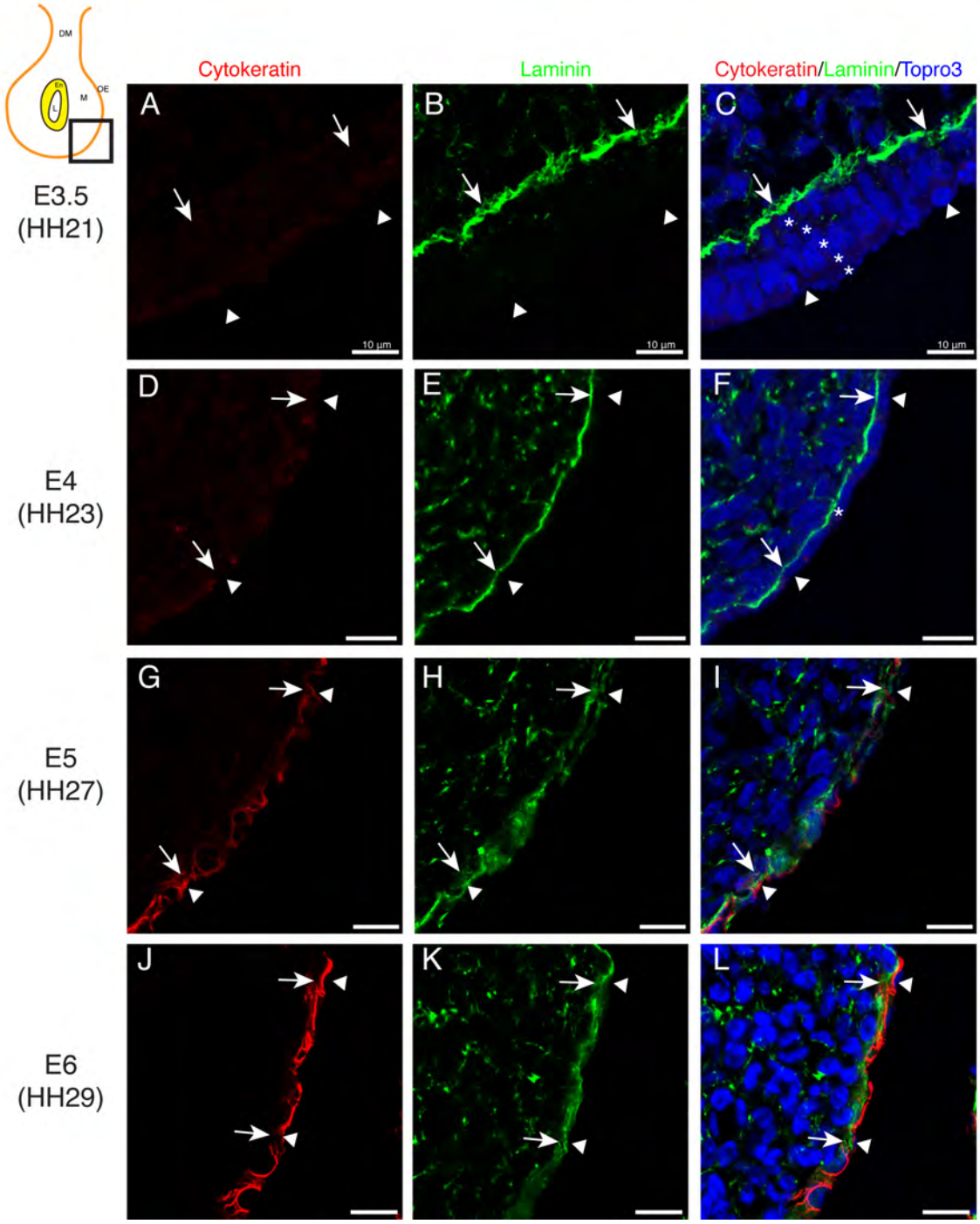
DM
OE
M
E3.5
(HH21)
E4
(HH23)
E5
(HH27)
E6
(HH29)
Cytokeratin
Laminin
Cytokeratin/Laminin/Topro3
A
B
C
D
E
F
G
H
I
J
K
L
10 µm

Figure 2.4 Mesothelial differentiation. Schematic in upper-left corner depicts the region of the gut tube that was imaged. **A-C**: At E3.5, the outer epithelium (arrowheads) was stratified (asterisks) and the basement membrane was continuous (arrows). No cytokeratin staining was evident at this time. **D-F**: At E4, the outer epithelium was a single cell layer thick (arrowheads) with a continuous basement membrane (arrows). Cytokeratin staining was weakly positive. **G-I**: At E5, laminin staining in the outer basement membrane was dispersed (arrows). Cytokeratin staining was present at low levels. **J-L**: At E6, laminin staining (arrows) was unbroken and cytokeratin staining was robust within the mesothelium (arrowheads). Scale bars: 10μm (A-L). DM, dorsal mesentery; En, endoderm; L, lumen; M, mesenchyme; OE, outer epithelium.

E5-E6 was concurrent with differentiation of the outer cell layer into a mature, cytokeratin positive mesothelium.

Expansion of the mesenchymal compartment

As described in Figures 2.2 and 2.3, the mesenchymal compartment underwent a dramatic expansion over these early stages of intestinal development. We next quantified the change in size of the mesenchymal compartment over time to determine if there was any correlation with basement membrane breakdown. We measured the distance between the endoderm and outer epithelial basement membranes at multiple medial-lateral positions to determine the average width of the mesenchymal compartment at each stage. The mesenchymal space at E1.9 (HH12) was narrow, averaging 7.5 μm in width. At E2.1 (HH14), despite the slight increase in the number of cells found in the mesenchymal space at this time, the overall average width was 6.4 μm. Between E2.1-E3.5 (HH14-HH21) the mesenchymal compartment expanded abruptly from 6.4 μm to 103 μm in width. This time period corresponded to the stages over which the outer basement membrane was broken down. Interestingly, after the basement membrane solidified again at E3.5, the distance between the two basement membranes decreased to 74 μm by E4. The second instance of outer basement membrane breakdown at E5 also correlated with a small increase in mesenchymal compartment width though generally the mesenchymal width trended downward between E3.5 and E6 (Figure 2.5 A).

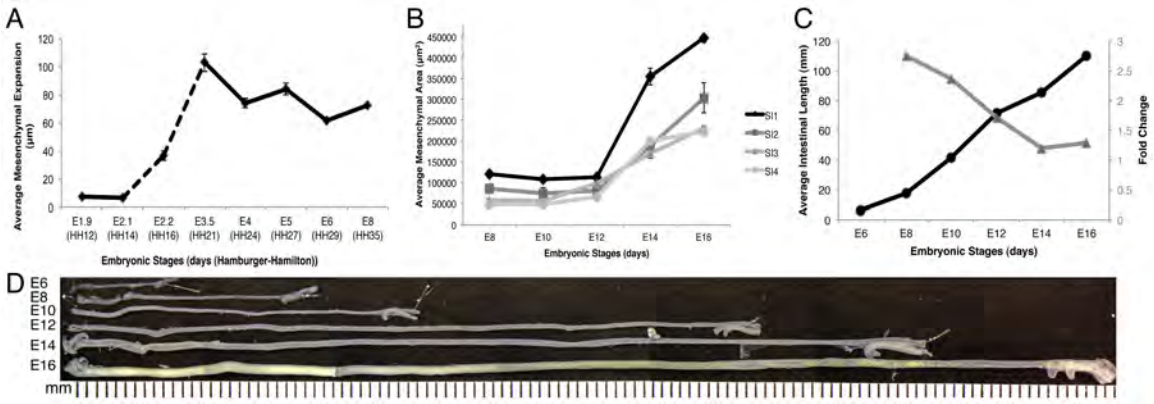

Figure 2.5 Expansion of the mesenchymal compartment over time. A: Graph of the distance between the outer epithelial and endodermal basement membranes measured at key stages between E1.9 and E8. The dashed line represents the time period over which the outer basement membrane was dispersed. Solid lines indicate a continuous outer basement membrane was present. **B**: Four regions along the anterior-posterior axis of the small intestine (SI 1-4) were analyzed individually for mesenchymal cross-sectional area between E8 and E16. The cross-sectional area of each region was graphed independently. **C**: Small intestinal length measured between E6 and E16 (left y-axis, black circles). Fold change in intestinal length over the same time period (right y-axis, grey triangles). **D**: Photomontage of isolated small intestines with mesentery and blood vessels removed and pinned out to demonstrate their length.

Over subsequent stages, the outer basement membrane was solid and the intestinal tube was closed. We next examined mesenchymal cross-sectional area and intestinal length to determine if these variables changed proportionately over time. We quantified mesenchymal cross-sectional area by outlining both the inner and outer basement membranes and calculating the intervening pixels using Metamorph software. We divided the small intestine into quarters along the length of the tube, small intestine (SI) 1-4, and analyzed each region individually at each stage. We also measured the length of the small intestine over the same stages by dissecting away the mesentery and extending the intestine out in a straight line. The anterior regions of the small intestine had consistently larger mesenchymal areas than the posterior regions over all stages examined. Between E8 and E12, the mesenchymal area of each region remained surprisingly constant (Figure 2.5 B). However, there was a dramatic increase in small intestinal length (17.6 mm at E8 to 71.1 mm at E12) over the same time period. Indeed, between E6 and E12, the small intestine roughly doubled in length every two days elongating at an average rate of 11 mm/day (Figure 2.5 C).

Between E12 and E16, there was a notable increase in cross-sectional area throughout all four regions of the small intestine (Figure 2.5 B). There was also an increase in small intestinal length over these stages. The rate of intestinal lengthening between E6 and E16 was relatively steady averaging close to 10 mm/day (Figure 2.5 C, black line). However, this steady rate of growth represented a 4-fold increase in length between E8 and E12 and only a 1.5-fold increase between E12 and E16 (Figure 2.5 C, gray line). Thus, the rapid increase

in mesenchymal cross-sectional area at E12 correlates with a decrease in the relative change in length.

Development of the muscularis layers and myofibroblasts

We next examined differentiation of the mesenchymal compartment. While initially uniform in appearance, the mature mesenchymal compartment is composed of varied tissue types including multiple layers of visceral smooth muscle that provide the force for peristaltic contractions. Other mesenchymal cells with limited contractile ability include the subepithelial myofibroblasts that closely surround the crypts and line the mucosa into the villi. Using studies of the chicken as a reference, we expected four layers of visceral smooth muscle to develop in the quail small intestine: inner longitudinal, inner circular, outer circular, and outer longitudinal (Gabella, 1985; Gabella, 2002). These layers are largely distinguished based on morphological features; however, the outer circular layer of the adult chicken can also be identified molecularly as α-smooth muscle actin (α-SMA) expression is almost entirely replaced by γ-smooth muscle actin (γ-SMA) expression (Gabella, 1985; Yamamoto, 1996).

We utilized immunofluorescence for α- and γ-SMA to generate a comprehensive timeline of visceral smooth muscle and myofibroblast development in the quail small intestine. Faint staining for both α- and γ-SMA was first observed at E6 in a rudimentary circular layer (OC) within the mesenchyme. SMA-negative mesenchymal cells were found on both the luminal

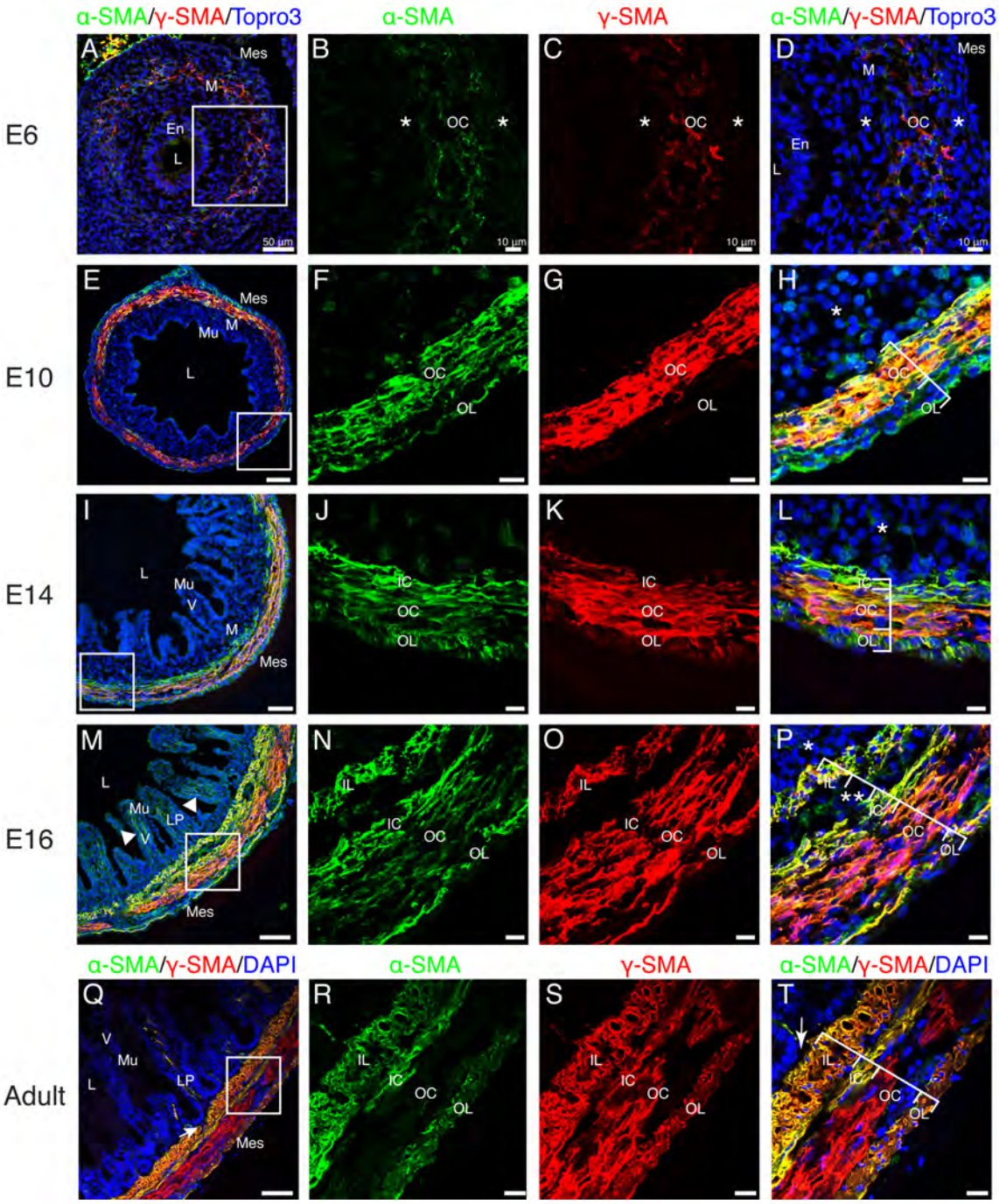
α-SMA/γ-SMA/Topro3
α-SMA
γ-SMA
α-SMA/γ-SMA/Topro3
E6
E10
E14
E16
Adult
α-SMA/γ-SMA/DAPI
α-SMA
γ-SMA
α-SMA/γ-SMA/DAPI
A
B
C
D
E
F
G
H
I
J
K
L
M
N
O
P
Q
R
S
T
Mes
M
En
L
Mu
V
LP
OC
OL
IC
IL
50 μm
10 μm

Figure 2.6 Differentiation of visceral smooth muscle. A-D: At E6, faint staining for α-SMA and γ-SMA defined the outer circular muscle layer. Asterisks represent SMA-negative mesenchymal cells bordering the outer circular muscle layer. **E-H**: Robust staining for α-SMA marked the outer circular and outer longitudinal muscle layers. γ-SMA was observed in the outer circular but not the outer longitudinal layer. SMA-negative submucosal mesenchyme was still present (asterisk). **I-L**: By E14, the inner circular layer (α-SMA-positive, weak γ-SMA) was evident. Asterisk denotes SMA-negative submucosal mesenchyme. **M-P**: At E16, four muscle layers were present including the inner longitudinal layer. All layers stained for both α-SMA and γ-SMA. Double asterisks denote submucosal neuronal plexus. Limited SMA-negative submucosal mesenchyme was present (asterisk). Arrowhead in M indicates SMA-positive staining within the villi. **Q-T**: In the adult intestine, the four visceral smooth muscle layers were directly subjacent to the lamina propria (arrow) with no intervening submucosal mesenchyme. The outer circular layer was α-SMA-negative. Scale Bars: 50μm (A, E, I, M, Q) and 10μm (B-D, F-H, J-L, N-P, R-T). En, endoderm; IC, inner circular; IL, inner longitudinal; LP, lamina propria; L, lumen; M, mesenchyme; Mes, mesothelium; Mu, mucosa; OC, outer circular; OL, outer longitudinal; V, villi.

and coelomic aspects (Figure 2.6 A-D, asterisks). At E10, an α-SMA-positive, γ-SMA-negative outer longitudinal (OL) layer was first observed within the submesothelial region (Figure 2.6 E-H). The inner circular (IC) layer was first distinguishable at E14 due to high levels of α-SMA and low levels of γ-SMA at the innermost aspect of the circular muscle layer (Figure 2.6 I-L). Also at E14, α-SMA-positive cells could occasionally be identified within the villi (data not shown). At E16, an α- and γ-SMA-positive inner longitudinal layer (IL) was visible and robust α-SMA-positive staining was present within the villi. The submucosal mesenchyme was concurrently reduced to a thin layer (asterisk) and the outer circular layer exhibited decreased staining for α-SMA (Figure 6.2 M-P). Finally, in the adult small intestine, γ-SMA was identified in all four layers of visceral smooth muscle but the outer circular layer did not stain for α-SMA at appreciable levels. Additionally, the intestinal crypts were directly adjacent to the inner longitudinal visceral smooth muscle layer without any intervening submucosal mesenchyme (Figure 2.6 Q-T, arrows). Thus, the structure of the adult quail small intestine is similar to other avians, including the chicken (Gabella, 1985). The current study demonstrates that contractile cell differentiation in the quail intestine occurs in the following progression: outer circular layer at E6, outer longitudinal layer at E10, inner circular layer at E14, and inner longitudinal layer and subepithelial myofibroblasts at E16.

The organization of the endothelial plexus

Elaboration of the vasculature is critical for organ formation. The vasculature of the intestine is housed within the mesenchymal layer. The major arteries supplying the intestine (mesenteric arteries) branch from the aorta and reach the intestine by means of a mesentery (two mesothelial membranes closely apposed to one another). Once the mesenteric arteries reach the intestine, the large, muscularized branches stay near the surface subjacent to the thin outer longitudinal layer of visceral smooth muscle. Other branches dive deep to supply a second tier of blood vessels that resides near the junction of the lamina propria and inner longitudinal smooth muscle layer. The third and most expansive tier is the extensive capillary network extending into the villi and localized just below the mucosal epithelium (Powell et al., 2011). The initial arrangement of the intestinal primordium with both basement membranes within microns of one another (at E2.1, (Meier, 1980)) allows a single, central endothelial plexus to contact both basement membranes and epithelia. The expansion of the mesenchyme necessitates growth and remodeling of the vascular plexus for this relationship to be maintained.

To understand how the vasculature of the intestine is remodeled from a single centrally located endothelial plexus into a multi-tiered vascular network, we utilized QH1 (quail endothelial cell marker) staining and Tg(*tie1*:H2B-eYFP) quail embryos. These transgenic embryos express an H2B-eYFP fusion protein under control of the endothelial specific *Tie1* promoter

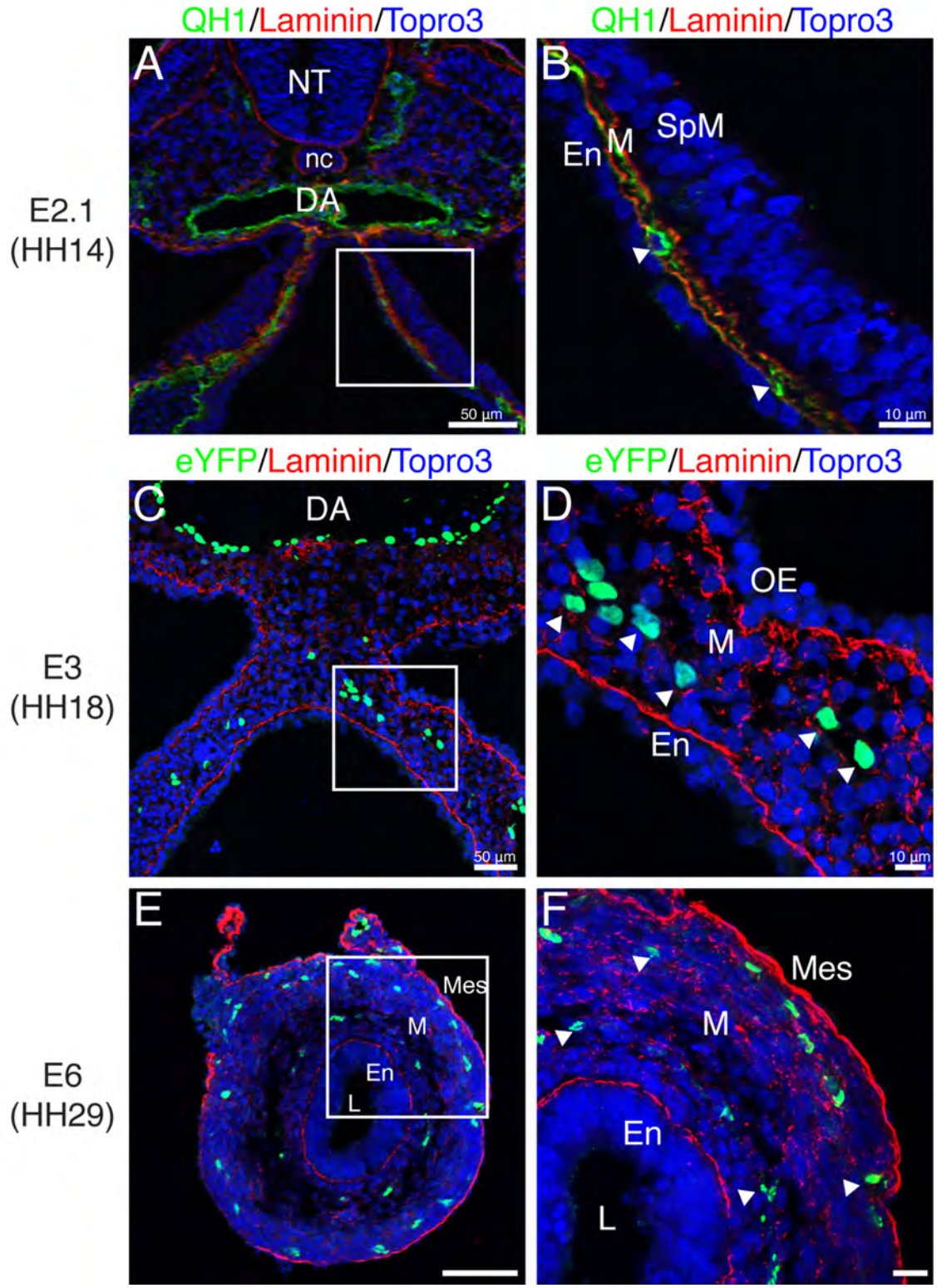
QH1/Laminin/Topro3
QH1/Laminin/Topro3
A
NT
nc
DA
50 µm
B
En
M
SpM
10 µm
E2.1
(HH14)
eYFP/Laminin/Topro3
eYFP/Laminin/Topro3
C
DA
50 µm
D
OE
M
En
10 µm
E3
(HH18)
E
Mes
M
En
L
F
Mes
M
En
L
E6
(HH29)

Figure 2.7 Generation of a two-tiered endothelial plexus. Laminin (basement membrane marker; red), QH1 and eYFP (endothelial markers; green) immunofluorescence. **A-B**: At E2.1, an endothelial plexus marked by QH1 (arrowheads) was present between the endoderm and splanchnic mesoderm. C-F: Sections through Tg(*tie1*:H2B-eYFP) quail intestinal primordia. **C-D**: At E3, the endothelial plexus (arrowheads) was detected in the middle of the multilayered mesenchyme. **E-F**: At E6, the endothelial plexus was organized into two concentric layers below the endoderm and mesothelium, respectively (arrowheads). Scale bars: 50μm (A, C, E) and 10μm (B, D, F). DA, dorsal aorta; En, endoderm; L, lumen; M, mesenchyme; Mes, mesothelium; nc, notochord; NT, neural tube; OE, outer epithelium; SpM, splanchnic mesoderm.

(Poynter and Lansford, 2008; Sato et al., 2010). At E2.1 (HH14), endothelial cells were in close approximation to both the endoderm and splanchnic mesoderm (Figure 2.7 A-B, arrowheads). At E3 (HH18), eYFP-positive endothelial cells were distributed along the medial-lateral axis of the intestinal primordium but remained within the middle of the mesenchymal layer thus losing close contact with both the endodermal and outer epithelial basement membranes (Figure 2.7 C-D, arrowheads). This configuration was maintained until E6 at which time the eYFP-positive cells were organized into two layers one subjacent to the mesothelium and another layer juxtaposed to the developing submucosal layer (Figure 7 E-F, arrowheads). The two tiered endothelial network visible at E6 was also reported in Nagy et al. (2009).

At E10, the external endothelial layer was localized below the newly differentiated outer longitudinal visceral smooth muscle cell layer thus occupying the same space where the major vessels will be found in the adult. At this stage, villi were also first observed in the anterior region of the small intestine (Figure 2.8 A-F) though the posterior region only had small ridges protruding into the lumen (Figure 2.8 G-L). Notably, endothelial cells of the internal plexus (arrowheads) throughout both the anterior and posterior small intestine did not extend into the villi or ridges (Figure 2.8 A-L). We first observed endothelial cells within the villi at E14 in low numbers, four days after villi were apparent in the anterior portion of the gut tube (Figure 2.9 A-C, arrowheads). By E16, endothelial cells were found in abundance within the villi (Figure 2.9 D-F, arrowheads). Cells within the outer endothelial tier became fewer in number over time (Figure 2.9 C,

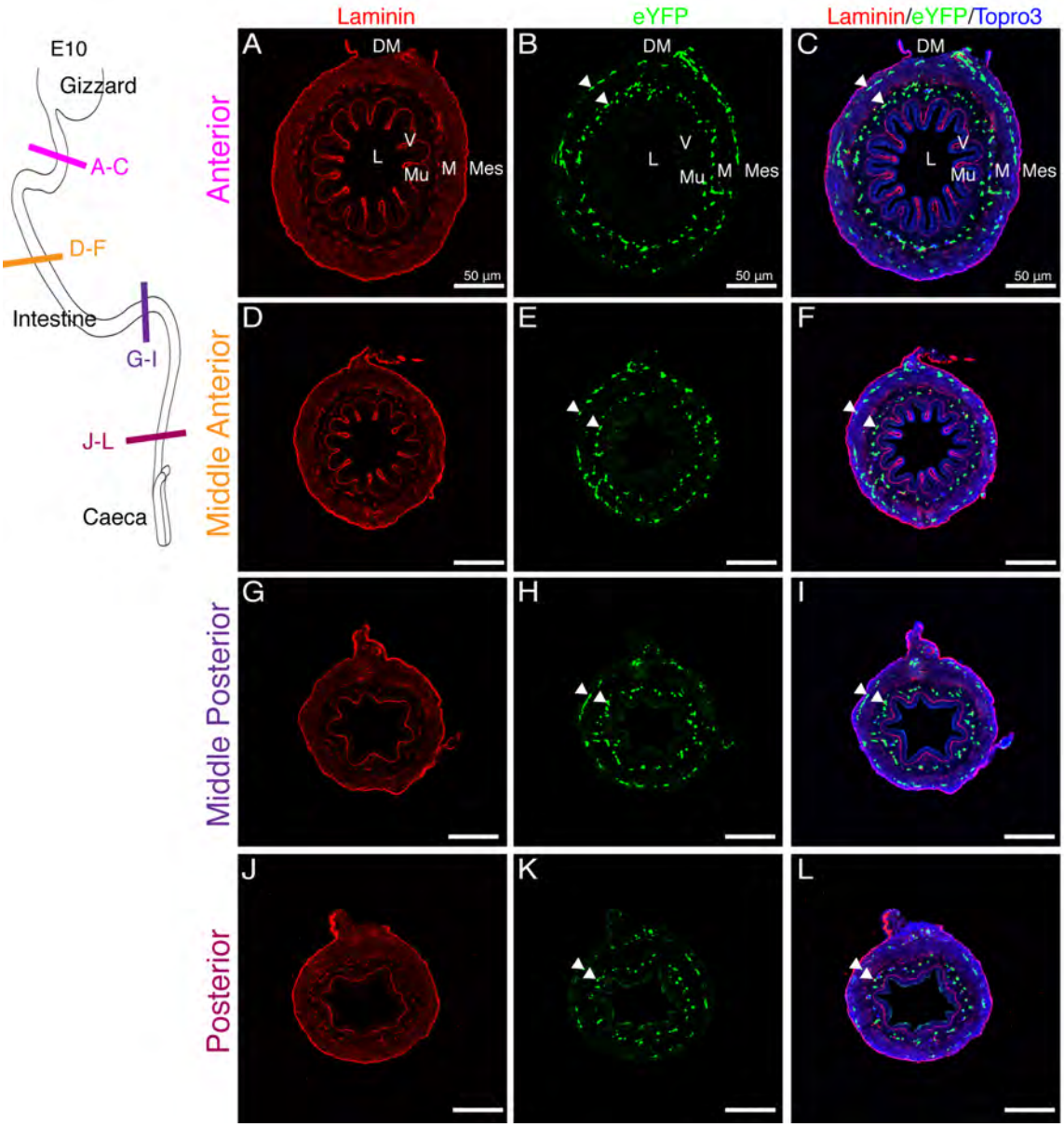

Figure 2.8 Endothelial plexus remodeling during villi formation. Schematic in upper-left corner depicts the regions of the intestine that were sectioned. E10 intestines were isolated from Tg(*tie1*:H2B-eYFP) embryos. **A-F**: Villi were present in the anterior region of the intestine. The endothelial plexus (eYFP-positive) was organized in two concentric rings (arrowheads) but did not extend into the villi. **G-L**: In the posterior small intestine, ridges but no villi were identified. The endothelial plexus remained organized in two concentric rings (arrowheads). Scale bars: 50µm (A-L). DM, dorsal mesentery; L, lumen; M, mesenchyme; Mes, mesothelium; Mu, mucosa, V, villi.

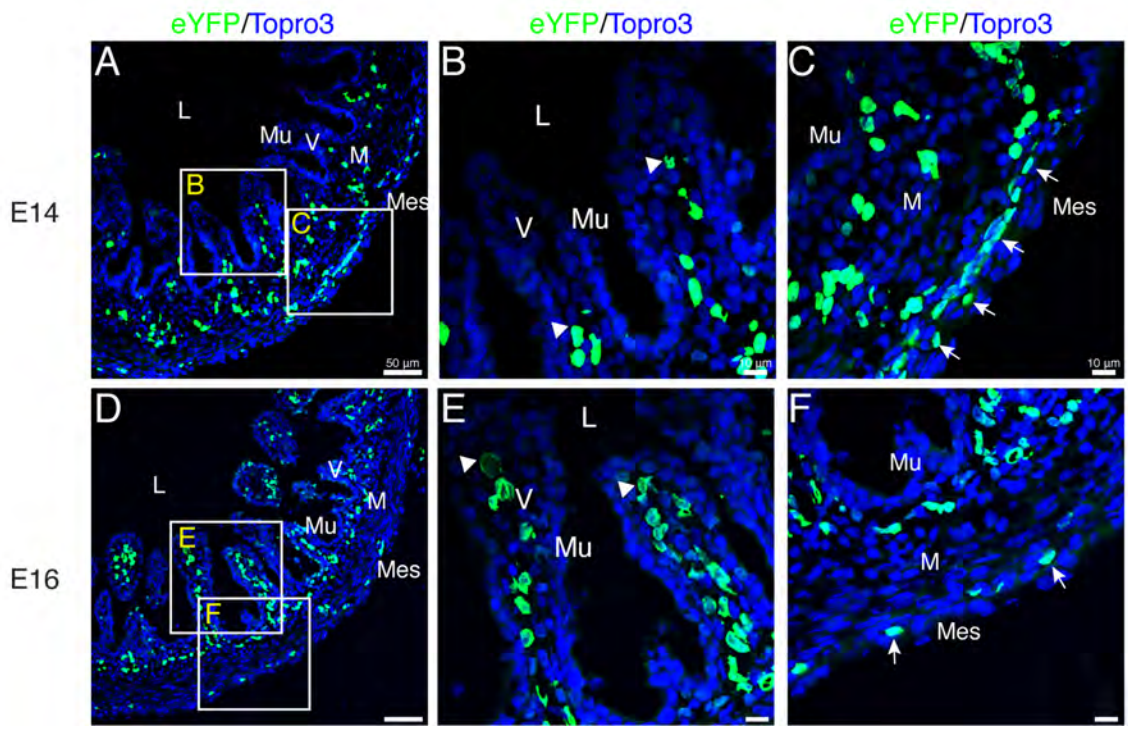

Figure 2.9 Extension of endothelial cells into the villi. Images are of sections through Tg(*tie1*:H2B-eYFP) quail intestines. **A-B**: At E14, eYFP-positive endothelial cells (arrowheads) were localized within the base of the villi in low numbers. **C**: The outer endothelial plexus was substantial at E14 (arrows). **D-E**: By E16, endothelial cells had reached the tip of the villi (arrowheads) and were present in high numbers. **F**: Thinning of the outer endothelial plexus was observed (arrows). Scale bars: 50µm (A, D), 10µm (B-C, E-F). L, lumen; M, mesenchyme; Mes, mesothelium; Mu, mucosa; V, villi.

F, arrows). Thus, development of the enteric endothelial network progresses through four phases. First, endothelial cells are scattered throughout the mesenchymal space. Second, they organize into two layers in the submesothelial region and submucosal mesenchyme, respectively. Third, differentiation of the outer longitudinal smooth muscle leads to localization of the external plexus below the muscle layer. Finally, endothelial cells penetrate the lamina propria of the villi.

Generation of muscularized surface blood vessels

While the vasculature of the villi remains as a capillary plexus, the vessels near the surface of the adult intestine are large caliber and muscularized. We next examined Tg(*tie1*:H2B-eYFP) intestines in whole mount to determine when large surface blood vessels were formed. At E6, the stage at which two distinct layers of endothelial cells were first apparent within the gut wall, there were not any major surface vessels (Figure 2.10 A-B). Instead, endothelial cells were uniformly distributed in a honeycomb-like pattern (Figure 2.10 B). By E10, mesenteric branches extending to the intestine were observed (arrows) though there were still no large vessels visible on the intestine proper (Figure 2.10 C-D). At E11, we first observed large blood vessels extending from the dorsal mesentery over the gut tube proper (Figure 2.10 E-F, arrowheads). Throughout subsequent stages, the major vessels elongated to encompass a greater portion of the intestinal circumference (E12, E13; Figure 2.10 G-J, arrowheads).

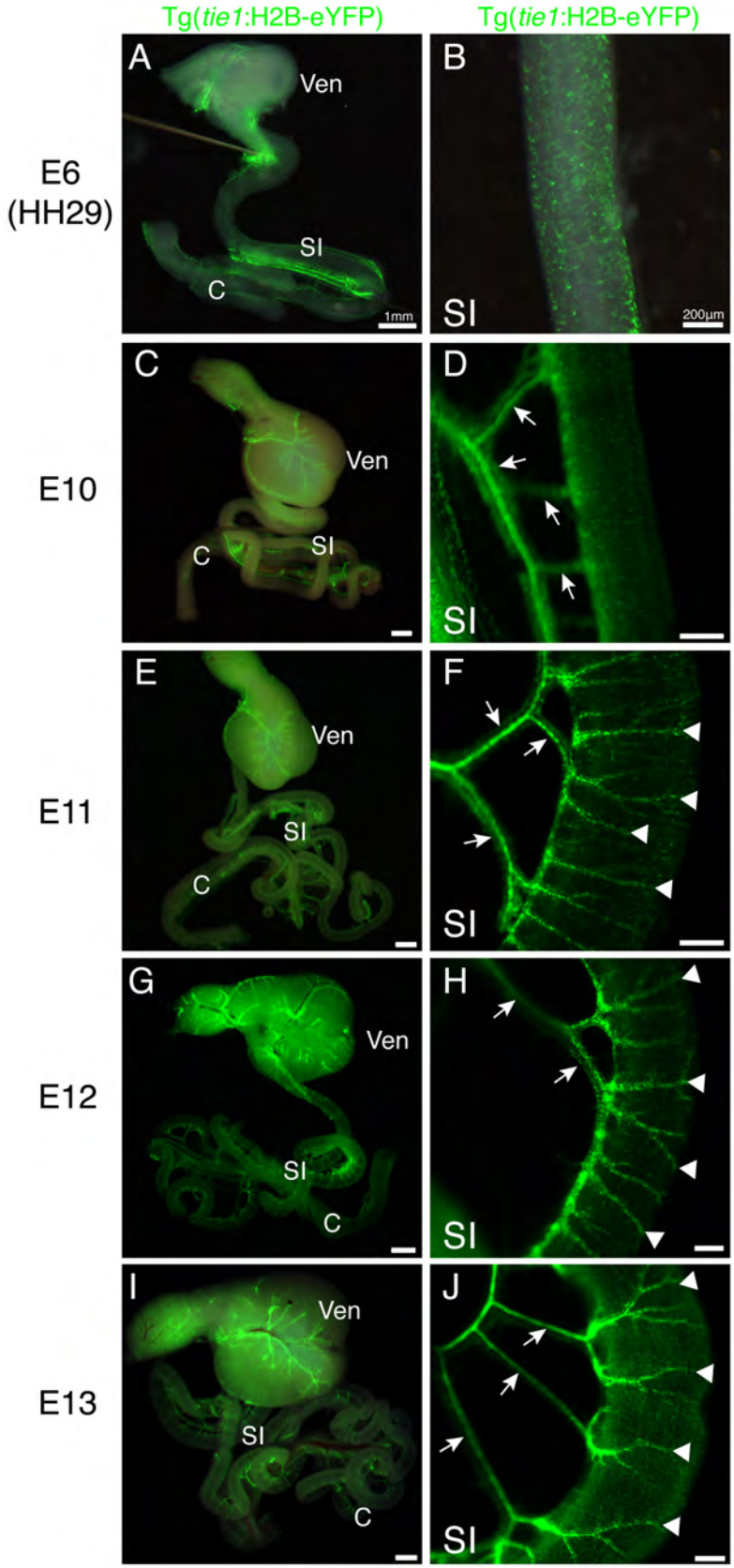
Tg(*tie1*:H2B-eYFP)
Tg(*tie1*:H2B-eYFP)
E6 (HH29)
E10
E11
E12
E13
A
B
C
D
E
F
G
H
I
J
Ven
SI
C
1mm
200μm

Figure 2.10 Development of large blood vessels of the small intestine. All panels are whole mount images of eYFP fluorescence in isolated gut tubes from Tg(*tie1*:H2B-eYFP) quail. **A-B**: At E6, eYFP-positive endothelial cells were evident in the wall of the small intestine in a honeycomb pattern. **C-D**: At E10, mesenteric vessels were visible (arrows) but large vessels on the small intestine proper were not observed. **E-F**: At E11, major vessels near the surface of the small intestine were present (arrowheads) extending from the mesentery (arrows). **G-J**: Major small intestinal vessels (arrows) displayed further branching at E12 and E13 (arrowheads). Scale bars: 1mm (A, C, E, G, I); 200μm (B, D, F, H, J). C, caeca; SI, small intestine; Ven; ventriculus.

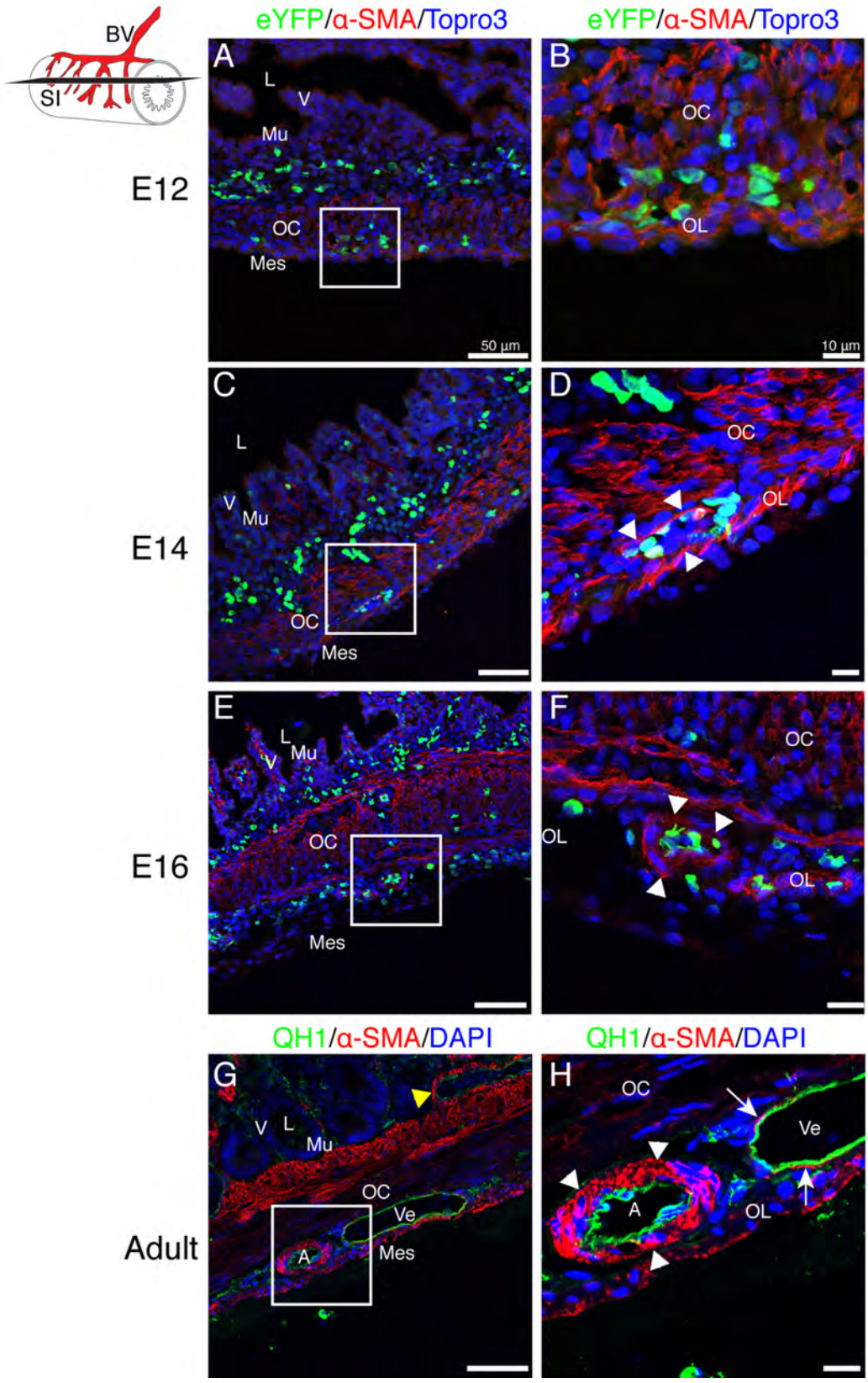
BV
SI
eYFP/α-SMA/Topro3
eYFP/α-SMA/Topro3
A
B
L
V
Mu
OC
Mes
50 μm
OL
10 μm
E12
C
D
L
V
Mu
OC
Mes
OL
E14
E
F
L
Mu
V
OC
Mes
OL
OL
E16
QH1/α-SMA/DAPI
QH1/α-SMA/DAPI
G
H
V
L
Mu
OC
Ve
A
Mes
OC
Ve
A
OL
Adult

Figure 2.11 Muscularization of small intestinal blood vessels. Schematic in upper-left corner represents the small intestine (SI), blood vessels (BV) and the orientation of sections (black slice). A-F: Sections from Tg(*tie1*:H2B-eYFP) intestines. **A-B**: At E12, eYFP-positive endothelial cells subjacent to the coelomic surface were in close proximity to the visceral smooth muscle layers (OC, OL) but were not invested by vascular smooth muscle cells. **C-D**: At E14, vascular smooth muscle cells (α-SMA-positive, arrowheads) arranged in a single layer were identified surrounding eYFP-positive endothelial cells localized near the coelomic surface of the small intestine. **E-F**: At E16, the vascular smooth muscle cells appeared more mature and were in multiple layers surrounding endothelial cells (arrowheads). **G-H**: QH1 staining of a wild type adult quail small intestine revealed mature vessels with multiple layers of vascular smooth muscle cells in large arteries (arrowheads) but only a single layer in veins (arrows). The second tier of blood vessels at the base of the villi was also muscularized in the adult (yellow arrowhead). Scale bars: 50μm (A, C, E, G) and 10μm (B, D, F, H). A, artery; L, lumen; Mes, mesothelium; Mu, mucosa; OC, outer circular muscle layer; Ve, vein; V, villi.

A further mark of blood vessel maturity is recruitment and differentiation of vascular smooth muscle cells. We used immunofluorescence for α-SMA to determine when cells of the intestinal vasculature were muscularized. At E12, α-SMA staining was present within the outer longitudinal and outer circular smooth muscle layers but was not identified surrounding the eYFP-positive endothelial cells (Figure 2.11 A-B). At E14, a single layer of α-SMA-positive cells surrounded the large blood vessels found near the surface of the intestine (Figure 2.11 C-D, arrowheads). At E16, rare blood vessels were observed containing multiple layers of vascular smooth muscle cells (Figure 2.11 E-F, arrowheads). In the adult intestine, large arteries with multiple layers of vascular smooth muscle were readily identified (Figure 2.11 G-H, arrowheads). Neighboring veins were large caliber though still poorly muscularized (Figure 2.11 G-H, arrows). Additionally, the second tier of blood vessels near the base of the villi were muscularized in the adult only (Figure 2.11 G, yellow arrowhead). Thus, the major blood vessels of the intestine are not muscularized until near hatching.

Discussion

Splanchnic mesoderm generates the bulk of the intestine and will diversify into serosa, connective tissue, musculature, and the enteric vasculature. However, relatively little is known about the development of the intestinal mesoderm. Our study provides a comprehensive examination of the major morphological changes that occur within the intestinal mesoderm starting with the

establishment of the intestinal primordium and ending with the definitive structure. Through concurrent examination of multiple features, we were able to identify temporal and spatial coordination between previously unlinked developmental events (Table 2.1). An examination of four critical time periods in intestinal mesoderm development is presented below highlighting novel correlations illustrated by this study. These data provide developmental biologists and clinicians with a detailed baseline of normal development—the context with which perturbations of intestinal development generated by experimental manipulation and disease can be evaluated. Finally, this comprehensive analysis reveals heretofore unidentified cell and tissue relationships that generate numerous questions for future study.

Appearance of the intestinal anlage.

Although not immediately apparent, the eventual architecture of the mature intestine is in fact represented in three features of the intestinal primordium. At the most fundamental level, the endoderm is localized ventrally and the mesoderm, dorsally in the flat intestinal anlage. Thus, when a tube is formed by folding the flat sheet ventrally, the endoderm will line the lumen and the mesoderm will form the coelomic surface reflecting their position in the adult structure. Second, the primordium is split into three compartments by two basement membranes, an arrangement maintained into maturity. Finally, from its earliest appearance, the vascular plexus is localized in the mesenchymal compartment juxtaposed to both basement membranes (Meier, 1980). These

Table 1. Key stages and pivotal developmental events that occur throughout quail intestine development

E1.9 (HH12)	E2.2 (HH16)	E3.5 (HH21)	E4 (HH23)	E5 (HH27)	E6 (HH29)
• Continuous outer basement membrane • Narrow mesenchymal space • Single layered endothelial plexus • Open gut tube (GT)	• Dispersed outer basement membrane • Scattered mesenchymal cells • Single endothelial plexus • Open GT	• Continuous outer basement membrane • Multilayered mesenchyme • Peak in mesenchymal width • Stratified outer epithelium • Anterior and posterior closure of GT	• Continuous outer basement membrane • Contraction of mesenchymal width • Single layered outer epithelium	• Dispersed outer basement membrane • Increased mesenchymal width • Cytokeratin-positive outer epithelium	• Continuous outer basement membrane • Decreased mesenchymal width • Mesothelium • Completely closed GT • Endothelial plexus splits into two layers • Outer circular muscle layer • Length: 6mm
E10	**E11**	**E12**	**E14**	**E16**	
• Villi present • Outer longitudinal muscle layer • Absence of SMA-negative submesothelial mesenchyme • Length: 42mm	• Large surface blood vessels	• Sharp increase in mesenchymal area • Length: 72mm	• Endothelial cells in base of villi • Myofibroblasts in lamina propria • Inner circular muscle layer • Single layer of vascular smooth muscle • Length: 85mm	• Endodermal basement membrane dispersed • Endothelial cells in tips of villi • Inner longitudinal muscle layer • Multilayered vascular media • Limited submucosal mesenchyme • Length: 110mm	

basic elements form the structural scaffold around which the flat sheet of the primordium folds to form a tube. Within this context, the mesenchymal space and its resident cells expand to generate the largest intestinal compartment, and the vasculature matures into a multi-tiered network.

Development of the mesenchymal compartment: E1.9-E5

Starting from this basic structure, the first significant change in intestinal mesoderm development is the generation of a multi-layered mesenchyme. Though forming the bulk of the intestine in the adult, this layer is essentially absent in the primordium—the endothelial plexus of the intestine is the only cell population to reside in the mesenchymal compartment and contacts the basement membranes of both the endoderm and splanchnic mesoderm. The rapid cellular expansion of the mesenchymal compartment between E2.2 and E3.5 occurred concurrently with a breakdown of the outer basement membrane likely due to an ingress of cells from the outer epithelium into the mesenchyme. At E3.5, the mesenchymal compartment peaked in width and the outer epithelial basement membrane returned to an unbroken configuration. Throughout the subsequent stages in which a solid basement membrane was present the width of the mesenchymal compartment gradually decreased. A slight increase in mesenchymal width was observed at E5, which correlated with a second brief breakdown of the outer epithelial basement membrane. These features suggest the following sequence: inward migration of cells from the outer epithelium into the mesenchyme, cessation of migration and repair of the basement membrane,

a second wave of inward migration, and final repair of the basement membrane. The potential of two temporally separated waves of migration into the mesenchymal space may indicate that specific mesenchymal lineages are added sequentially as suggested but not conclusively proven by cell lineage tracing studies (Wilm et al., 2005; Winters et al., 2012).

Completion of intestinal tube formation: E5-E6

The next major change in intestinal development is the completion of tube formation that occurs at E6. At this stage, the mesothelium is fully differentiated, SMA is first observed in the outer circular visceral smooth muscle layer and the endothelial plexus splits into two layers. Each of these topics is considered below.

Mesothelial differentiation in the intestine has only recently been studied in any detail (Kawaguchi et al., 2007; Wilm et al., 2005; Winters et al., 2012). In contrast, mesothelial development in the heart has been examined extensively. Cardiac mesothelium is derived from a localized, extrinsic progenitor pool that migrates to the heart. Once at the surface of the heart, individual mesothelial cells undergo an epithelial-mesenchymal transition (EMT) to invade the underlying myocardium and give rise to vascular smooth muscle cells and intracardiac fibroblasts (Dettman et al., 1998; Guadix et al., 2006; Männer, 1999; Mikawa and Gourdie, 1996; Pérez-Pomares et al., 2002). Mesothelial cells of the intestine have a similar potential demonstrated by genetic lineage tracing in the mouse but are derived from a broadly distributed progenitor population intrinsic to the forming gut tube (Wilm et al., 2005). The second brief breakdown of the outer

basement membrane of the intestine occurred as the outer epithelium differentiated into a mesothelial layer. Thus, the second wave of inward migration into the mesenchyme may be specific to mesothelial cells or their progenitors providing cells of the future vascular or fibroblast lineage. The molecular regulation of EMT of the cardiac mesothelium has been investigated utilizing multiple murine genetic models (Baek and Tallquist, 2012; Wu et al., 2010). It may be of interest to examine these genetic models in the context of intestinal development to determine if a similar molecular network regulates EMT of mesothelia in the two organs.

In addition to contributing cells, mesothelium is also a signaling center during development (Olivey and Svensson, 2010; Svensson, 2010; White, 2006). The first visceral smooth muscle layer of the intestine differentiates in close proximity to the mesothelium with only a small layer of intervening SMA-negative cells. Endodermal Shh signals are known to be repressive to visceral smooth muscle differentiation in the chick thus positioning the initial layer at a distance from the mucosa (Gabella, 2002; Sukegawa et al., 2000). However, both *Shh* and *Ihh* knockouts in the mouse led to reduced visceral smooth muscle differentiation suggesting the role of Shh is not repressive alone (Mao et al., 2010; Ramalho-Santos et al., 2000). Intestinal mesothelial signaling has not been investigated though frequently, developmental patterning is the result of integration of signals from two opposing sources (Irish et al., 1989; Meinhardt, 2009). Precise positioning of the initial circular muscle layer and subsequent layers of smooth muscle may be the result of both endodermal and mesothelial

signaling events though further investigation is required.

The endothelial plexus also divides into two layers at E6 (Nagy et al., 2009). Signals that pattern the intestinal vasculature are currently unknown. As cells are added to the mesenchyme, the endothelial plexus remains centrally located with increasing distance separating it from both basement membranes; thus, hypoxia might be proposed as a potential regulatory signal. However, quantification of the width of the mesenchymal compartment revealed there is actually a decrease in the distance separating the two basement membranes between E3.5 and E6. Thus, division of the endothelial plexus into two layers at this time may not be related simply to increased hypoxia due to mesenchymal growth. The division into two layers that reside near the mesothelial and mucosal surface, respectively, suggests chemotactic cues may originate from both epithelia to produce this pattern though further research is needed in this area.

Maturation of visceral smooth muscle and vascular components: E6-E16

The next major changes that occur within the mesenchymal compartment include differentiation of the remaining visceral smooth muscle cell layers, vascular remodeling and maturation, and extensive growth. It is unknown what directs the sequential differentiation of individual visceral smooth muscle cell layers though, as described above, roles for both the endoderm and mesothelium are possible. Interestingly, the appearance of the villi is temporally associated with generation of the outer circular and outer longitudinal visceral smooth muscle cell layers suggesting a potential mechanical relationship.

In studies of murine intestinal development, endothelial cells appear to play an important role in villus formation and remain in close association with the endoderm throughout (Hashimoto et al., 1999; Kim et al., 2007). In the quail, villi form independent of a close morphological relationship with the vasculature. Indeed, endothelial cells do not invade the villi until days after they are formed. The cues leading to endothelial ingrowth into the villi are unknown. Also of potential interest, subepithelial myofibroblasts differentiate concurrent with endothelial migration into villi. Endothelial cells in endodermally-derived organs function in paracrine signaling independent of their function in supplying vascular flow to an area (Jacquemin et al., 2006; Lammert et al., 2001; Matsumoto et al., 2001; Yoshitomi and Zaret, 2004). Thus, regulation of villus maturation and myofibroblast differentiation may be related to signaling events from the nearby endothelial cells.

Finally, while the endothelial plexus of the intestinal primordium is thought to be derived from the splanchnic mesoderm (Drake et al., 1997; Meier, 1980; Pardanaud et al., 1989), the origin of the large surface blood vessels is unclear. They are first visible in the mesentery and subsequently over the intestine suggesting they may grow via angiogenesis from the vitelline artery. Alternatively, they may be derived completely from remodeling of the existing endothelial plexus.

As detailed above, there remains much to be understood about intestinal development. Knowledge of the morphological underpinnings is vital if investigations of intestinal formation are to be placed into the larger context in

which they occur. These studies provide a timeline of intestinal mesodermal development integrating information about multiple foundational features. With a broad view of intestinal development, potential interactions can be identified that range from the level of gene function, through cellular interactions, to tissue morphogenesis leading to the establishment of the definitive structure.

References

Ainsworth, S. J., Stanley, R. L. and Evans, D. J. R. (2010). Developmental stages of the Japanese quail. *J Anat* **216**, 3-15.

Appelman, H. D. (2011). Morphology of gastrointestinal stromal tumors: Historical perspectives. *J Surg Oncol* **104**, 874-881.

Baek, S. T. and Tallquist, M. D. (2012). Nf1 limits epicardial derivative expansion by regulating epithelial to mesenchymal transition and proliferation. *Development* **139**, 2040-2049.

Burns, A. J., Roberts, R. R., Bornstein, J. C. and Young, H. M. (2009). Development of the enteric nervous system and its role in intestinal motility during fetal and early postnatal stages. *Semin Pediatr Surg* **18**, 196-205.

Coulombre, A. J. and Coulombre, J. L. (1958). Intestinal development. I. Morphogenesis of the villi and musculature. *J Embryol Exp Morphol* **6**, 403-411.

Dauça, M., Bouziges, F., Colin, S., Kedinger, M., Keller, M. K., Schilt, J., Simon-Assmann, P. and Haffen, K. (2007). Development of the vertebrate small intestine and mechanisms of cell differentiation. *Int J Dev Biol* **34**, 205-218.

Dettman, R. W., Denetclaw, W., Ordahl, C. P. and Bristow, J. (1998). Common epicardial origin of coronary vascular smooth muscle, perivascular fibroblasts, and intermyocardial fibroblasts in the avian heart. *Dev Biol* **193**, 169-181.

Drake, C. J., Brandt, S. J., Trusk, T. C. and Little, C. D. (1997). TAL1/SCL is expressed in endothelial progenitor cells/angioblasts and defines a dorsal-to-ventral gradient of vasculogenesis. *Dev Biol* **192**, 17-30.

Eddinger, T. J. (2009). Unique contractile and structural protein expression in dog ileal inner circular smooth muscle. *J Smooth Muscle Res* **45**, 217-230.

Gabella, G. (1985). Structure of the musculature of the chicken small intestine. *Anat Embryol (Berl)* **171**, 139-149.

Gabella, G. (2002). Development of visceral smooth muscle. *Results Probl Cell Differ* **38**, 1-37.

Grey, R. D. (1972). Morphogenesis of intestinal villi. I. Scanning electron microscopy of the duodenal epithelium of the developing chick embryo. *J Morphol* **137**, 193-213.

Grosse, A. S., Pressprich, M. F., Curley, L. B., Hamilton, K. L., Margolis, B., Hildebrand, J. D. and Gumucio, D. L. (2011). Cell dynamics in fetal intestinal epithelium: implications for intestinal growth and morphogenesis. *Development* **138**, 4423-4432.

Guadix, J. A., Carmona, R., Muñoz-Chápuli, R. and Pérez-Pomares, J. M. (2006). In vivo and in vitro analysis of the vasculogenic potential of avian proepicardial and epicardial cells. *Dev Dyn* **235**, 1014-1026.

Guzman, M. A., Prasad, R., Duke, D. S. and De Chadarévian, J.-P. (2011). Multiple intestinal atresias associated with angiodysplasia in a newborn. *J Pediatr Surg* **46**, 1445-1448.

Hamburger, V. and Hamilton, H. L. (1992). A series of normal stages in the development of the chick embryo. 1951. *Dev Dyn* **195**, 231-272.

Hashimoto, H., Ishikawa, H. and Kusakabe, M. (1999). Development of vascular networks during the morphogenesis of intestinal villi in the fetal mouse. *Kaibogaku zasshi. J Anat* **74**, 567-576.

Heanue, T. A. and Pachnis, V. (2007). Enteric nervous system development and Hirschsprung disease: advances in genetic and stem cell studies. *Nat Rev Neurosci* **8**, 466-479.

Hiramatsu, H. and Yasugi, S. (2004). Molecular analysis of the determination of developmental fate in the small intestinal epithelium in the chicken embryo. *Int J Dev Biol* **48**, 1141-1148.

Hirota, S., Isozaki, K., Y, M., Hashimoto, K., Nishida, T., Ishiguro, S., Kawano, K., Hanada, M., Kurata, A., Takeda, M., Muhammad Tunio, G., Matsuzawa, Y., Kanakura, Y., Shinomura, Y. and Kitamura, Y. (1998). Gain-of-function mutations of c-kit in human gastrointestinal stromal tumors. *Science* **279**, 577-580.

Huss, D., Poynter, G. and Lansford, R. (2008). Japanese quail (Coturnix japonica) as a laboratory animal model. *Lab Anim (NY)* **37**, 513-519.

Irish, V., Lehmann, R. and Akam, M. (1989). The Drosophila posterior-group gene nanos functions by repressing hunchback activity. *Nature* **338**, 646-648.

Jacobson, L. F. and Noer, R. J. (1952). The vascular pattern of the intestinal villi in various laboratory animals and man. *Anat Rec* **114**, 85-101.

Jacquemin, P., Yoshitomi, H., Kashima, Y., Rousseau, G. G., Lemaigre, F. P. and Zaret, K. S. (2006). An endothelial-mesenchymal relay pathway regulates early phases of pancreas development. *Dev Biol* **290**, 189-199.

Kawaguchi, M., Bader, D. M. and Wilm, B. (2007). Serosal mesothelium retains vasculogenic potential. *Dev Dyn* **236**, 2973-2979.

Kim, K. E., Sung, H.-K. and Koh, G. Y. (2007). Lymphatic development in mouse small intestine. *Dev Dyn* **236**, 2020-2025.

Lammert, E., Cleaver, O. and Melton, D. (2001). Induction of pancreatic differentiation by signals from blood vessels. *Science* **294**, 564-567.

Lefebvre, O., Sorokin, L., Kedinger, M. and Simon-Assmann, P. (1999). Developmental expression and cellular origin of the laminin alpha2, alpha4, and alpha5 chains in the intestine. *Dev Biol* **210**, 135-150.

Louw, J. H. and Barnard, C. N. (1955). Congenital intestinal atresia; observations on its origin. *Lancet* **269**, 1065-1067.

Madison, B. B., Braunstein, K., Kuizon, E., Portman, K., Qiao, X. T. and Gumucio, D. L. (2005). Epithelial hedgehog signals pattern the intestinal crypt-villus axis. *Development* **132**, 279-289.

Männer, J. (1999). Does the subepicardial mesenchyme contribute myocardioblasts to the myocardium of the chick embryo heart? A quail-chick chimera study tracing the fate of the epicardial primordium. *Anat Rec* **255**, 212-226.

Mao, J., Kim, B.-M., Rajurkar, M., Shivdasani, R. A. and Mcmahon, A. P. (2010). Hedgehog signaling controls mesenchymal growth in the developing mammalian digestive tract. *Development* **137**, 1721-1729.

Matsumoto, K., Matsumoto, K., Yoshitomi, H., Rossant, J. and Zaret, K. S. (2001). Liver organogenesis promoted by endothelial cells prior to vascular function. *Science* **294**, 559-563.

Mazur, M. T. and Clark, H. B. (1983). Gastric stromal tumors. Reappraisal of histogenesis. *Am J Surg Pathol* **7**, 507-519.

Mchugh, K. M. (1995). Molecular analysis of smooth muscle development in the mouse. *Dev Dyn* **204**, 278-290.

Meier, S. (1980). Development of the chick embryo mesoblast: pronephros, lateral plate, and early vasculature. *J Embryol Exp Morphol* **55**, 291-306.

Meinhardt, H. (2009). Models for the generation and interpretation of gradients. *Cold Spring Harb Perspect Biol* **1**, a001362.

Mikawa, T. and Gourdie, R. G. (1996). Pericardial mesoderm generates a population of coronary smooth muscle cells migrating into the heart along with ingrowth of the epicardial organ. *Dev Biol* **174**, 221-232.

Milgrom-Hoffman, M., Harrelson, Z., Ferrara, N., Zelzer, E., Evans, S. M. and Tzahor, E. (2011). The heart endocardium is derived from vascular endothelial progenitors. *Development* **138**, 4777-4787.

Mitjans, M., Barniol, G. and Ferrer, R. (1997). Mucosal surface area in chicken small intestine during development. *Cell Tissue Res* **290**, 71-78.

Mutsaers, S. E. (2002). Mesothelial cells: their structure, function and role in serosal repair. *Respirology* **7**, 171-191.

Mutsaers, S. E. (2004). The mesothelial cell. *Int J Biochem Cell Biol* **36**, 9-16.

Nagy, N., Mwizerwa, O., Yaniv, K., Carmel, L., Pieretti-Vanmarcke, R., Weinstein, B. M. and Goldstein, A. M. (2009). Endothelial cells promote migration and proliferation of enteric neural crest cells via beta1 integrin signaling. *Dev Biol* **330**, 263-272.

Newgreen, D. and Young, H. M. (2002). Enteric nervous system: Development and developmental disturbances--Part 1. *Pediatr Dev Pathol* **5**, 224-247.

Olivey, H. E. and Svensson, E. C. (2010). Epicardial-myocardial signaling directing coronary vasculogenesis. *Circ Res* **106**, 818-832.

Pardanaud, L., Yassine, F. and Dieterlen-Lievre, F. (1989). Relationship between vasculogenesis, angiogenesis and haemopoiesis during avian ontogeny. *Development* **105**, 473-485.

Pérez-Pomares, J.-M., Carmona, R., González-Iriarte, M., Atencia, G., Wessels, A. and Muñoz-Chápuli, R. (2002). Origin of coronary endothelial cells from epicardial mesothelium in avian embryos. *Int J Dev Biol* **46**, 1005-1013.

Powell, D. W., Pinchuk, I. V., Saada, J. I., Chen, X. and Mifflin, R. C. (2011). Mesenchymal cells of the intestinal lamina propria. *Annu Rev Physiol* **73**, 213-237.

Poynter, G. and Lansford, R. (2008). Generating transgenic quail using lentiviruses. *Methods Cell Biol* **87**, 281-293.

Ramalho-Santos, M., Melton, D. A. and Mcmahon, A. P. (2000). Hedgehog signals regulate multiple aspects of gastrointestinal development. *Development* **127**, 2763-2772.

Sanders, K. M. (1996). A case for interstitial cells of Cajal as pacemakers and mediators of neurotransmission in the gastrointestinal tract. *Gastroenterology* **111**, 492-515.

Sato, Y., Poynter, G., Huss, D., Filla, M. B., Czirók, A., Rongish, B. J., Little, C. D., Fraser, S. E. and Lansford, R. (2010). Dynamic analysis of vascular morphogenesis using transgenic quail embryos. *PloS one* **5**, e12674.

Savin, T., Kurpios, N. A., Shyer, A. E., Florescu, P., Liang, H., Mahadevan, L. and Tabin, C. J. (2011). On the growth and form of the gut. *Nature* **476**, 57-62.

Simon-Assmann, P., Kedinger, M., De Arcangelis, A., Rousseau, V. and Simo, P. (1995). Extracellular matrix components in intestinal development. *Experientia* **51**, 883-900.

Spence, B., Lauf, R. and Shroyer, N. (2011). Vertebrate intestinal endoderm development. *Dev Dyn* **240**, 501-520.

Streutker, C. J., Huizinga, J. D., Driman, D. K. and Riddell, R. H. (2007). Interstitial cells of Cajal in health and disease. Part I: normal ICC structure and function with associated motility disorders. *Histopathology* **50**, 176-189.

Sukegawa, A., Narita, T., Kameda, T., Saitoh, K., Nohno, T., Iba, H., Yasugi, S. and Fukuda, K. (2000). The concentric structure of the developing gut is regulated by Sonic hedgehog derived from endodermal epithelium. *Development* **127**, 1971-1980.

Svensson, E. C. (2010). Deciphering the signals specifying the proepicardium. *Circ Res* **106**, 1789-1790.

Wells, J. M. and Melton, D. A. (1999). Vertebrate endoderm development. *Annu Rev Cell Dev Biol* **15**, 393-410.

White, A. C. (2006). FGF9 and SHH signaling coordinate lung growth and development through regulation of distinct mesenchymal domains. *Development* **133**, 1507-1517.

Wilm, B., Ipenberg, A., Hastie, N. D., Burch, J. B. E. and Bader, D. M. (2005). The serosal mesothelium is a major source of smooth muscle cells of the gut vasculature. *Development* **132**, 5317-5328.

Winters, N. I., Thomason, R. T. and Bader, D. M. (2012). Identification of a novel developmental mechanism in the generation of mesothelia. *Development* **139**, 2926-2934.

Wu, M., Smith, C. L., Hall, J. A., Lee, I., Luby-Phelps, K. and Tallquist, M. D. (2010). Epicardial spindle orientation controls cell entry into the myocardium. *Dev Cell* **19**, 114-125.

Yamamoto, Y., Kubota, T, Atoji, Y, Suzuki, Y. (1996). Distribution of alpha-vascular smooth muscle actin in the smooth muscle cells of the gastrointestinal tract of the chicken. *J Anat* **189**, 623.

Yoshitomi, H. and Zaret, K. S. (2004). Endothelial cell interactions initiate dorsal pancreas development by selectively inducing the transcription factor Ptf1a. *Development* **131**, 807-817.

Young, H., Bergner, A., Anderson, R., Enomoto, H., Milbrandt, J., Newgreen, D. and Whitington, P. (2004). Dynamics of neural crest-derived cell migration in the embryonic mouse gut. *Dev Biol* **270**, 455-473.

Young, H. M. and Newgreen, D. (2001). Enteric neural crest-derived cells: origin, identification, migration, and differentiation. *Anat Rec* **262**, 1-15.

Yung, S. and Chan, T. M. (2007). Mesothelial cells. *Perit Dial Int* **27 Suppl 2**, S110-115.

Zorn, A. M. and Wells, J. M. (2009). Vertebrate endoderm development and organ formation. *Annu Rev Cell Dev Biol* **25**, 221-251.

CHAPTER III

IDENTIFICATION OF A NOVEL DEVELOPMENTAL MECHANISM IN THE GENERATION OF MESOTHELIA

This chapter was accepted by *Development* on 22 May 2012 under the same title by the following authors:

Nichelle I. Winters, Rebecca T. Thomason, David M. Bader

Abstract

Mesothelium is the surface layer of all coelomic organs and critical for the generation of their vasculature. Still, our understanding of the genesis of this essential cell type is restricted to the heart where a localized, exogenous population of cells, the proepicardium, migrates to and envelops the myocardium supplying mesothelial, vascular, and stromal cell lineages. Currently it is unknown whether this pattern of development is specific to the heart or applies broadly to other coelomic organs. Using two independent long term lineage tracing studies, we demonstrate that mesothelial progenitors of the intestine are intrinsic to the gut tube anlage. Furthermore, a novel chick-quail chimera model of gut morphogenesis reveals these mesothelial progenitors are broadly distributed throughout the gut primordium and are not derived from a localized and exogenous proepicardium-like source of cells. These data demonstrate an

intrinsic origin of mesothelial cells to a coelomic organ and provide a novel mechanism for the generation of mesothelial cells.

Introduction

The vertebrate coelom, or body cavity, and internal organs housed therein are all lined by a simple squamous epithelium called mesothelium. In the healthy adult, mesothelia are relatively quiescent—their primary function is to form a non-adhesive surface for the movement of organs (Mutsaers and Wilkosz, 2007). However, mesothelia are also recognized as critical players in peritoneal sclerosis (Chegini, 2008; Yung and Chan, 2009), for regulation of the injury microenvironment in myocardial infarction (Zhou et al., 2011) and for their ability to promote revascularization of diverse tissues including the heart (Takaba et al., 2006; Zhang et al., 1997). These functions of mesothelium in injury and repair reflect the dynamic behavior of mesothelia in embryonic development. While mesothelia are universally distributed in the pericardial, pleural and peritoneal cavities of all vertebrates, our understanding of mesothelial development is largely restricted to one organ, the heart.

Manasek (1969) and Ho and Shimada (1978) demonstrated that cardiac mesothelium (epicardium) originated from a discrete population of cells termed the proepicardium (PE) localized outside of the initial heart tube (Ho and Shimada, 1978; Manasek, 1969). Originating from the region of the sinus venosus, these cells migrate as an epithelium across the pericardial space to

contact the naked myocardium (Ishii et al., 2010). Further dorsal-ventral migration of this epithelium over the heart tube leads to formation of the epicardium. Thus, epicardial precursors do not arise in situ but are recruited from a localized cell source exogenous to the splanchnic mesoderm of the developing organ.

Subsequent lineage tracing studies revealed that specific cells within the epicardium undergo epithelial-mesenchymal transition (Wu et al., 2010), invade the myocardium, and differentiate into fibroblasts, vascular smooth muscle, and endothelial cell populations (Dettman et al., 1998; Mikawa and Gourdie, 1996). Hepatic, pulmonary, and intestinal mesothelia have since been shown to provide vasculogenic and stromal populations to their respective organs (Asahina et al., 2011; Eralp et al., 2005; Morimoto et al., 2010; Perez-Pomares et al., 2004; Que et al., 2008; Wilm et al., 2005).

Wilm et al. demonstrated that the mesothelial marker *Wilms' tumor protein 1 (Wt1)* first appeared in the mesentery of the intestine and then later encompassed the gut tube in a dorsal-ventral direction. This expression pattern mirrored the dorsal-ventral migration of the epicardium seen in the heart and, from these data, our group hypothesized that "non-resident cells migrate to and over the gut to form the serosal mesothelium" (Wilm et al., 2005). These data in conjunction with the shared vasculogenic potential of mesothelia suggested the mechanism of mesothelial development and the function of this cell type in embryogenesis may be conserved in diverse coelomic cavities.

In contrast to the extensive analysis of epicardial development, careful

examination of the primary literature reveals that little if anything is known about the origin of mesothelial cells in any coelomic organ other than the heart. Additionally, a change in terminology contributes to confusion in the literature regarding this cell type. The term “mesothelium” originally referred to the entire epithelial component of mesoderm as differentiated from the loose mesenchyme (Minot, 1890). The term did not refer to the specific simple squamous cell type we currently identify as mesothelium. Still, a review authored by Minot in 1890 using this original terminology appears to form the basis for the modern description on the origin of vertebrate coelomic mesothelia (Moore and Persaud, 1998; Mutsaers, 2002). An extensive review of the literature reveals no primary data addressing the origin of mesothelium. Taken together, it is clear that the program of proepicardial/epicardial development stands alone as a definitive model of development of this widely distributed cell type that is so critical for vertebrate organogenesis.

A question arises: Is there a common mechanism of mesothelial development? Fundamental to the resolution of this question is determining the origin of mesothelial precursors in diverse coelomic organs. Thus, we examined intestinal development to determine whether mesothelium originated from an exogenous, localized source as seen in the heart or, conversely a resident population of mesothelial progenitors within the gut itself. Using three independent experimental models, we demonstrate that the intestine derives its mesothelial layer from progenitor cells broadly resident within the splanchnic mesoderm and not from a PE-like structure extrinsic to the developing organ.

These data provide new information concerning a fundamental process of intestinal development and reveal diversity in mechanisms regulating the generation of mesothelia.

Materials and Methods

In situ hybridization (ISH)

ISH was performed according to standard protocols (McGlinn and Mansfield, 2011). *Wt1* template (GenBank accession number AB033634.1) was kindly provided by Dr. Jorg Manner (Georg-August University of Gottingen, Germany) (Schulte et al., 2007).

Immunohistochemistry (IHC) and co-localization analysis

Immunohistochemical analysis of sectioned chick (Gallus gallus) or quail (Coturnix japonica) embryos was as published (Osler and Bader, 2004). All animal procedures were performed in accordance with institutional guidelines and IACUC approval. Chick embryos were staged according to Hamburger and Hamilton (Hamburger and Hamilton, 1992). The following primary antibodies were used: Anti-GFP (Invitrogen A11122, 1:200); Anti-laminin (Abcam Ab11575, 1:50); Anti-Laminin (DSHB 31 or 31-2 1:25); Anti-neurofilaments (DSHB RT97 1:50); Anti-smooth muscle actin (Sigma A2547 1:200), Anti-smooth muscle actin (Abcam Ab5694 1:200), QCPN (DSHB undiluted), 8F3 (DSHB 1:25), Anti-PGP9.5 (Zymed 38-1000, 1:200); Anti-cytokeratin (Abcam Ab9377, 1:100), QH1

(DSHB, 1:200). The following secondary antibodies were used at a 1:500 dilution: Alexa fluor 488 or 568 Goat anti-rabbit (Invitrogen); Alexa fluor 488 or 568 Goat anti-mouse (Invitrogen). TOPRO-3 (Invitrogen T3605) at 1 μmol/L was applied for 20 min. Sections were imaged in Z-stacks using a LSM510 META Confocal with 0.4 μm optical slices. Each optical slice was analyzed for co-localization of the red and green channels using ImageJ followed by Z-projection for counting of cells. All IHC images presented in figures are Z-projections.

Microinjection

Windowed chick embryos (HH14-17) were lightly stained by placing a dried strip of neutral red (0.2 mg/mL) in 1% agar on top of the embryo. For contrast, 0.2 uL of 10% fast green solution (sterile filtered) was added to 5 μl viral or pCIG suspension (7 μg/μL) and then loaded into a pulled glass needle. The agar strip was removed and approximately 25-30 nanoliters were injected into both lateral cavities with aid of a micromanipulator and use of a Narishige IM300 microinjector with 2msec pulses at 38PSI.

Electroporation

pCIG-GFP in which GFP expression is driven by the chicken β-actin promoter was kindly provided by Dr. Michael Stark (Brigham Young University, Provo, UT, USA) (Lassiter et al., 2007). Chick eggs incubated 2.5 days were windowed by withdrawing 4 ml of albumin and cutting a hole in the top of the egg shell. The vitelline membrane over the posterior region of windowed HH14-HH17

embryos was removed with a tungsten needle. After pCIG-GFP microinjection, a small hole was made outside of the vascularized region through which the positive electrode was inserted below the embryo. The negative electrode was placed on top of the embryo and 5-7, 10 msec pulses at 15 V were delivered (ECM 830 electroporator; BTX Harvard Apparatus). After addition of Tyrode's salts solution with 1% pen/strep, the eggs were resealed with tape and incubated 8 days.

Production of pSNID retrovirus

The following plasmids were used: pSNID with both a GFP and βgal reporter a generous gift of Dr. Jeanette Hyer (UCSF, San Francisco, CA, USA) (Venters et al., 2008); pCI-VSVG (Addgene 1733); pCAGGS Gag/Pol (generous gift of Dr. Connie Cepko, Harvard University, Cambridge, MA, USA). Virus was produced in Phoenix-GP cells. PheonixGP cells (ATCC SD-3514) were grown to 70-80% confluence in DMEM supplemented with 10% FBS and split 1:3 onto four, 10 cm plates the night prior to transfection. Media was exchanged prior to transfection. For each plate, 4 ug DNA (2 ug pSNID, 1 ug VSV-G, 1 ug Gag/pol) was diluted in 100 uL serum free DMEM. To the DNA suspension, 24 uL PEI (1 mg/mL PEI, pH7; MW25K, Polysciences Inc 23966-2) was added, mixed by vortexing, incubated 15 min at room temperature, added to the cells overnight. Media was exchanged, media collected after 24 hrs, and stored at -80°C. 5 ml new media was added, media collected at 48 hrs, pooled with 24 hr collection, syringe filtered (0.45 micrometer PES) and concentrated by ultracentrifugation

(SW-28 rotor, 18000 RPM, 43000 x g, 2 hours, 4°C). Supernatant was discarded and the ultracentrifuge tube drained by inverting for 60 sec. The viral pellet was resuspended in media that remained in the ultracentrifuge tube (~50-80 uL). Polybrene (Sigma H9268) was added to the viral suspension at final concentration of 100 ug/mL. After microinjection, infected cells were detected by GFP expression in whole mount using a fluorescent dissecting microscope or in section by staining with an anti-GFP antibody.

Titer assay

D17 cells were grown to 60% confluence in 6-well plates. Fresh media (DMEM + 7% FBS + 1% penicillin/streptomycin) with 10 µg/ml polybrene was added to the plates prior to infection. Concentrated viral suspension was serially diluted and added to the 6-well plates. At 48 hrs, cells were stained with Xgal to detect viral infection. The total number of positive clones in a well were counted to determine the total number of virions added. Viral titers reaching at least 10^7 virions/mL were aliquoted and stored at -80°C.

Generation of chick-quail chimeras

Splanchnopleure was dissected away from quail embryos staged 14-17. Dissection was carried out in sterile Tyrode's salt solution. Isolated splanchnopleure was bisected into anterior and posterior regions by cutting at the vitelline artery and then anterior and posterior splanchnopleure was further subdivided into 3-4 pieces. Chick embryos in windowed eggs were lightly stained

with a strip of neutral red in agar. The vitelline membrane was removed with a tungsten needle and a small hole made through the somatopleure over the vitelline artery. The quail splanchnopleure graft was transferred into the chick egg and pushed through the hole with forceps and a tungsten needle into the right lateral cavity. Tyrode's salt solution with 1% penicillin/steptomycin was added to replace volume and eggs were then sealed with tape and incubated for 1-14 days. The number of graft and host derived mesothelial cells was determined by analyzing a subset of graft-derived gut tubes at multiple levels. The mesothelial layer was distinguished by morphology combined with cytokeratin or laminin staining. Nuclei within the mesothelial layer were manually identified and then subsequently identified as either QCPN or 8F3 positive.

Results

Trilaminar organization of the intestine is established prior to tube formation

The adult intestine is composed of three subdivisions or compartments: the inner mucosa with an underlying basement membrane, the middle "mesenchymal" layers harboring stromal and visceral smooth muscle cells, and the outer mesothelium with its own basement membrane. We used immunohistochemical staining for cytokeratin, an intermediate filament expressed by epithelia, and laminin, a component of basement membranes, to examine the intestine for establishment of these three compartments. By close examination of formation of these compartments, we sought to identify any

potential mesothelial progenitor population within the gut tube either of a proepicardial-like morphology or any other tissue arrangement.

The splanchnopleure posterior to the heart tube of chick embyos was examined at early stages of intestinal morphogenesis, prior to gut tube closure. At the earliest stage examined, HH13, the splanchnopleure was bilaminar composed of endoderm and splanchnic mesoderm with almost no intervening mesenchymal cells (Figure 1 A-C, arrowhead). Each layer was individually underlain by a laminin-positive basement membrane that extended along the entire dorsal-ventral axis of the splanchnopleure (Figure 1 A-C, arrows).

At HH15, the splanchnopleure transitioned from having two major compartments to three. This was due to the establishment of a mesenchymal layer between the two basement membranes of the splanchnopleure (Figure 1 D-F). For ease of reference, we termed the three compartments endoderm, mesenchyme, and outer epithelium though at this time the outer epithelium does not express cytokeratin (Figure 3.1 F'). The transition to three compartments occurred evenly throughout the splanchnopleure, and no localized PE-like structure was observed throughout the entirety of the peritoneal cavity. The outer epithelium remained stratified/pseudostratified, was underlain by a fragmented basement membrane (yellow arrow) and formed a uniform layer over the mesenchyme (Figure 3.1 D-F). With the appearance of the mesenchymal layer, the splanchnopleure was now in a trilaminar configuration which, as described above, is the basic organization of the adult intestine. The mesenchymal layer

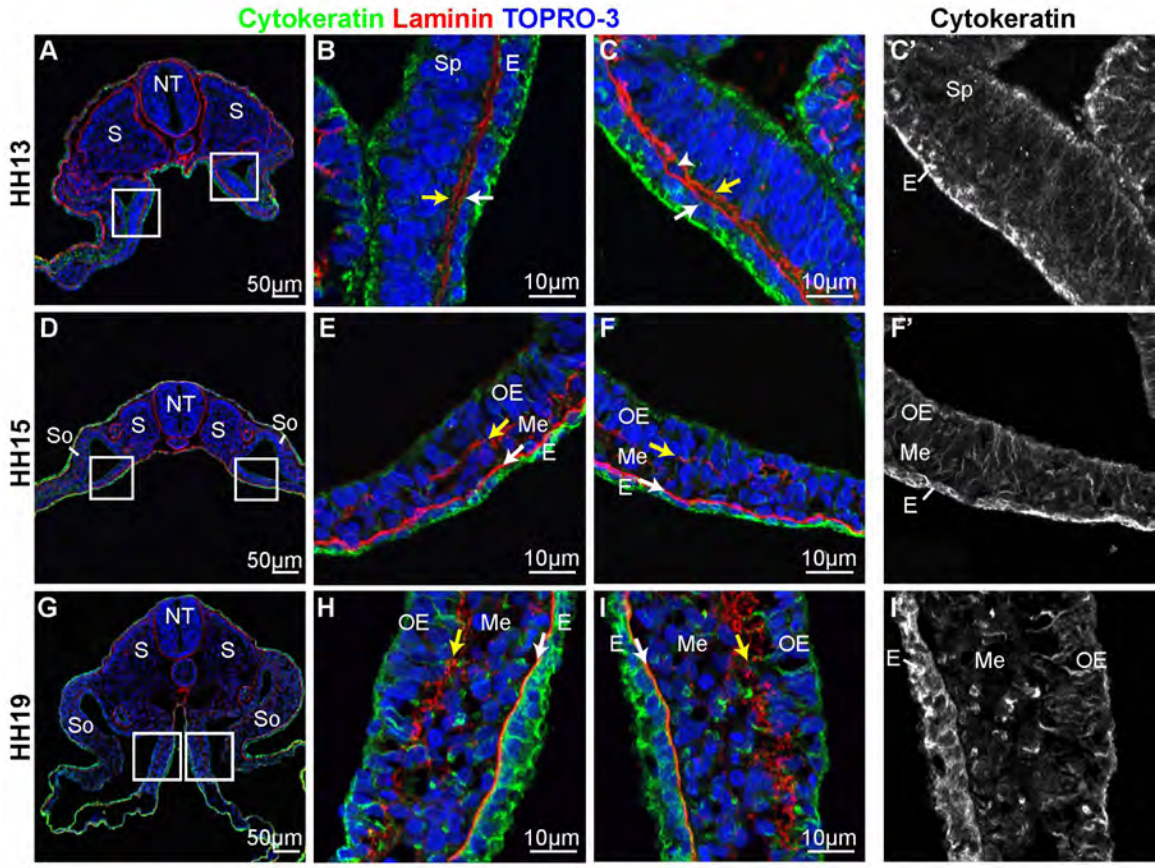

Figure 3.1 A trilaminar gut tube was generated by HH15. A: HH13 splanchnopleure was composed of two layers. **B-C**: Boxed regions shown in A). The splanchnic mesoderm appeared stratified and was underlain by a basement membrane (yellow arrow). The endoderm had its own basement membrane (white arrow). Arrowhead in C indicates a single mesenchymal cell. **C'**: The endoderm but not the splanchnic mesoderm was cytokeratin positive at HH13. **D-F**: At HH15, a mesenchymal layer was observed residing between the aforementioned basement membranes (arrows). **F'**: The outer epithelium was not cytokeratin positive at HH15. **G-I**: At HH19 the mesenchymal layer had expanded (space between two arrows) and the basement membrane of the outer epithelium had fragmented (outer arrow). **I'**: The endoderm but not the outer epithelium was cytokeratin positive. E, endoderm; Me, mesenchyme; NT, neural tube; OE, outer epithelium; S, somite; So, somatic mesoderm; Sp, splanchnic mesoderm.

expanded through HH19 and the basement membrane of the outer epithelium remained fragmented (Figure 3.1 G-I, yellow arrow). The mesothelial marker *Wt1* was, however, not expressed specifically in the outer epithelium at these stages though *Wt1* staining was observed in the mesothelial component of the PE over the same period of time (Figure 3.2). Four days after the initial appearance of the outer epithelium (HH29, day 6) the layer attained the simple squamous morphology and robust cytokeratin expression of a definitive mesothelium (Figure 3.3 A-D). Thus, the three compartments of the intestine including a potential mesothelial progenitor layer, the outer epithelium, are established very early in development prior even to intestinal tube formation.

Mesothelial progenitors are resident to the splanchnic mesoderm

As a first step in identifying the origin of mesothelial progenitors, it was necessary to determine whether the outer epithelium was derived from resident cells of the splanchnic mesoderm layer or a migratory progenitor population undetected by the analyses described above. Thus, we devised a method to label and trace cells of the splanchnic mesoderm over time. A reporter plasmid expressing green fluorescent protein (GFP) from the chick β-actin promoter was injected into the lateral cavities of HH14 chick embryos, the stage prior to establishment of the mesenchymal layer (Figure 3.4 A). Microinjection was followed by electroporation with the electrodes oriented directly above and below the embryo to direct the DNA ventrally into the splanchnic mesoderm.

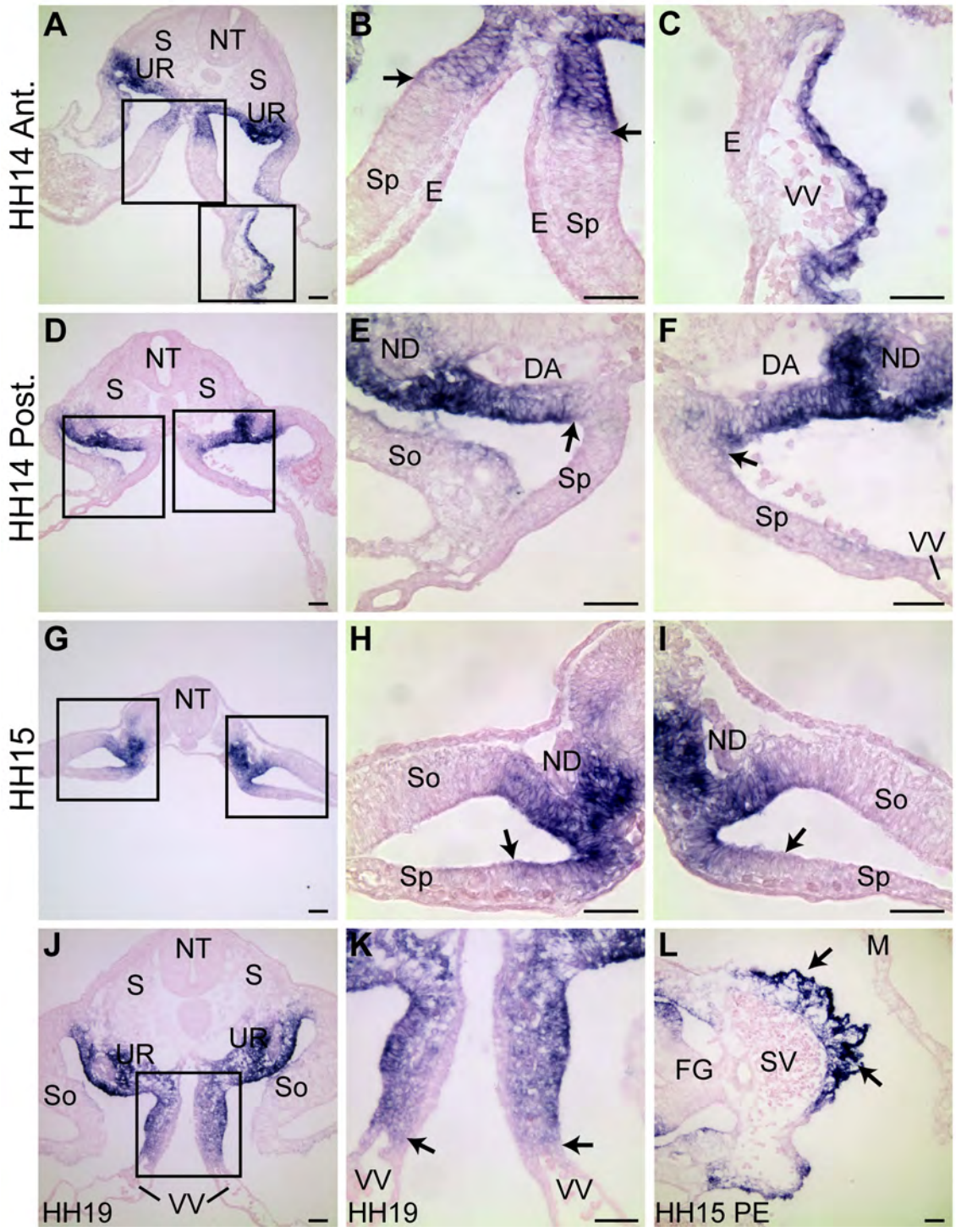
HH14 Ant.
HH14 Post.
HH15
A
S
NT
UR
S
UR
B
Sp
E
E
Sp
C
E
VV
D
NT
S
S
E
ND
DA
So
Sp
F
DA
ND
Sp
VV
G
NT
H
So
ND
Sp
I
ND
So
Sp
J
NT
S
S
UR
UR
So
So
VV
HH19
K
VV
VV
HH19
L
M
FG
SV
HH15 PE

Figure 3.2 In situ hybridization for *Wt1*. Nephric precursors and the urogenital ridge expressed Wt1 at all stages examined (HH13-HH19). Arrows denote the ventral boundary of positive staining. **A-B)**: At HH14, *Wt1* was not present within the anterior splanchnopleure except at the most dorsal aspect (arrows). **C**: The mesoderm over the vitelline vein (VV) also was *Wt1* positive anteriorly at HH14. **D-F**: In the posterior region of HH14 embryos, *Wt1* not identified in the splanchnopleure. **G-I**: At HH15, *Wt1* expression was variable along the A-P axis though expression did extend into the splanchnic mesoderm at some levels. Expression was not clearly restricted to the outer epithelium (arrows). **J-K**: At HH19, expression of *Wt1*, while still variable, was found extending throughout the entire splanchnic mesoderm up to the vitelline veins and including the mesenchymal layer (arrows). **L**: Representative image demonstrating *Wt1* expression in the PE (arrows). Note the lack of staining over the myocardium (M). DA, dorsal aorta; E; endoderm; FG, foregut; ND, nephric duct; NT, neural tube; S, somite; So, somatic mesoderm; Sp, splanchnic mesoderm; SV, sinus venosus; UR, urogenital ridge; VV, vitelline vein. Scale bar 40 μm.

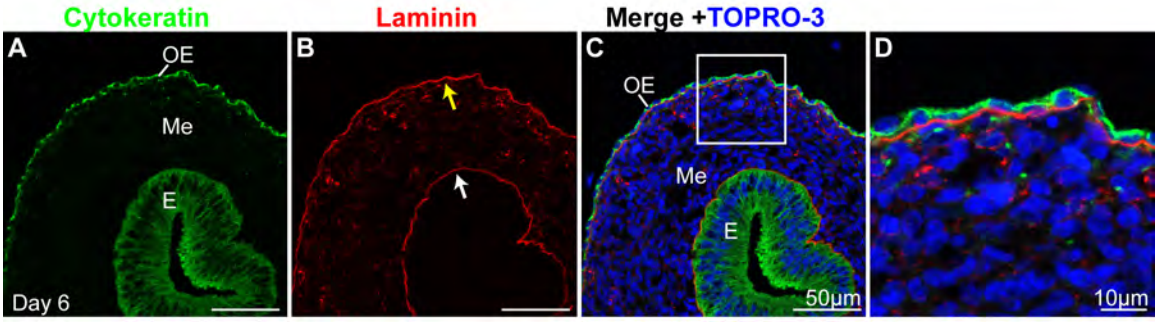

Figure 3.3 Definitive intestinal mesothelium is present at HH29 (Day 6). A: At day 6, a simple squamous, cytokeratin positive (green) mesothelium is present surrounding the intestine. **B**: A basement membrane underlies the mesothelium (red, yellow arrow). White arrow indicates the endodermal basement membrane. **C**: Merge. **D**: Higher magnification of boxed region shown in C). E, endoderm; Me, mesenchyme; OE, outer epithelium.

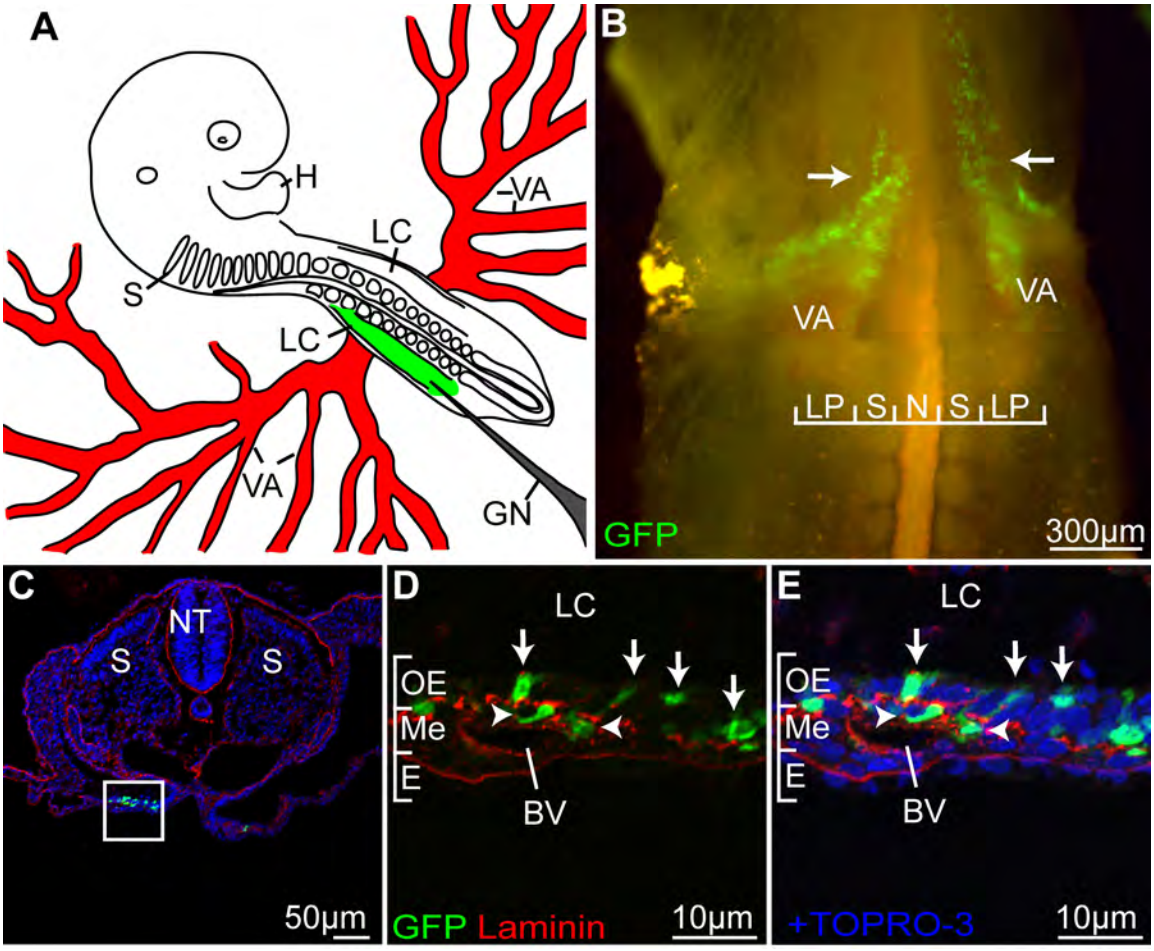

Figure 3.4 Electroporation of the splanchnic mesoderm at HH14 demonstrates labeling of the outer epithelium and mesenchyme. A: Schematic demonstrating injection of the GFP reporter plasmid into the right lateral cavity of an embryo in ovo. **B**: Wholemount image of the ventral surface of an embryo electroporated at HH14 and then incubated for 6 hours. Electrodes were placed near the vitelline artery. GFP was observed in the region near the vitelline artery and was restricted to the lateral plates (arrows). **C**: GFP-positive cells localized to the splanchnic mesoderm. **D**: Boxed area shown in C). GFP-positive cells were found primarily within the outer epithelium (arrows) with a few cells within the mesenchymal layer (arrowheads). No GFP-positive cells were identified in the endoderm. **E**: Merge with TOPRO-3. BV, blood vessel; GN, glass needle; H, heart; LC, lateral cavity; LP, lateral plate; Me, mesenchymal layer; N, notochord; NT, neural tube; OE, outer epithelium; S, somite, VA, vitelline artery.

Embryos were incubated for six hours post-electroporation to allow for GFP to accumulate to a detectable level and also encompass the time over which the splanchnopleure transitions from two to three layers. Whole mount imaging of electroporated embryos revealed bilateral GFP expression restricted to the region of the lateral plate near the vitelline arteries demonstrating the accuracy of the targeting method (Figure 3.4 B, arrows). Fluorescent imaging of sections through the targeted regions at six hours post-electroporation demonstrated that GFP-positive cells were present predominantly within the outer epithelium (71%; 454/640 total cells counted from four embryos, arrows) but also in the underlying mesenchyme (29%, 186/640 total cells counted, Fig. 3C-E, arrowheads). At no time was endoderm labeled with this method. Embryos electroporated between HH15-HH17 demonstrated similar labeling with 66% of GFP-positive cells within the outer epithelium (316/482 total cells counted, Figure 3.5). The presence of labeled cells in the outer epithelium and mesenchyme indicates the splanchnic mesoderm provides cells to both layers.

We next sought to determine if cells of the splanchnic mesoderm later gave rise to the mesothelium. For this experiment, embryos were electroporated between HH15-HH17 and incubated for eight days (the limit of GFP detection using this method) to day 10 of chick development. Examination of resulting small intestines revealed labeled cells were clearly resident within the mesothelial layer. These GFP-positive cells exhibited features typical of mesothelium including a close association with the basal lamina and a squamous morphology (Figure 3.6 A-D, arrows). In addition to the mesothelium,

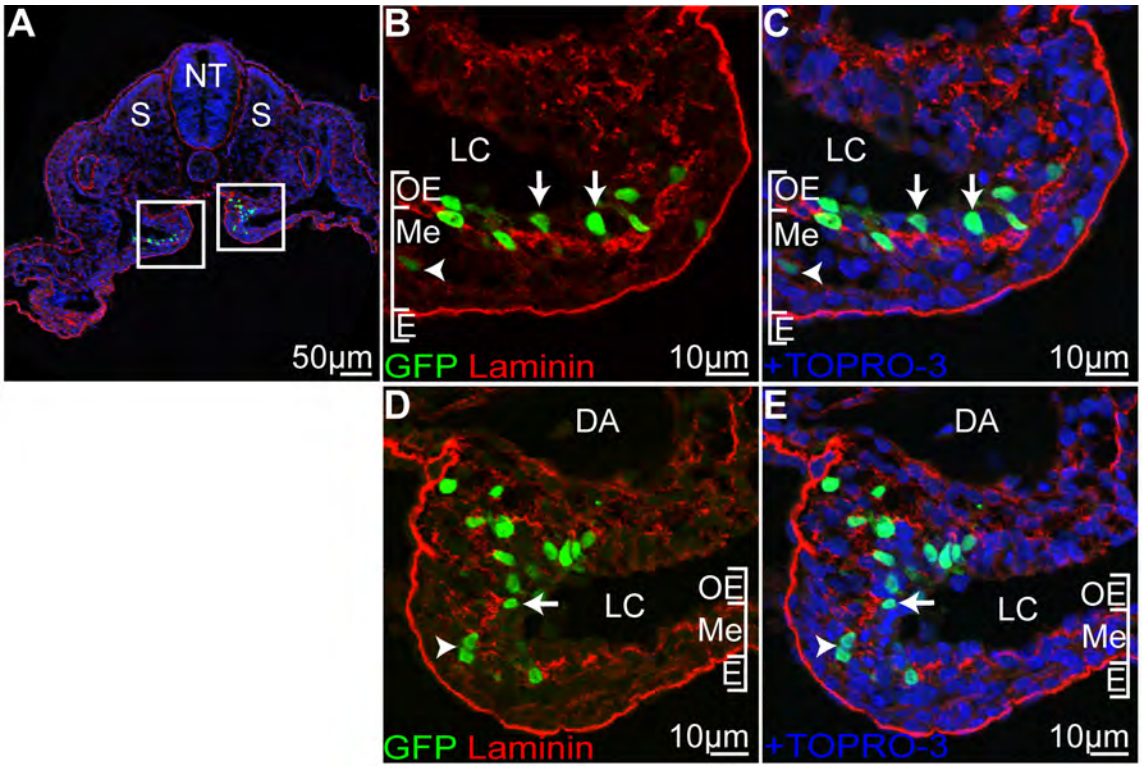

Figure 3.5. Electroporation of the splanchnic mesoderm at HH15. A) Section though an embryo 6 hours post-electroporation. Both right and left sides of the embryo were targeted (boxed areas) **B-E)** Higher power views of boxed areas. Cells within the outer epithelium (arrows) and mesenchyme (arrowheads) were GFP-positive. DA, dorsal aorta; E, endoderm; LC, lateral cavity; Me, mesenchymal layer; NT, neural tube; OE, outer epithelium; S, somite.

GFP-positive cells were identified throughout the gut tube including the muscularis externa (arrows) and penetrating as deep as the submucosa (arrowhead, Figure 3.6 E-H). Labeled cells were never observed in the endodermal mucosa. These data demonstrate that mesothelial precursors are resident to the splanchnic mesoderm and outer epithelial layer of the primitive intestine.

We utilized a second direct labeling approach to confirm and extend our findings. For these experiments, we used a replication incompetent retrovirus with broad tropism and a GFP reporter gene. Incorporation of the retroviral genome into infected cells allows for long term tracing without dilution of the label through cell division. High titer retrovirus was injected into the lateral cavities of HH14-17 embryos in the same manner as the electroporation plasmid to label the surface cells throughout the time points at which the splanchnopleure transitions between two to three compartments. Embryos were then incubated 14 days (to day 17 of development, hatching occurs at day 21) before the gut tubes were harvested.

Isolated gut tubes were first examined in whole mount for GFP expression. In embryos infected at HH14, a time prior to appearance of the middle mesenchymal layer, GFP-positive cells were present throughout the gut tube and mesentery and many appeared localized to the surface (Figure 3.7 A, arrows). GFP-positive cells also clearly associated with the vascular tree (Figure 3.7 B-B', arrows) and distributed in deep layers (Figure 3.7 C, arrows).

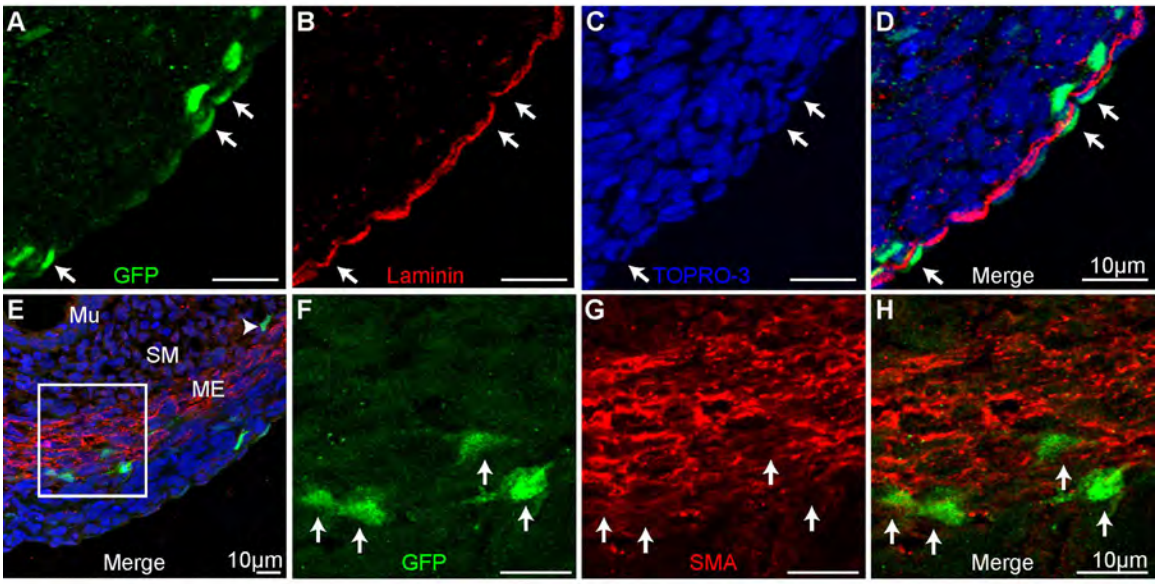

Figure 3.6 DNA electroporation demonstrates that splanchnic mesoderm harbors mesothelial progenitors. Sections through gut tubes of embryos electroporated at HH15-HH17 and incubated 8 days. **A-D**: GFP-positive cells (arrows) were identified within the squamous mesothelial layer of the intestine associated closely with the basement membrane (laminin, red). **E**: GFP-positive cells were also identified within the forming alpha-smooth muscle actin (SMA) positive muscularis externa (boxed region) and into the submucosa (arrowhead). **F-H**: Higher magnification of boxed region. GFP-positive cells within the muscularis externus were not SMA-positive (arrows). ME, muscularis externa; Mu, mucosa; SM, submucosa.

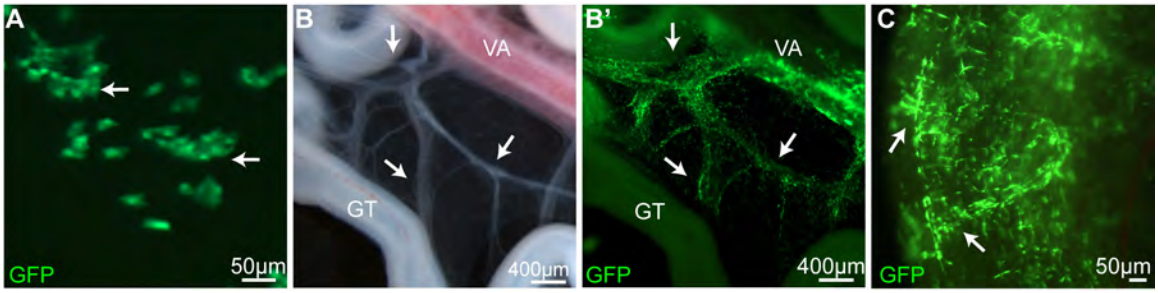

Figure 3.7 Long term retroviral lineage tracing of splanchnic mesoderm. Wholemount images of intestine from embryos infected with virus between HH14-HH17 and analyzed 14 days later. **A**: High magnification of intestinal surface demonstrated cells resembling mesothelium with prominent nuclei and broad cell processes (arrows). **B**: Brightfield image of gut tube demonstrating the vasculature (arrows). **B'**: GFP fluorescence of gut tube pictured in B). GFP-positive cells surrounded the vasculature within the mesentery and intestine (arrows). **C**: GFP-positive cells were also found distributed deeply in the intestine (arrows). GT, gut tube; VA, vitelline artery.

Upon sectioning, surface GFP-positive mesothelial cells with a squamous morphology were clearly identified in close association with the external basal lamina (Figure 3.8 A-B, arrowhead). GFP-positive vascular smooth muscle cells were also present consistent with previously published data (Wilm et al., 2005). Other GFP-positive, SMA-negative cells were identified peripheral to the vascular media within the adventitia (Figure 3.8 C-D). We did not identify any GFP-positive endothelial cells. GFP-positive cells were also identified within the submucosa and muscularis externa but not within the mucosal epithelium (Figure 3.8 E). Only 5% of GFP-positive cells localized within the muscularis externa were visceral smooth muscle cells (alpha-smooth muscle actin (SMA)-positive and spindle shaped) (Figure 3.8 F-H, arrowheads). The phenotype of the remaining cells could not be identified by morphology or by specific markers of smooth muscle, neurons, or epithelia and might best be characterized as stromal/mesenchymal by their location within the organ wall (Figure 3.8 J, L and data not shown). In embryos infected with the retrovirus between stages 15-17, after division of the splanchnic mesoderm into outer epithelium and mesenchyme, the same GFP-positive populations were identified at day 17 of development (Figure 3.8 I-L). This independent assay confirmed that resident splanchnic mesoderm was the origin of mesothelium and that these cells are maintained within the definitive mesothelium.

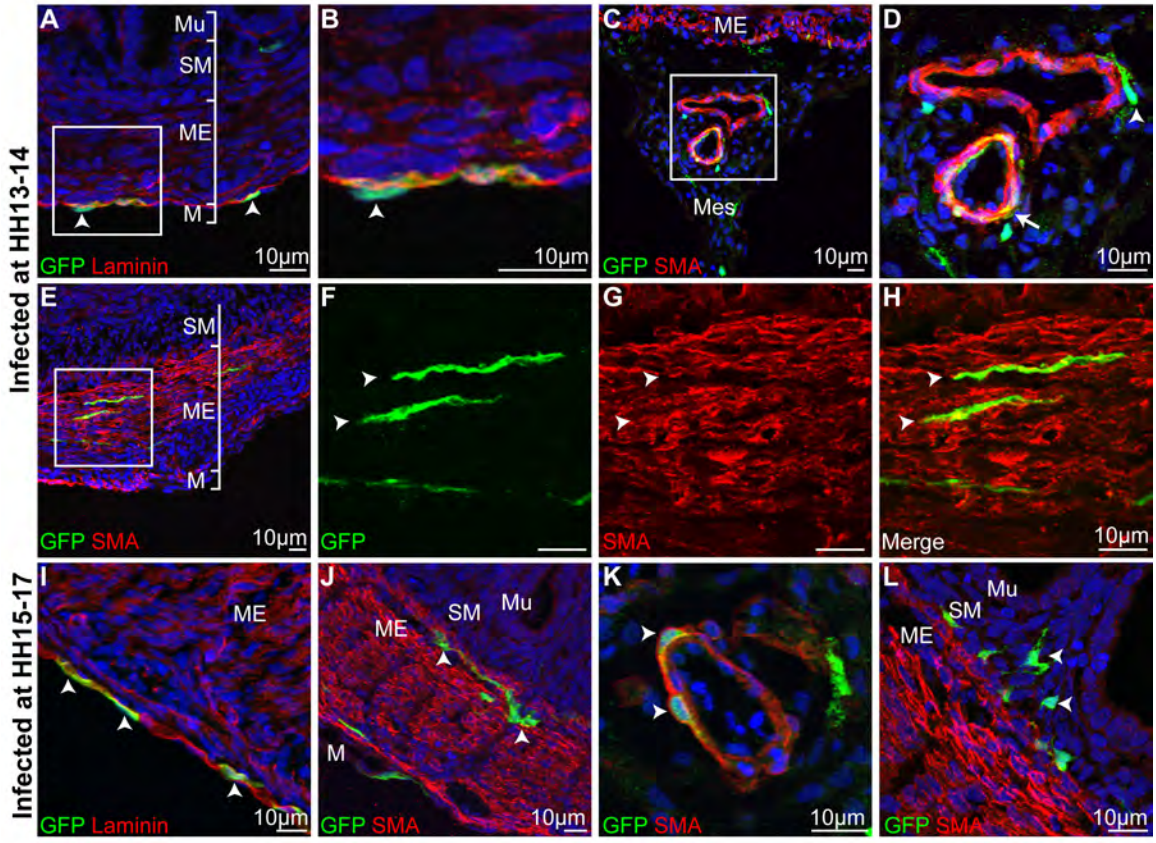

Figure 3.8 Lineage tracing of splanchnic mesoderm reveals mesothelial, perivascular, and mesenchymal derivatives. A-H: Sections of intestine from embryos infected between HH13-14 and isolated 14 days later. **A**: Squamous GFP-positive cells frequently populated the mesothelium (arrowheads) closely associating with the basement membrane (red, laminin). **B**: High magnification of boxed area in A). **C**: GFP-positive cells associated with large mesenteric blood vessels. **D**: High magnification of boxed area in C) demonstrates GFP-positive vascular smooth muscle cells (arrow) and perivascular cells (arrowhead). **E**: GFP-positive cells were identified within the muscularis externa. **F-H**: High magnification of boxed area shown in E). A rare population of GFP-positive cells found within the muscularis externus were spindle shaped and SMA-positive (arrowheads). **I-L**: Sections of intestine from embryos infected between HH15-17 and isolated 14 days later. **I**: Squamous GFP-positive cells populated the mesothelium (arrowheads) closely associating with the basement membrane (red, laminin). **J**: SMA-negative mesenchymal cells within the muscularis externa layer (arrowheads). **K**: GFP-positive vascular smooth muscle cells (arrowheads). **L**: Submucosal GFP-positive, SMA-negative cells. M, mesothelium; ME, muscularis externus; Mes, mesentery; Mu, mucosa, SM, submucosa.

Intestinal mesothelial progenitors are localized broadly throughout the splanchnic mesoderm

The current data establish that cells resident to the splanchnic mesoderm give rise to intestinal mesothelium. We next sought to determine if the majority of cells were derived from this resident population of progenitors and if the potential to generate mesothelium from resident cells was distributed broadly throughout the splanchnic mesoderm or restricted to subdivisions of the gut.

To address these questions, we developed a chick-quail chimera assay to analyze gut development. Bilateral splanchnopleure was isolated from HH13-17 quail embryos, divided into 6-7 pieces along the A-P axis, and then transplanted individually into the right lateral cavities (precursor to the coelomic cavity) of chick embryos staged between HH16-18 (Figure 3.9 A). The host chick embryos were incubated for 14 days post-transplantation (corresponding to day 16.5 of quail development) and then harvested to identify where the transplanted tissue incorporated and whether mesothelial differentiation transpired.

Strikingly, the transplanted splanchnopleure did not incorporate into the host gut tube but rather formed an independent “gut tube” within the coelomic cavity connected to the host only through a mesentery (Figure 3.9 B). At 14 days post-transplantation, graft-derived gut tubes were similar to a normally developing small intestine with an elongated tubular shape and a single dorsal mesentery (Figure 3.9 C, brackets) housing a well organized vasculature (Figure 3.9 D, arrowheads; observed in 16 chick-quail chimeras). Transverse sections through graft-derived gut tubes demonstrated a remarkable intestinal

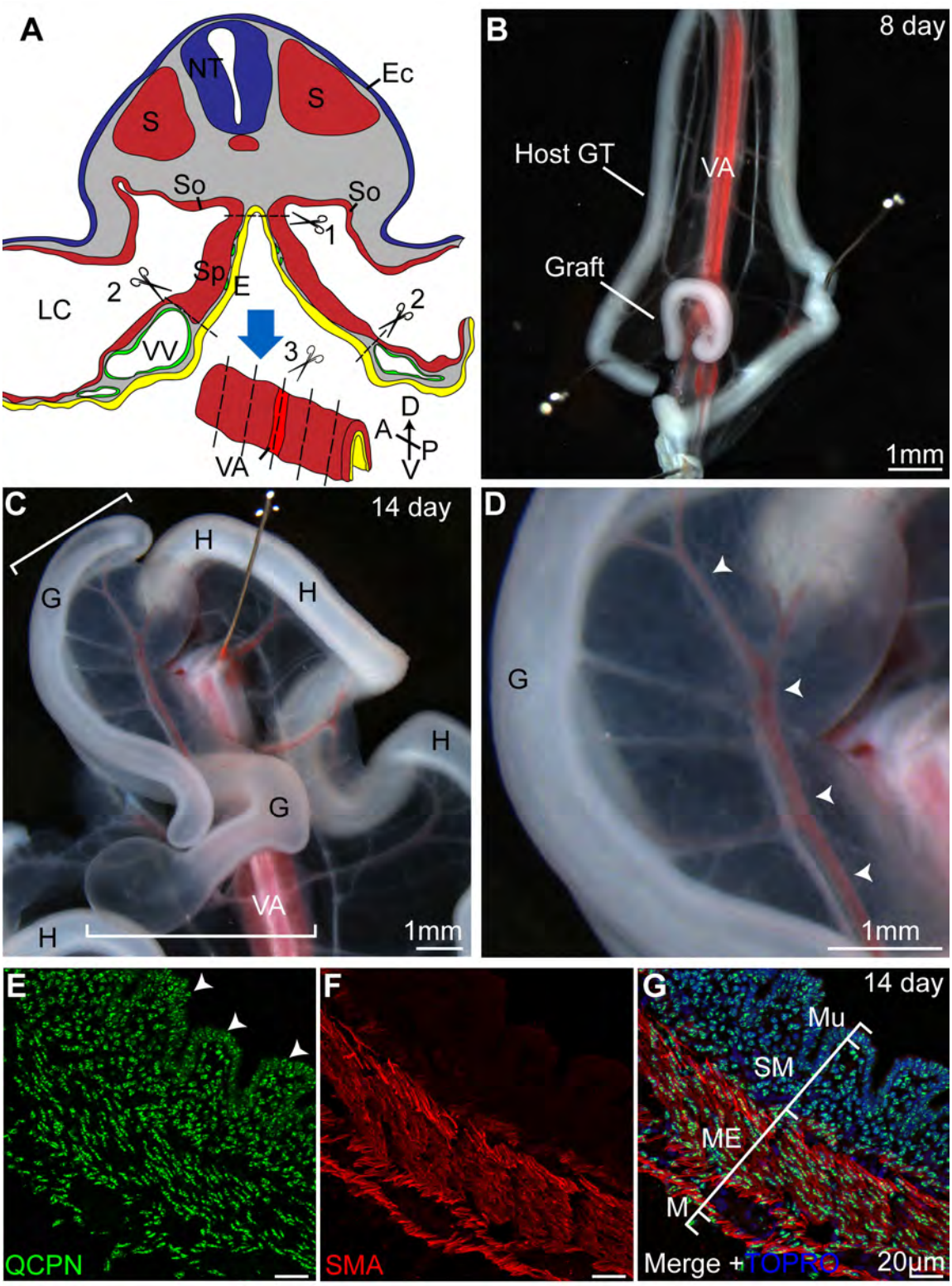
A
NT
Ec
S
S
So
So
1
2
Sp
E
LC
2
VV
3
D
A
P
V
VA
B
8 day
Host GT
VA
Graft
1mm
C
14 day
H
G
H
H
G
VA
H
1mm
D
G
1mm
E
QCPN
F
SMA
G
14 day
Mu
SM
ME
M
Merge +TOPRO
20μm

Figure 3.9 Transplanted splanchnopleure forms a highly structured gut tube. A: Transplants were generated by cutting along the dorsal aspect of the splanchnopleure (1) and the ventral edges near the vitelline veins (2). The splanchnopleure was then cut along the A-P axis (3) to generate 6-7 pieces for transplantation. **B**: A representative graft-derived gut tube 8 days after transplantation. The graft had generated a tube and attached to the mesentery of the host gut tube. **C**: A representative graft-derived gut tube 14 days after transplantation (G, bracketed). The graft-derived gut tube was attached to the host (H) via a mesentery. **D**: The mesentery of the graft-derived gut tube contained a regular arrangement of blood vessels (arrowheads). **E-G**: Sections through the graft-derived gut tube demonstrated normal morphogenesis with villi (arrowheads), submucosa (SM), and a SMA-positive muscularis externus layer. All layers were derived from quail cells (QCPN-positive, green). E, endoderm; Ec, ectoderm; G, graft-derived gut tube; H, host gut tube; LC, lateral cavity; M, mesothelium; ME, muscularis externa; Mu, mucosa; NT, neural tube; S, somite; So, somatic mesoderm; Sp, splanchnic mesoderm; SM, submucosa; VA, vitelline artery; VV, vitelline vein.

organization with an inner mucosa with villus folds (arrowheads), a submucosa, and a muscularis externa with smooth muscle differentiation (Figure 3.9 E-G). Staining for quail specific QCPN demonstrated all layers of the graft were quail derived (Figure 3.9 E-G). Specific regions in the graft did not stain with QCPN but were positive for a pan-neuronal marker, PGP9.5 (Figure 3.10 A-E asterisks). Co-staining for a marker of chick cells (8F3) and PGP9.5 confirmed these cells originated from host neural crest cells (Figure 3.10 F-J). Interestingly, the host-derived neural crest cells that invaded the graft organized into typical submucosal and myenteric plexuses (Figure 3.10). Transplanted splanchnopleure isolated both prior to (HH13-HH14) and after (HH15-17) establishment of a trilaminar configuration produced identical results (Figure 3.11).

Co-staining for QCPN with cytokeratin revealed that mesothelium covering the graft-derived gut tube and within the mesentery originated from transplanted quail splanchnopleure (Figure 3.11 A-F, arrowheads). We quantified the number of mesothelial cells in graft-derived gut tubes that were QCPN-positive and found that on average 85% of mesothelial cells were quail derived. Furthermore, 94% of mesothelial cells in graft-derived gut tubes were negative for a marker specific to chick cells (8F3) (Figure 3.11 G-I). The difference between the two percentages is likely due to the variation in staining patterns; QCPN is a perinuclear antigen often with distinct puncta of staining while 8F3 is cytoplasmic and more easily visualized (Figure 3.11 J-L). Both figures denote the great majority of graft-derived mesothelial cells were derived from transplanted tissue.

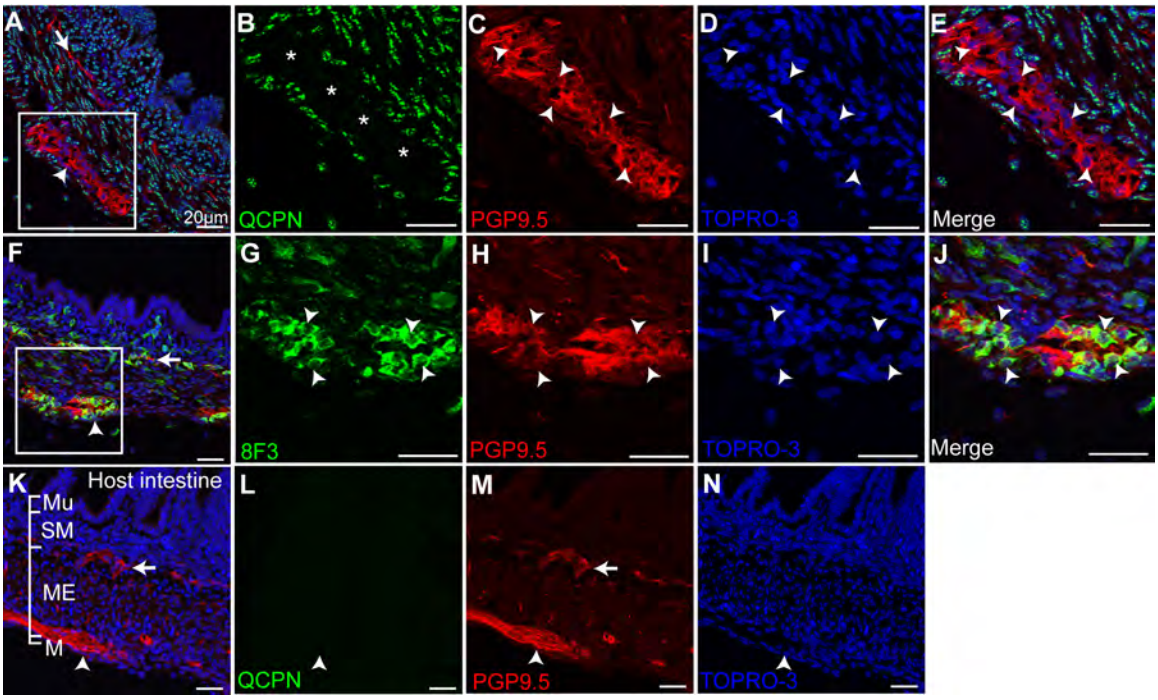

Figure 3.10 Invasion of graft-derived gut tube by chick neural crest. A: Neuronal cells identified by PGP9.5 staining were found throughout the graft-derived gut tube organized into submucosal (arrow) and myenteric plexuses (arrowhead). **B-E**: Higher magnification of boxed area in A). QCPN-negative cells within the graft (asterisks) were PGP9.5-positive (arrowheads). **F-J**: Staining for the chick cell marker 8F3 co-localized with PGP9.5 staining (arrowheads). **K-N**: Immunostaining for QCPN and PGP9.5 in a host gut tube demonstrating the typical organization into submucosal (arrow) and myenteric (arrowhead) plexuses. **L**: QCPN-positive cells were not found within the host gut tube. M, mesothelium; ME, muscularis externa; Mu, mucosa; SM, submucosa.

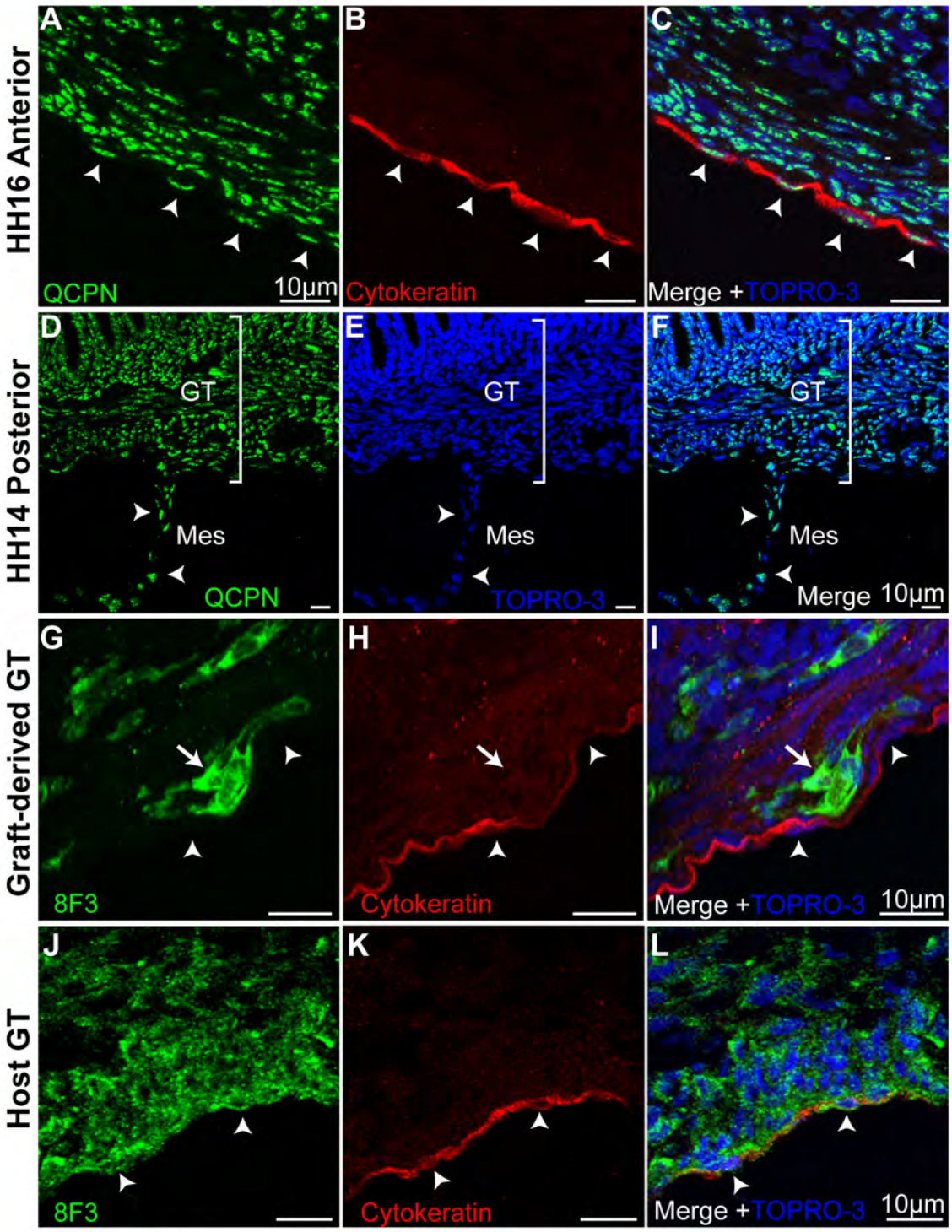
HH16 Anterior
A
QCPN
10μm
B
Cytokeratin
C
Merge +TOPRO-3
HH14 Posterior
D
GT
Mes
QCPN
E
GT
Mes
TOPRO-3
F
GT
Mes
Merge 10μm
Graft-derived GT
G
8F3
H
Cytokeratin
I
Merge +TOPRO-3 10μm
Host GT
J
8F3
K
Cytokeratin
L
Merge +TOPRO-3 10μm

Figure 3.11 Graft mesothelium is quail derived. A-C: Section of graft-derived gut tube generated from tissue isolated from the anterior splanchnopleure of a HH16 quail donor. Co-staining for QCPN and cytokeratin demonstrated that the mesothelial cells lining the graft were quail derived (arrowheads). **D-F**: Section of a graft-derived gut tube generated from the posterior splanchnopleure of a HH14 quail donor. QCPN staining demonstrates the mesenteric mesothelium is quail derived (arrowheads). **G-H**: Host-derived cells (8F3-positive) were also identified within the graft (arrows). However, 8F3-positive chick cells were only rarely (6%) identified within the mesothelial layer (arrowheads) of the graft-derived gut tube. **J-L**: Staining of a chick (host) gut tube reveals mesothelial cells (arrowheads) robustly label with the chick marker 8F3. GT, gut tube; Mes, mesentery.

Tissue morphogenesis was identical between both anterior and posterior derived grafts and, critical to the current studies, the mesothelium was always quail-derived regardless of whether the graft was obtained from an anterior or posterior location in the source splanchnopleure (100% of cases examined, Figure 3.11 A-F). Taken together, these data demonstrate that mesothelial progenitors are broadly distributed along the A-P axis of the intestine and there is not a localized or restricted PE-like source of mesothelial cells.

Discussion

Mesothelia are essential for the generation of diverse cell types within all coelomic organs investigated thus far (Asahina et al., 2011; Eralp et al., 2005; Mikawa and Gourdie, 1996; Perez-Pomares et al., 2004; Que et al., 2008; Wilm et al., 2005). Despite the importance of this cell type in organogenesis, the origin of mesothelium had only been established in the heart where mesothelium is derived from a localized, extrinsic cell population, the PE. Identification of the origin of mesothelial cells is essential for studies of the molecular regulation of mesothelial differentiation, vascular formation, and mesothelial-dependent signaling in intestinal development and organogenesis in general. Here, using three independent methods, we demonstrate that intestinal mesothelium is derived from a resident population of cells broadly distributed within the splanchnic mesoderm. Thus, gut mesothelium does not arise in the same manner as described in the heart and reveals a novel paradigm for the

generation of this essential cell type. Discovery of the origin of gut mesothelium is critical for further analysis of regulatory mechanisms governing mesothelial development, repair in the adult, and origin of disease.

Previously, we demonstrated through a genetic lineage tracing study in mouse that vascular smooth muscle cells of the intestine were derived from mesothelium. Furthermore, expression of *Wt1* was first observed in the mesentery and then progressively encompassed the intestinal tube suggesting a migratory mesothelial population may exist as observed in the heart (Wilm et al., 2005). However, a PE-like structure or clear evidence of a migratory population was not identified. Furthermore, *Wt1* is not a marker specific only to mesothelium (Zhou et al., 2011). Here, through the use of direct labeling and transplantation studies in the avian embryo, we have demonstrated that mesothelial progenitors of the intestine are broadly resident to the splanchnic mesoderm and not derived from an exogenous migratory source. This progenitor population is present prior to tube formation but does not specifically express *Wt1*. While there may be variation between species in intestinal mesothelial origin and *Wt1* expression patterns, it is possible that murine mesothelial progenitors are also resident broadly in the intestine and *Wt1* is expressed in a dorsal-ventral direction as mesothelial differentiation proceeds. Still, further experimentation is needed to resolve this issue amongst different species.

The intestines, lungs, liver, and pancreas are all gut tube derivatives formed from endoderm or endodermal buds that are surrounded by splanchnic mesoderm. In contrast, the heart wall is not a gut tube derivative but rather is

derived solely from splanchnic mesoderm excluding endoderm dorsally. The splanchnic mesoderm comprising the majority of the heart wall is not thought to contain mesothelial progenitors (Gittenberger-de Groot et al.; Manner et al., 2005). In contrast, the present study demonstrates that mesothelial precursors are resident broadly to the surface of the developing gut splanchnic mesoderm prior to endodermal budding and mucosal differentiation. Considering the unique features of cardiac development and the early specialization of the cardiac splanchnic mesoderm (i.e. it is a contractile tube before PE-derived mesothelium contacts the organ), we postulate mesothelial development in the lungs, liver and pancreas as gut tube derivatives will be found to more closely resemble the intestinal rather than the cardiac model of mesothelial development.

The molecular foundation for the variation in proepicardial and intestinal mesothelial development is currently unknown. However, Ishii et al. report that the liver bud is at least partially responsible for induction of markers of the PE including *Wt1*, *Tbx18* and *capsulin*. Liver bud transplanted ectopically into the lateral embryo distal to the heart induced *Wt1* in the closely adjoining tissue. Interestingly, the lung bud and stomach did not have similar inductive capabilities in that system (Ishii et al., 2007). For the majority of the mesothelium not in contact with the liver bud, alternative inductive tissues and signals must be involved. Other studies have uncovered potential roles for BMP in villous protrusion of the PE (Ishii et al., 2010), a behavior observed in cardiac but not intestinal mesothelial development (from the current study), and for both BMP and FGF signals in the lineage specification of epicardial cells (Kruithof et al.,

2006; Schlueter et al., 2006). With identification of the fundamental mechanism of intestinal mesothelial formation, studies on the molecular regulation of behaviors unique to either the intestinal or cardiac mesothelium can proceed.

While the origin of mesothelial cells in the intestine and heart are clearly divergent, there do exist conserved features of mesothelial development and differentiation. The presence of a small number of host mesothelial cells in graft-derived gut tubes suggests that intestinal mesothelium can be migratory as previously observed with epicardial mesothelium. Whether this is a normally occurring event in gut development or simply a “blending” of cells in this particular experimental model, it is evident that mesothelial progenitors of the gut and/or definitive gut mesothelium are capable of movement or active migration. Mesothelial cells in the heart, lungs, intestines, and liver all give rise to stromal cells including vascular smooth muscle, endothelium, fibroblasts, and other “mesenchymal” cells (Asahina et al., 2011; Dettman et al., 1998; Eralp et al., 2005; Mikawa and Gourdie, 1996; Perez-Pomares et al., 2004; Que et al., 2008; Wilm et al., 2005). Both cardiac and peritoneal mesothelia of the adult retain the ability to generate stromal progeny. When stimulated, adult omental mesothelial cells differentiate into vascular smooth muscle cells and can directly contribute cells to an injured blood vessel (Kawaguchi et al., 2007; Shelton et al., 2012). Fibroblast and vascular smooth muscle cell differentiation from previously quiescent mesothelium has also been observed following myocardial infarction (Zhou and Pu, 2011). Thus, while the mechanism generating intestinal

mesothelial cells is different from that of the heart, once established, these two progenitor populations appear to have similar differentiative potentials.

Other disease processes involving mesothelia reflect the developmental potential of this cell type. For example, peritoneal sclerosis, a fibrotic thickening of the abdominal serosal membranes, is frequently observed following peritoneal dialysis (Devuyst et al., 2010). Mesothelial cells have recently been recognized both as a source of fibrotic cells and a signaling center for aberrant vasculogenesis (Aroeira et al., 2005; Braun et al., 2011; Yanez-Mo et al., 2003; Yung and Chan, 2009). In another example, pulmonary fibrosis is first observed as a fibrotic thickening just below the pulmonary mesothelium that progressively moves inward (King et al., 2011). The role of mesothelium in this disease has also recently been the focus of studies and reviews as a signaling center or source of fibrotic cells (Acencio et al., 2007; Decologne et al., 2007; Mutsaers et al., 2004). These pathologies have a direct root in the developmental potential of mesothelium to give rise to fibroblasts and vascular smooth muscle. Thus, investigation of the diversity of mesothelial populations is critical to understanding their behavior in these various organs systems and disease processes.

Following discovery of the proepicardium, studies on development of cardiac mesothelium were able to rapidly progress. Currently, our understanding of epicardial biology encompasses the detailed cell lineage, mechanisms of molecular differentiation during development, and pathological behavior. We are now poised to move forward with similar studies of non-cardiac mesothelial populations. Mesothelial cells of diverse organs and body cavities have been

considered a uniform population due to their ultrastructural similarity and apparent shared developmental potential. Our data demonstrate that at least cardiac and intestinal mesothelia are heterogeneous populations with varied developmental histories that must be considered independently. Understanding the developmental origin of diverse mesothelia is essential for understanding the role mesothelial, vascular, and stromal cells may play in the development and homeostasis of these organs in the adult.

References

Acencio, M. M., Vargas, F. S., Marchi, E., Carnevale, G. G., Teixeira, L. R., Antonangelo, L. and Broaddus, V. C. (2007). Pleural mesothelial cells mediate inflammatory and profibrotic responses in talc-induced pleurodesis. *Lung* **185**, 343-348.

Aroeira, L. S., Aguilera, A., Selgas, R., Ramirez-Huesca, M., Perez-Lozano, M. L., Cirugeda, A., Bajo, M. A., del Peso, G., Sanchez-Tomero, J. A., Jimenez-Heffernan, J. A. et al. (2005). Mesenchymal conversion of mesothelial cells as a mechanism responsible for high solute transport rate in peritoneal dialysis: role of vascular endothelial growth factor. *Am J Kidney Dis* **46**, 938-948.

Asahina, K., Zhou, B., Pu, W. T. and Tsukamoto, H. (2011). Septum transversum-derived mesothelium gives rise to hepatic stellate cells and perivascular mesenchymal cells in developing mouse liver. *Hepatology* **53**, 983-995.

Braun, N., Alscher, D. M., Fritz, P., Edenhofer, I., Kimmel, M., Gaspert, A., Reimold, F., Bode-Lesniewska, B., Ziegler, U., Biegger, D. et al. (2011). Podoplanin-positive cells are a hallmark of encapsulating peritoneal sclerosis. *Nephrol Dial Transplant* **26**, 1033-1041.

Chegini, N. (2008). TGF-beta system: the principal profibrotic mediator of peritoneal adhesion formation. *Semin Reprod Med* **26**, 298-312.

Decologne, N., Kolb, M., Margetts, P. J., Menetrier, F., Artur, Y., Garrido, C., Gauldie, J., Camus, P. and Bonniaud, P. (2007). TGF-beta1 induces progressive pleural scarring and subpleural fibrosis. *J Immunol* **179**, 6043-6051.

Dettman, R. W., Denetclaw, W., Jr., Ordahl, C. P. and Bristow, J. (1998). Common epicardial origin of coronary vascular smooth muscle, perivascular fibroblasts, and intermyocardial fibroblasts in the avian heart. *Dev Biol* **193**, 169-181.

Devuyst, O., Margetts, P. J. and Topley, N. (2010). The pathophysiology of the peritoneal membrane. *J Am Soc Nephrol* **21**, 1077-1085.

Eralp, I., Lie-Venema, H., DeRuiter, M. C., van den Akker, N. M., Bogers, A. J., Mentink, M. M., Poelmann, R. E. and Gittenberger-de Groot, A. C. (2005). Coronary artery and orifice development is associated with proper timing of epicardial outgrowth and correlated Fas-ligand-associated apoptosis patterns. *Circ Res* **96**, 526-534.

Gittenberger-de Groot, A. C., Vrancken Peeters, M. P., Bergwerff, M., Mentink, M. M. and Poelmann, R. E. (2000). Epicardial outgrowth inhibition leads to compensatory mesothelial outflow tract collar and abnormal cardiac septation and coronary formation. *Circ Res* **87**, 969-971.

Hamburger, V. and Hamilton, H. L. (1992). A Series of Normal Stages in the Development of the Chick-Embryo, (Reprinted from Journal of Morphology, Vol 88, 1951). *Developmental Dynamics* **195**, 231-272.

Ho, E. and Shimada, Y. (1978). Formation of the epicardium studied with the scanning electron microscope. *Dev Biol* **66**, 579-585.

Ishii, Y., Garriock, R. J., Navetta, A. M., Coughlin, L. E. and Mikawa, T. (2010). BMP signals promote proepicardial protrusion necessary for recruitment of coronary vessel and epicardial progenitors to the heart. *Dev Cell* **19**, 307-136.

Ishii, Y., Langberg, J. D., Hurtado, R., Lee, S. and Mikawa, T. (2007). Induction of proepicardial marker gene expression by the liver bud. *Development* **134**, 3627-3637.

Kawaguchi, M., Bader, D. M. and Wilm, B. (2007). Serosal mesothelium retains vasculogenic potential. *Dev Dyn* **236**, 2973-2979.

King, T. E., Jr., Pardo, A. and Selman, M. (2011). Idiopathic pulmonary fibrosis. *Lancet* **378**, 1949-1961.

Kruithof, B. P., van Wijk, B., Somi, S., Kruithof-de Julio, M., Perez Pomares, J. M., Weesie, F., Wessels, A., Moorman, A. F. and van den Hoff, M. J. (2006). BMP and FGF regulate the differentiation of multipotential pericardial mesoderm into the myocardial or epicardial lineage. *Dev Biol* **295**, 507-522.

Lassiter, R. N., Dude, C. M., Reynolds, S. B., Winters, N. I., Baker, C. V. and Stark, M. R. (2007). Canonical Wnt signaling is required for ophthalmic trigeminal placode cell fate determination and maintenance. *Dev Biol* **308**, 392-406.

Manasek, F. J. (1969). Embryonic development of the heart. II. Formation of the epicardium. *J Embryol Exp Morphol* **22**, 333-348.

Manner, J., Schlueter, J. and Brand, T. (2005). Experimental analyses of the function of the proepicardium using a new microsurgical procedure to induce loss-of-proepicardial-function in chick embryos. *Dev Dyn* **233**, 1454-1463.

McGlinn, E. and Mansfield, J. H. (2011). Detection of gene expression in mouse embryos and tissue sections. *Methods Mol Biol* **770**, 259-292.

Mikawa, T. and Gourdie, R. G. (1996). Pericardial mesoderm generates a population of coronary smooth muscle cells migrating into the heart along with ingrowth of the epicardial organ. *Dev Biol* **174**, 221-232.

Minot, C.-S. (1890). The mesoderm and the coelom of vertebrates. *The American Naturalist* **24**, 877-898.

Moore, K. L. and Persaud, T. V. N. (1998). The developing human : clinically oriented embryology. Philadelphia: Saunders.

Morimoto, M., Liu, Z., Cheng, H. T., Winters, N., Bader, D. and Kopan, R. (2010). Canonical Notch signaling in the developing lung is required for determination of arterial smooth muscle cells and selection of Clara versus ciliated cell fate. *J Cell Sci* **123**, 213-224.

Mutsaers, S. E. (2002). Mesothelial cells: their structure, function and role in serosal repair. *Respirology* **7**, 171-191.

Mutsaers, S. E., Prele, C. M., Brody, A. R. and Idell, S. (2004). Pathogenesis of pleural fibrosis. *Respirology* **9**, 428-440.

Mutsaers, S. E. and Wilkosz, S. (2007). Structure and function of mesothelial cells. *Cancer Treat Res* **134**, 1-19.

Osler, M. E. and Bader, D. M. (2004). Bves expression during avian embryogenesis. *Dev Dyn* **229**, 658-667.

Perez-Pomares, J. M., Carmona, R., Gonzalez-Iriarte, M., Macias, D., Guadix, J. A. and Munoz-Chapuli, R. (2004). Contribution of mesothelium-derived cells to liver sinusoids in avian embryos. *Dev Dyn* **229**, 465-474.

Que, J., Wilm, B., Hasegawa, H., Wang, F., Bader, D. and Hogan, B. L. (2008). Mesothelium contributes to vascular smooth muscle and mesenchyme during lung development. *Proc Natl Acad Sci U S A* **105**, 16626-16630.

Schlueter, J., Manner, J. and Brand, T. (2006). BMP is an important regulator of proepicardial identity in the chick embryo. *Dev Biol* **295**, 546-558.

Schulte, I., Schlueter, J., Abu-Issa, R., Brand, T. and Manner, J. (2007). Morphological and molecular left-right asymmetries in the development of the proepicardium: a comparative analysis on mouse and chick embryos. *Dev Dyn* **236**, 684-695.

Shelton, E., Poole, S., Reese, J. and Bader, D. (2012). Omental grafting:a cell-based therapy for blood vessel repair. *J Tissue Eng Regen Med*, doi:10.1002/term.528.

Takaba, K., Jiang, C., Nemoto, S., Saji, Y., Ikeda, T., Urayama, S., Azuma, T., Hokugo, A., Tsutsumi, S., Tabata, Y. et al. (2006). A combination of omental flap and growth factor therapy induces arteriogenesis and increases myocardial perfusion in chronic myocardial ischemia: evolving concept of biologic coronary artery bypass grafting. *J Thorac Cardiovasc Surg* **132**, 891-899.

Venters, S. J., Dias da Silva, M. R. and Hyer, J. (2008). Murine retroviruses re-engineered for lineage tracing and expression of toxic genes in the developing chick embryo. *Dev Dyn* **237**, 3260-3269.

Wilm, B., Ipenberg, A., Hastie, N. D., Burch, J. B. and Bader, D. M. (2005). The serosal mesothelium is a major source of smooth muscle cells of the gut vasculature. *Development* **132**, 5317-5328.

Wu, M., Smith, C. L., Hall, J. A., Lee, I., Luby-Phelps, K. and Tallquist, M. D. (2010). Epicardial spindle orientation controls cell entry into the myocardium. *Dev Cell* **19**, 114-125.

Yanez-Mo, M., Lara-Pezzi, E., Selgas, R., Ramirez-Huesca, M., Dominguez-Jimenez, C., Jimenez-Heffernan, J. A., Aguilera, A., Sanchez-Tomero, J. A., Bajo, M. A., Alvarez, V. et al. (2003). Peritoneal dialysis and epithelial-to-mesenchymal transition of mesothelial cells. *N Engl J Med* **348**, 403-413.

Yung, S. and Chan, T. M. (2009). Intrinsic cells: mesothelial cells -- central players in regulating inflammation and resolution. *Perit Dial Int* **29** Suppl 2, S21-7.

Zhang, Q. X., Magovern, C. J., Mack, C. A., Budenbender, K. T., Ko, W. and Rosengart, T. K. (1997). Vascular endothelial growth factor is the major angiogenic factor in omentum: mechanism of the omentum-mediated angiogenesis. *J Surg Res* **67**, 147-154.

Zhou, B., Honor, L. B., He, H., Ma, Q., Oh, J. H., Butterfield, C., Lin, R. Z., Melero-Martin, J. M., Dolmatova, E., Duffy, H. S. et al. (2011). Adult mouse epicardium modulates myocardial injury by secreting paracrine factors. *J Clin Invest* **121**, 1894-1904.

Zhou, B. and Pu, W. T. (2011). Epicardial epithelial-to-mesenchymal transition in injured heart. *J Cell Mol Med* **15**, 2781-2783.

CHAPTER IV

CELLULAR POTENTIAL VARIES BETWEEN HEART AND INTESTINAL MESOTHELIAL CELL POPULATIONS IN THE EMBRYO

This chapter contains unpublished data and is formatted for submission to *Development* as a Research Report with the following authors:

Rebecca T. Thomason, Nichelle I. Winters, David M. Bader

Abstract

Mesothelium is an epithelial sheet that covers organs in the coelomic cavity and is involved in development of the vascular system. In the developing heart, the proepicardial organ (PE), migrates to and over the heart to form the epicardium, and undergoes epithelial-mesenchymal transition (EMT) to give rise to the cells of the coronary blood vessels. The gut mesothelium serves as a major source of vascular smooth muscle cells for the gut tube in development. Based on current data, mesothelial cells play important roles in organ protection and formation of blood vessels in the heart and gut tube, suggesting similarities between the two populations. Thus, we hypothesize that heart and intestinal mesothelial cell populations possess similar cellular competencies and will integrate into any coelomic organ. First, we characterized the intestinal mesothelium in the avian embryo using histological and molecular techniques to determine the cell types present at time of transplantation. In addition,

mesothelial isolates were cultured to determine differentiative capacity. To test the plastic nature of mesothelial cells, we utilized the chick-quail chimera system to transplant quail PE and epicardial cells into the peritoneal cavity of a chick embryo and quail intestinal mesothelial cells into chick pericardial cavity. Our initial findings revealed that both cell types migrate into coelomic organs. Intestinal mesothelial cells incorporated into the endogenous epicardium and contributed vascular smooth muscle cells, fibroblasts, and myofibroblasts to the heart. However, PE and epicardial cells did not incorporate into the endogenous gut mesothelium, but retained epithelial characteristics. Taken together, our current data suggest divergent cellular characteristics and potential between heart and intestinal mesothelial cell populations.

Introduction

Mesothelia are simple squamous epithelia that cover organs and line all coeloms in vertebrates. In the adult, this ubiquitous cell type functions to provide a lubricated and smooth surface upon which organs move in their respective coelomic cavity (Mutsaers, 2004). While seemingly innocuous in appearance, mesothelia have well documented roles in diverse disease states and repair models.

Interestingly, mesothelia are absent from all primordia at the initiation of organogenesis. To date, the mesothelial field has focused on deciphering the developmental origins in and contributions to the heart. During early heart

development, an epithelial sheet of cells (the proepicardium or PE) arising from the region of the sinus venosus migrates to and over the organ establishing a definitive mesothelium (Ho and Shimada, 1978; Ishii et al., 2007; Manasek, 1969; Männer, 1992; Nahirney et al., 2003; van Wijk et al., 2009; Virágh and Challice, 1973). Specific cells within this mesothelium undergo epithelial-to-mesenchymal transition (EMT) to produce a freely migratory population of progenitors which in turn differentiate into vascular smooth muscle and pericytes, and stromal cells of the myocardial wall (Dettman et al., 1998; Gittenberger-de Groot et al., 1998; Männer, 1999; Mikawa and Gourdie, 1996; Vrancken Peeters et al., 1999; Wessels and Pérez-Pomares, 2004). The PE also provides endothelial cells for coronary vasculogenesis although their relationship to the mesothelial epithelium of the PE has not been definitively resolved (Katz et al., 2012; Mikawa and Gourdie, 1996; Red-Horse et al., 2010). Thus, the PE represents an exogenous and localized group of progenitors whose descendants produce organ mesothelium and are essential for vasculogenesis within the heart.

Recently, our group analyzed the generation of mesothelium in a second model system. Using long-term lineage tracing and chimeric analysis, Winters and colleagues demonstrated that gut mesothelium is generated in a completely different manner from that previously observed in the heart (Winters et al., 2012). In the case of the small intestine, mesothelial progenitors were not present as a migratory and exogenous cell population but, instead were widely distributed within the splanchnic mesoderm and endogenous to the gut anlagen. While the mechanism of generating this type of mesothelium is completely different from

that observed in the heart, gut mesothelium is the major contributor of vasculogenic smooth muscle in the developing gastrointestinal tract (Wilm et al., 2005).

Based on data demonstrating that both heart and gut mesothelial cells cover organs, undergo EMT, and contribute cells to the vasculature and mesenchyme of the organ, I hypothesized that there is a comparative development potential between heart and gut mesothelium. However, in light of new data demonstrating varying origins of the mesothelial populations (Winters et al., 2012), we also asked: do progenitor populations share this same interchangeable potential? Using chick-quail chimera techniques, mesothelial populations were transplanted into opposing cavities to determine if exogenous mesothelium would contribute known cell types to that organ. In this study, I demonstrated that only transplanted intestinal mesothelium does indeed possess an exchangeable capacity in the heart, contributing to the endogenous mesothelial population, vascular smooth muscle cells, and mesenchymal cells. Interestingly, transplanted PE and epicardial cells did not possess this same interchangeable potential when transplanted in the peritoneum. The implications of this work are significant in establishing embryonic mesothelial properties as well as the critical potential of these cells when utilized in therapies and regeneration in the adult.

Material and Methods

Immunohistochemical Analysis

All embryos and organ tissue were fixed in a 4% formaldehyde (Sigma F1635) in phosphate buffer solution (1X PBS, pH 7.4) at 4°C or at room temperature depending on tissue size. The samples were washed with 1X PBS (pH 7.4), cryoprotected in 30% sucrose, embedded in OCT (TissueTek 4583) and sectioned at 5μm -7μm. Slides were rehydrated and washed with 1X PBS, then perforated with a 0.2% Triton-X 100 (Sigma T9284) for ten minutes, washed again with 1xPBS, and blocked in 10% Goat Serum (Invitrogen 16210-072), 1% BSA (Sigma A2153) in 1X PBS. Samples were then treated with primary antibodies (QCPN (DSHB) and αSMA (Abcam ab5694; 1:200)) overnight at 4°C. Slides were then washed with PBS and treated with secondary antibodies (Alexa 488 and 568 (Invitrogen A11001, A11004; 1:500) and DAPI (Invitrogen D3571; 1:10,000)). For four-channel labeling, slides were viewed using an Olympus FV-1000 confocal microscope (Vanderbilt CISR) to determine the locations of $QCPN^{+}$ cells, and then direct labeled using the Zenon Alexa Fluor Antibody Labeling Kits (Invitrogen: Z-25008, Z-25308, Z-25108) for laminin (Abcam ab11575), cytokeratin (Abcam ab9377), and MF20 (DSHB)). Slides were washed and mounted with ProLong mounting agent (Invitrogen P36930).

Characterizing Mesothelial Isolates

Mesothelia was isolated from E8, E10, or E12 embryonic hearts and intestine via microdissection from quail (*Coturnix coturnix japonicia*) embryos were staged accordingly (Ainsworth et al., 2010). Isolates were fixed for 1 hour in 4% formaldehyde in 1XPBS (pH 7.4), washed with 1XPBS, then sectioned and antibody labeled using the same techniques as described above in Immunohistochemical Analysis. All samples were imaged on the Olympus FV-1000 confocal microscope (CISR Core).

RT-PCR

PE and gut mesothelial tissues were isolated from chick and quail embryos. RNA was extracted from the isolates and cDNA was synthesized with Multiscribe reverse transcriptase (Invitrogen 4311235) and random primers, and then used in PCR reactions with the following primers (5'-3'): *Wt1* GGGACTCCGAGCTACGGCCA and AGGGTTTCACACCTGTGTGTCGT, *Tbx18* TCAGGACGTAACAGAATGGGACTGG and TCCGTACAGCGCACAGGGACT, *GAPDH* CAGCCTTCACTACCCTCTTG and ACGCCATCACTATCTTCCAG.

Mesothelial Cultures

Mesothelial isolates were dissected from HH14-16 PEs and E6, E8, E10, and E12 hearts, foregut and midguts in quail embryos. PE, epicardium, and gut mesothelial tissue were gently treated with Collagenase Type I (BD Biosciences 354236) and dissected into small pieces. The isolates were placed on

fibronectin-coated eight well slides (Nunc 154534) and cultured in Medium199 medium (Hyclone SH3025301) supplemented with 10% FBS (Hyclone SH3007103) and 1:1000 Penicillin/Streptomycin (Hyclone SV30010). Cultures were incubated at 37°C in 5% CO_2 for four to five days. The cells were fixed in 4% formaldehyde and labeled with antibodies including: cytokeratin (epithelial), QH1 (endothelial), and αSMA (smooth muscle) (see Immunohistochemical Analysis). All slides were then mounted with Prolong Gold (Invitrogen P36930) and imaged on the Olympus FV-1000 confocal microscope (CISR Core).

PE, Epicardial, and Gut Mesothelial Transplants

Quail tissue was dissected in 1XPBS from HH14-16 (PE) and E6, E8, E10 or E12 staged embryos. Non-mesothelial tissue was gently teased away from mesothelium, and then dissected into small pieces. 1% BSA coated pipette tips were used to carefully transfer isolates into 96-well plates containing a 3% neutral red solution (Sigma 4628) dissolved in Medium199 and placed in a 37°C incubator for 15 minutes. Samples were gently washed before transplantation. Chicken eggs (*Gallus gallus domesticus*) were windowed and embryos were lightly stained with a strip of neutral red (0.2mg/ml) in 1% agar then staged at HH13-17. Using forceps and a tungsten needle, a small hole was made in the pericardial cavity or between the splanchnic and somatic mesoderm in the chick embryo and the mesothelial isolate was placed. 1XPBS containing 1% penicillin/streptomycin solution was added to replace the volume in the egg, then the window was sealed with tape and eggs were incubated for 2-15 days.

Embryos were dissected, fixed, embedded, sectioned, and antibody labeled for analysis. Immunohistochemical analysis was performed as described above.

Results

Mesothelial isolates label with epithelial markers

Mesothelial cells are simple squamous epithelial sheets that cover coelomic organs. During development, some mesothelial cells undergo EMT, migrating into the layers of tissue beneath the mesothelial surface (Männer, 1999; Mikawa and Gourdie, 1996; Vrancken Peeters et al., 1999). Previous studies have demonstrated that mesothelial cells can be successfully cultured to determine the cell types to which mesothelia give rise (Bax et al., 2011; Cross et al., 2011; Kawaguchi et al., 2007; Yung and Chan, 2007). Additionally, PE cells have been transplanted *in vivo* to elucidate cell potential and lineage within an organism (Gittenberger-de Groot et al., 1998; Männer, 1999; Pérez-Pomares et al., 1997). In order to confirm that our isolates (PE, epicardium, and intestinal mesothelium) were epithelial in composition, we performed antibody labeling and RT-PCR analysis before transplantation. The isolates from the epicardium and intestine mesothelium were dissected, prepared for sectioning and antibody labeled. Epicardial and intestinal mesothelial isolates stained positive for laminin, cytokeratin, and fibronectin, confirming these tissues were comprised of epithelial cells (Figure 4.1 A-C, F-H). To determine if the isolates contained any vascular markers, they were labeled with the endothelial marker QH1 and smooth muscle

marker, αSMA (Figure 4.1 D-E, I-J, arrowhead). Few endothelial cells were identified and no smooth muscle cells were labeled in the isolates, confirming that the isolates were mainly epithelial.

More specific markers for mesothelium include the two transcription factors *Wt1* and *Tbx18*. Both *Wt1* and *Tbx18* were expressed in quail PE isolates and intestinal mesothelial isolates at E8, E10 and E12 in both quail and chick (Figure 4.1 K, L). We observed reduced expression of *Tbx18* in E8 isolates, in comparison to E10 and E12 isolates (Figure 4.1 K, L). This result indicates that *Tbx18* may be transiently expressed in the gut mesothelium. Overall, these data demonstrate that our starting product was epithelial in nature and did not contain any smooth muscle cells when transplanted into the host embryo.

Cultured mesothelial isolates differentiate into smooth muscle cells

Mesothelial cells are readily cultured and utilized to study the potential differentiative properties (Bax et al., 2011; Cross et al., 2011; Kawaguchi et al., 2007). To establish that cultured tissue can differentiate into smooth muscle cells in culture, PE, epicardial, and intestinal mesothelial isolates were each dissected from quail embryos and placed in culture. When grown for four to five days, the isolates migrated in a radial manner throughout the culture dish and labeled with epithelial markers, cytokeratin, and vascular markers, specifically SMA and QH1 (Figure 4.2 A-I). Most PE cells retained cytokeratin labeling and abundant smooth muscle cells at the leading edges (Figure 4.2 A, B). Epicardial cells in culture for this time period were mostly smooth muscle

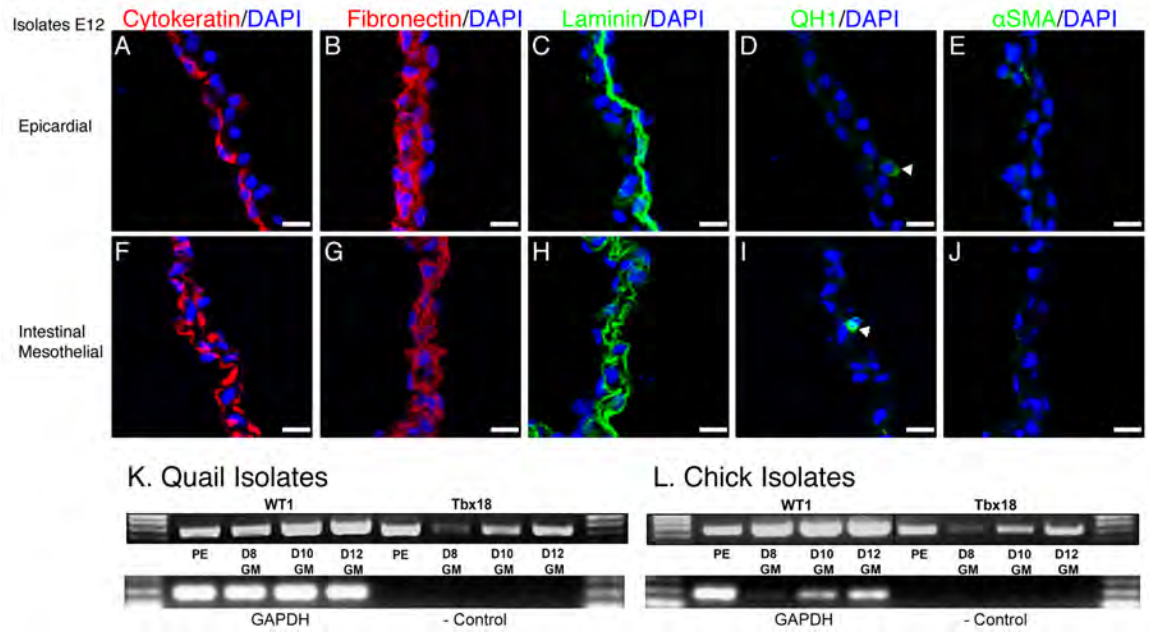

Figure 4.1 Mesothelial isolates are epithelial and contain no smooth muscle cells. A-E: Isolated quail epicardium at E12. **F-J**: Isolated quail gut mesothelium at E12. All isolates were labeled with epithelial markers (A, F cytokeratin; B, G fibronectin; C, H laminin) to confirm mesothelial nature of isolates before transplantation. Few cells in the isolates labeled for vascular markers QH1 (endothelial cells; D, I) and no cells labeled with αSMA (α-smooth muscle actin; E, J). **K-L**: RT-PCR of quail PE and intestinal mesothelial isolates revealed expression for *Wt1* and *Tbx18* E8, E10, and E12 quail and chick isolates. GAPDH expression was present in all samples as a positive control. All scale bars 10μm.

positive with a few cytokeratin cells interspersed between (Figure 4.2 D, E). Intestinal mesothelial cultures contained very few cytokeratin cells and were smooth muscle positive at the leading edges and throughout most of the culture (Figure 4.2 G, H). Interestingly, αSMA in the intestinal mesothelial isolates was much more robust than in the epicardial cells (compare Figure 4.2 E with Figure 4.1 H). This observation suggests that smooth muscle cells derived from epicardial isolates *in vitro* fluctuate in differentiate potential compared to intestinal mesothelial isolates. Additionally, in all cultures we observed some endothelial positive cells, most likely originating from the isolate (Figure 4.2 C, F, I). These data provide evidence that cultured mesothelial cells give rise to the same cell types, although differences in cell differentiation were observed. Due to this variability, we next investigated the potential of each isolate *in vivo*.

Transplanted intestinal mesothelial cells incorporate into analogous heart structures

Once mesothelial cells cover organs, their histology and function appear almost synonymous (Gittenberger-de Groot et al., 1998; Mikawa and Gourdie, 1996; Wilm et al., 2005). Thus, we hypothesized that the gut mesothelium would recapitulate migration of PE cells and differentiate into vascular cells when transplanted into the pericardial cavity. Using the chick-quail chimera system, quail mesothelia microdissected from the foregut and midgut was positioned near the heart of a chick host. Images of antibody labeled cells positive for QCPN (Quail not-Chicken Perinuclear marker) revealed that transplanted mesothelial

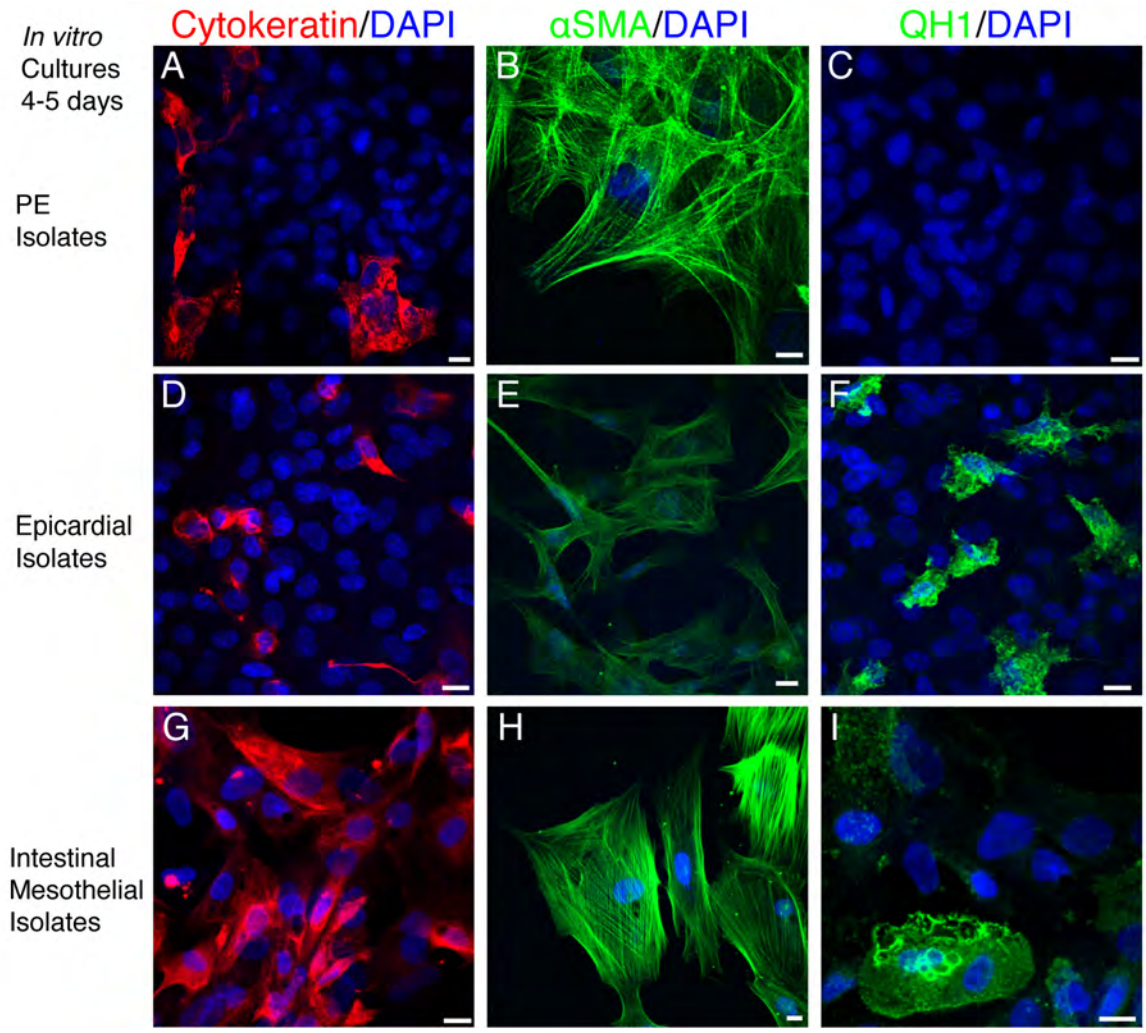

Figure 4.2 Cultured mesothelial isolates differentiate into smooth muscle cells. A-I: PE, epicardial, and intestinal mesothelial isolates labeled cytokeratin, αSMA, and QH1. **A-C:** PE isolates differentiated into smooth muscle (αSMA) (B) but not endothelial cells (C). **D-F**: Epicardial cells displayed weak smooth muscle but robust endothelial differentiation. **G-I:** Intestinal mesothelial cells retained their mesothelial identity as evidenced by cytokeratin staining (G) but also exhibited smooth muscle and endothelial phenotypes (H, I). All images were collected using comparable exposure settings. All scale bars 10μm.

cells migrated into the heart, spread throughout the endogenous epicardium and through many layers of tissue including the submesothelial space and myocardium (Figure 4.3 A-D). The incorporation of QCPN-positive cells into the epicardium was corroborated by co-labeling with cytokeratin (Figure 4.3 B-D, arrowheads). In samples grown to older stages (E17), sections through the heart confirmed the presence of smooth muscle cells within the coronary vessels as indicated by αSMA staining (Figure 4.3 F-M, arrowheads). However, in these samples, few cells were identified in the myocardium (Figure 4.3 J-M, yellow arrowhead). In comparing younger samples to older samples, we observed differences in the number of QCPN-positive cells, location of cells in blood vessels, and cells found in the endogenous mesothelium. These data demonstrate the plasticity of gut mesothelial cells when transplanted into an analogous environment. The mesothelial isolates like those of the PE are capable of incorporating into mesothelial structures and contributing of smooth muscle and fibroblast cells to the heart.

Epicardial cells integrate into organs in the peritoneum

Epicardial cells are derived from PE cells that have migrated over the heart and spread to form a single-layer sheet of cells. Some epicardial cells delaminate and dive into the myocardium via EMT to contribute fibroblasts, vascular smooth muscle cells, and pericytes to the heart (Gittenberger-de Groot et al., 1998; Mikawa and Gourdie, 1996). After testing the potential of gut mesothelial cells, we next asked if epicardial cells possess the same ability to

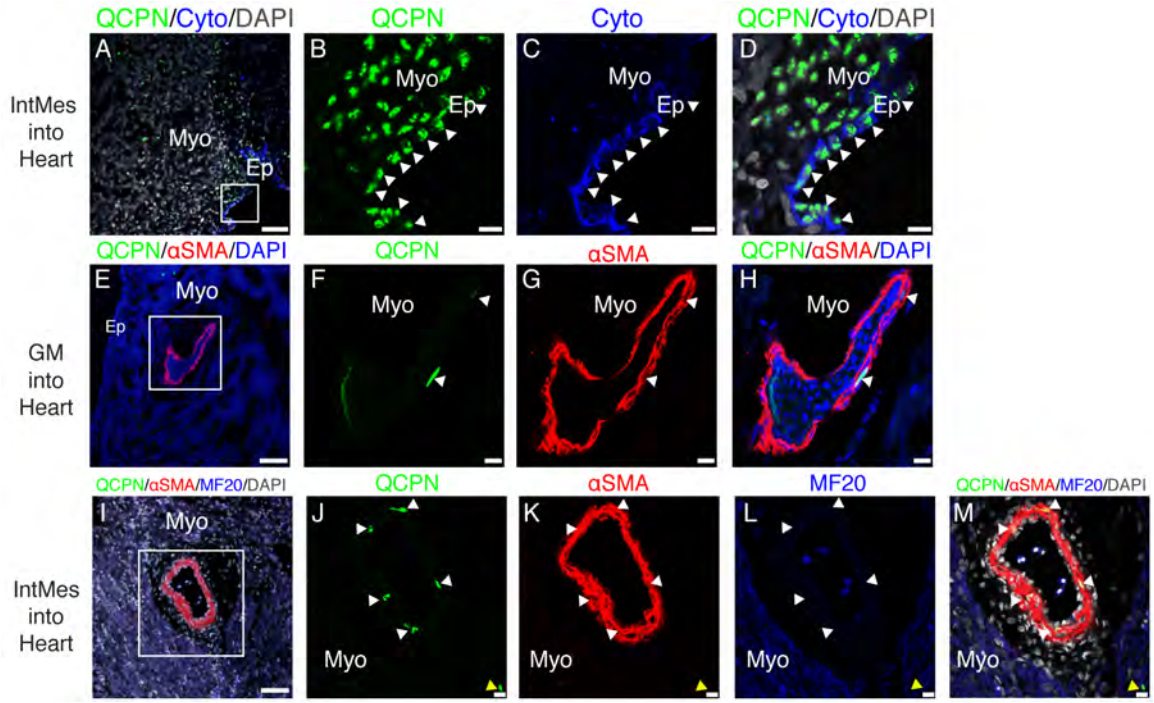

Figure 4.3 Gut mesothelium incorporates into epicardium and coronary vessels. Quail intestinal gut mesothelial isolates transplanted into the pericardial cavity of a chick host. **A**: E8 intestinal mesothelium transplanted into a HH17 chick host then analyzed three days later. **B-D**: Boxed region from A. Quail gut mesothelial cells (QCPN (Quail not-Chicken Perinuclear marker), green, arrowheads) assimilate into chicken epicardium and labeled with cytokeratin (Cyto, blue, arrowheads). Merge is shown in D (nuclei are in gray scale). **E**: E13 gut mesothelium placed in the pericardial cavity of a HH13 chick host, then analyzed 14 days later reveal quail cells in the heart. **F-G**: Quail mesothelial cells (QCPN, green, arrowheads) in a blood vessel (αSMA, red). **H**: Merge of F and G, QCPN-positive cells were also αSMA-positive. **I**: E10 intestinal mesothelium transplanted into a HH16 chick host then examined 14 days later. **J-M**: QCPN-positive cells (green, while arrowheads) were identified in a blood vessel (αSMA, red, white arrowheads) and among myocardial cells (MF20, blue, yellow arrowhead). QCPN cells clearly co-labeled with αSMA. Nuclei are in gray scale. Scale bars: 50μm (A, E, I) and 10μm (B-D, F-H, J-M). Ep, epicardium; GM, gut mesothelium; IntMes, intestinal mesothelium; Myo, myocardium.

migrate throughout the intestine and contribute vascular smooth muscle cells to this organ system. As a positive control, epicardial cells transplanted back into the pericardial cavity migrated throughout the organ, contributing cells to the epicardium and myocardium as labeled with QCPN (Figure 4.4 A-E). Transplanted quail epicardial cells were identified in the host chick epicardium via cytokeratin staining (Figure 4.4 B-E, white arrowheads). Quail cells were also identified in the subepicardial space and some retained cytokeratin staining (yellow arrowheads) while few cells stained positive for αSMA (data not shown). In contrast, epicardial cells transplanted into the peritoneum migrated into the small intestine but retained cytokeratin markers within the mesenchymal layer, or muscle layer (Figure 4.4 F-N). Additionally, a few cells in the mesenchyme were αSMA-positive (arrowheads) (Figure 4.4 G-J). We found these observations perplexing in that epicardial cells retained cytokeratin staining after migrating into the organ, but did not incorporate into the endogenous gut mesothelium. Collectively these data demonstrate a possible bias for the epicardial cells. When transplanted into the analogous environment these cells do not seem to acquire either mesothelial characteristics or other predicted phenotypes such as smooth muscle in vessels.

The developmental program of PE cells shifts when transplanted

As previously discussed, mesothelial cells in the heart and gut are different in origin and initial formation. Of the two, proepicardial (PE) cells are the progenitor cells of the epicardium and have been well characterized in terms of

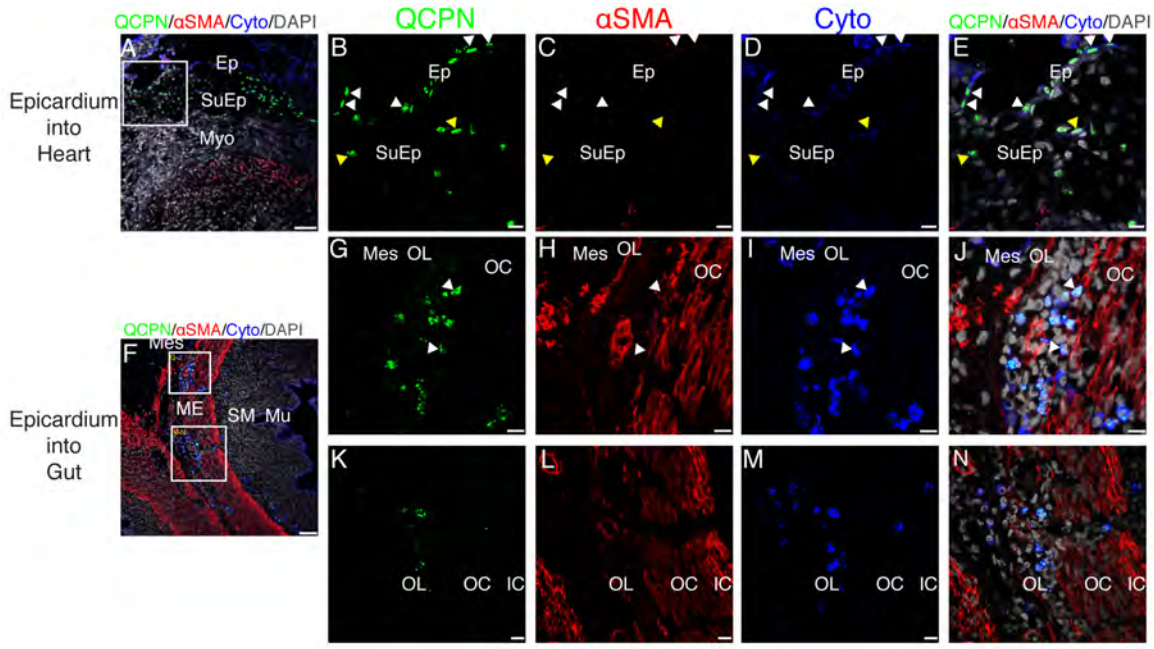

Figure 4.4 Epicardial cells possess a limited capacity to incorporate into intestinal tissues. Isolated quail epicardium transplanted into the pericardial and peritoneal cavities of chick hosts revealed limited potential of the cells to contribute to the analogous structure. **A**: Quail epicardium (E10.5; labeled with QCPN, green) transplanted into the pericardial cavity of HH16 chick host spread throughout the endogenous epicardium, subepicardium and myocardium. **B-E**: Inset from A. QCPN positive cells incorporate and co-label with cytokeratin (blue, white arrows) in the chick epicardium. A few quail cells in the subepicardial space also co-label with cytokeratin (yellow arrows). **F**: Transplanted E8 quail epicardium into the peritoneal cavity of HH17 chick host, then analyzed 14 days later. QCPN-positive cells migrate into the muscle and submucosa of the intestine. **G-J**: Higher magnification of F, upper inset. Quail cells are located in the muscle layers (αSMA, red) of the intestine (green) and only a few co-label with αSMA (arrowheads). **K-N**: Higher magnification of lower inset. QCPN-positive cells co-label with cytokeratin (blue) but not αSMA. No cells incorporated into the endogenous gut mesothelium or blood vessels. All nuclei are labeled in gray scale. Scale bars: 50μm (A, F) and 10μm (B-E, G-J, K-N). Ep, epicardium; IL, inner longitudinal muscle layer; ME, muscularis externa; Mes, mesothelium; Mu, mucosa; Myo, myocardium, OC, outer circular muscle layer; OL, outer longitudinal muscle layer; SM, submucosa SuEp, subepicardium.

cellular interactions, signaling pathways, histology, and regeneration (reviewed in (Pérez-Pomares and de la Pompa, 2011). Based on the differing programs of the mesothelial progenitor cells, we tested the potential of the PE cells by transplanting them into the pericardial cavity of a chick host. As shown in previous studies, the PE cells migrate over the endogenous epicardial tissue, incorporate into the epicardium, and migrate into the myocardium (Figure 4.5 A). In the inverse experiment, isolated PE cells were transplanted into peritoneum and the cells incorporated into several developing organs including the gut, liver, and/or kidney (data not shown). Interestingly these cells were capable of migrating into the organ, but instead of spreading they remained grouped and epithelial in nature, staining positive for fibronectin (Figure 4.5 B-I). In both samples reported here, the transplanted PE cells were more columnar in shape and no cells incorporated into the gut mesothelium. We observed this phenotype in several samples and in various coelomic organs. These results suggest that the PE cells undergo a shift in developmental program when placed in a seemly analogous environment and will not incorporate into the mesothelium or blood vessels of that organ.

Discussion

Mesothelial cells are a major component of the epicardium in the heart and serosa of the intestine. In development, mesothelial cells cover the heart and intestine, and will contribute important cell types to each organ. While these developmental properties are similar, our data suggest that the plastic nature of

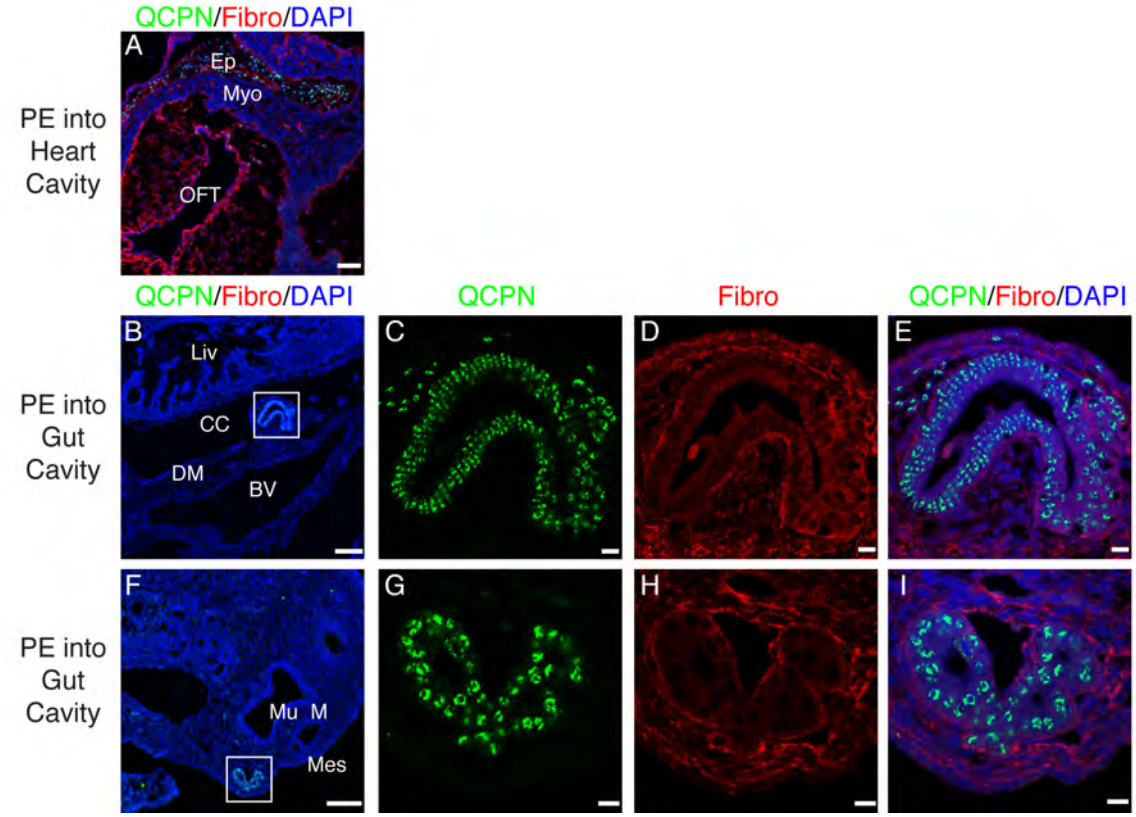

Figure 4.5 Transplanted PE cells do not incorporate into the gut mesothelium. Quail PE cells were transplanted into chick hosts then analyzed. **A**: Representative image of PE cells transplanted into chick pericardial cavity. Quail cells (QCPN, green) migrate around and incorporate into endogenous chick epicardium, as marked by fibronectin (Fibro, red). Cells also migrate into the myocardium. **B**: Quail PE cells (HH14, QCPN, green) transplanted into the peritoneal cavity of a HH16 host then assessed three days later revealed cells in the intestinal mesentery, but just below the mesothelial surface. **C-E**: Higher magnification of B. QCPN positive cells (C) also co-labeled with fibronectin (D, Fibro, red), indicating retained epithelial characteristics. **F**: In another sample, HH15 PE cells are placed in a HH13.5 chick peritoneal cavity, and analyzed two days later. **G-I**: QCPN-positive cells (G) again migrate into the gut tube, organize and cluster just below the gut mesothelial surface. These cells also retain epithelial characteristics as per labeling with fibronectin (H, red). Scale bars: 50μm (A, B, F) and 10μm (C-E, G-I). BV, blood vessel; CC, coelomic cavity; DM, dorsal mesentery; Ep, epicardium; Myo, myocardium; OFT, outflow tract.

mesothelial cells differ among the populations. Intestinal mesothelial cells will migrate into any coelomic organ, but were the only mesothelial cell type that incorporated into endogenous epicardium and contributed smooth muscle cells to the major vessels of the heart. While transplanted epicardial or PE cells also migrated into coelomic organs, they did not incorporate into the endogenous mesothelium, or differentiate into non-epithelial cell types. These data identify unique incompatibilities between heart and intestinal mesothelial cell capacities, which suggest that only heart mesothelial cells are specified and restricted to the heart during organogenesis.

During examination of the mesothelial plasticity, we predicted that established mesothelium, such as the epicardium and intestinal mesothelium, retained similar capabilities upon transplantation. However, distinctive differences between epicardial and intestinal mesothelial potential began to emerge. These studies demonstrated the plastic nature of intestinal mesothelium in integrate with the heart but an absence in this potential in the epicardium to the intestine. These data corroborated previously posed concepts regarding the difference between the development of heart and intestinal mesothelial cells, including intestinal mesothelial origin (Winters et al., 2012). Thus, the heart mesothelium exhibits nonconforming characteristics during development among the coelomic organs. These data also lead to questions concerning cell specification within coelomic organs, including cell autonomy or regional determination. Previous studies have focused on signaling in development of the epicardium and cell differentiation, whereas few studies investigate signaling in the intestinal

mesothelium. Fundamental analysis of mesothelial signaling and differentiation in the intestine are required to determine the mechanisms involved in cell specification and communication between intestinal tissues.

Transplantation of the PE, the progenitor cell population of the epicardium, resulted in similar observed phenotypes to the transplanted epicardium. PE cells migrated into coelomic organs, but did not incorporate into intestinal mesothelium or intestinal cell types. These data were of particular interest, since they demonstrated that progenitor cells might possess differing programs from developed mesothelial tissues. As demonstrated in Figure 4.3, epicardial mesothelial isolates transplanted into coelomic cavities presented a similar migratory and nonconforming phenotype as the PE. Further analysis, is necessary to determine if heart mesothelial cells possess intrinsic properties, such as direction towards a specific cell type or if the environment, or organs, are signaling inhibiting cues to the PE cells, and thus driving them to retain cell polarity when placed in an analogous cavity.

Overall, these data suggest that the PE and epicardial cells appear to abide by their own developmental program regarding origin and cell potential. Conversely, intestinal mesothelial cells maintain a level of plasticity that permits incorporation and contribution in both heart and gut organs. Continued investigation is required to ascertain the developmental similarities and differences between heart and intestinal mesothelia. Importantly, these data provide novel evidence of the similar, yet distinct potential of mesothelial cell populations. Understanding the flexibility of intestinal mesothelial cells will allow

researchers and clinicians to develop targeted therapies for patients following injury.

References

Ainsworth, S. J., Stanley, R. L. and Evans, D. J. R. (2010). Developmental stages of the Japanese quail. *J. Anat.* **216**, 3-15.

Bax, N. a. M., Van Oorschot, A. a. M., Maas, S., Braun, J., Van Tuyn, J., De Vries, A. a. F., Groot, A. C. G.-D. and Goumans, M. J. (2011). In vitro epithelial-to-mesenchymal transformation in human adult epicardial cells is regulated by TGFβ-signaling and WT1. *Basic Res Cardiol* **106**, 829-847.

Cross, E. E., Thomason, R. T., Martinez, M., Hopkins, C. R., Hong, C. C. and Bader, D. M. (2011). Application of Small Organic Molecules Reveals Cooperative TGFβ and BMP Regulation of Mesothelial Cell Behaviors. *ACS Chem Biol* **6**, 952-961.

Dettman, R. W., Denetclaw, W., Ordahl, C. P. and Bristow, J. (1998). Common epicardial origin of coronary vascular smooth muscle, perivascular fibroblasts, and intermyocardial fibroblasts in the avian heart. *Dev Biol* **193**, 169-181.

Gittenberger-De Groot, A. C., Vrancken Peeters, M. P., Mentink, M. M., Gourdie, R. G. and Poelmann, R. E. (1998). Epicardium-derived cells contribute a novel population to the myocardial wall and the atrioventricular cushions. *Circ Res* **82**, 1043-1052.

Hamburger, V. and Hamilton, H. L. (1992). A series of normal stages in the development of the chick embryo. 1951. *Dev Dyn* **195**, 231-272.

Ho, E. and Shimada, Y. (1978). Formation of the epicardium studied with the scanning electron microscope. *Dev Biol* **66**, 579-585.

Ishii, Y., Langberg, J. D., Hurtado, R., Lee, S. and Mikawa, T. (2007). Induction of proepicardial marker gene expression by the liver bud. *Development* **134**, 3627-3637.

Katz, T. C., Singh, M. K., Degenhardt, K., Rivera-Feliciano, J., Johnson, R. L., Epstein, J. A. and Tabin, C. J. (2012). Distinct compartments of the proepicardial organ give rise to coronary vascular endothelial cells. *Dev Cell* **22**, 639-650.

Kawaguchi, M., Bader, D. M. and Wilm, B. (2007). Serosal mesothelium retains vasculogenic potential. *Dev Dyn* **236**, 2973-2979.

Manasek, F. J. (1969). Embryonic development of the heart. II. Formation of the epicardium. *J Embryol Exp Morphol* **22**, 333-348.

Männer, J. (1992). The development of pericardial villi in the chick embryo. *Anat Embryol* **186**, 379-385.

Männer, J. (1999). Does the subepicardial mesenchyme contribute myocardioblasts to the myocardium of the chick embryo heart? A quail-chick chimera study tracing the fate of the epicardial primordium. *Anat Rec* **255**, 212-226.

Mikawa, T. and Gourdie, R. G. (1996). Pericardial mesoderm generates a population of coronary smooth muscle cells migrating into the heart along with ingrowth of the epicardial organ. *Dev Biol* **174**, 221-232.

Mutsaers, S. E. (2004). The mesothelial cell. *Int J Biochem Cell Biol* **36**, 9-16.

Nahirney, P. C., Mikawa, T. and Fischman, D. A. (2003). Evidence for an extracellular matrix bridge guiding proepicardial cell migration to the myocardium of chick embryos. *Dev Dyn* **227**, 511-523.

Pérez-Pomares, J.-M. and De La Pompa, J. L. (2011). Signaling during epicardium and coronary vessel development. *Circ Res* **109**, 1429-1442.

Pérez-Pomares, J. M., Macías, D., García-Garrido, L. and Muñoz-Chápuli, R. (1997). Contribution of the primitive epicardium to the subepicardial mesenchyme in hamster and chick embryos. *Dev Dyn* **210**, 96-105.

Red-Horse, K., Ueno, H., Weissman, I. L. and Krasnow, M. A. (2010). Coronary arteries form by developmental reprogramming of venous cells. *Nature* **464**, 549-553.

Van Wijk, B., Van Den Berg, G., Abu-Issa, R., Barnett, P., Van Der Velden, S., Schmidt, M., Ruijter, J. M., Kirby, M. L., Moorman, A. F. M. and Van Den Hoff, M. J. B. (2009). Epicardium and myocardium separate from a common precursor pool by crosstalk between bone morphogenetic protein- and fibroblast growth factor-signaling pathways. *Circ Res* **105**, 431-441.

Virágh, S. and Challice, C. E. (1973). Origin and differentiation of cardiac muscle cells in the mouse. *J Ultrastruct Res* **42**, 1-24.

Vrancken Peeters, M. P., Gittenberger-De Groot, A. C., Mentink, M. M. and Poelmann, R. E. (1999). Smooth muscle cells and fibroblasts of the coronary arteries derive from epithelial-mesenchymal transformation of the epicardium. *Anat Embryol* **199**, 367-378.

Wessels, A. and Pérez-Pomares, J. M. (2004). The epicardium and epicardially derived cells (EPDCs) as cardiac stem cells. *Anat Rec* **276**, 43-57.

Wilm, B., Ipenberg, A., Hastie, N. D., Burch, J. B. E. and Bader, D. M. (2005). The serosal mesothelium is a major source of smooth muscle cells of the gut vasculature. *Development* **132**, 5317-5328.

Winters, N. I., Thomason, R. T. and Bader, D. M. (2012). Identification of a novel developmental mechanism in the generation of mesothelia. *Development* **139**, 2926-2934.

Yung, S. and Chan, T. M. (2007). Mesothelial cells. *Perit Dial Int* **27 Suppl 2**, S110-115.

CHAPTER V

CONCLUSIONS AND FUTURE DIRECTIONS

Conclusions

This dissertation provides a descriptive baseline for mesoderm derived tissue morphogenesis. My data focus on the mesodermal development in the small intestine and the plasticity of heart and gut mesothelial cell populations. The most important finding of this work is that mesothelial development in the heart and gut is fundamentally different, despite exhibiting similar cellular characteristics and differentiative capacities. Until now, researchers have regarded the heart as the gold standard for all mesothelial morphogenesis. However, my data provide evidence that the initial developmental processes of heart mesothelia are not conserved in the gut. The experiments described in the previous chapters focus on the development of the gut mesothelium and establish novel mechanisms that: reveal cellular location and association with neighboring tissues, the origin of the intestinal mesothelial cells, and the ability to form similar cell types in distinct organs (Figure 5.1 A-E). This work will enable the field to take new directions regarding the molecular and genetic programs regulating the development and function of mesothelia.

Chapter II of this dissertation established a detailed timeline of the mesodermal compartment development in the small intestine. These data

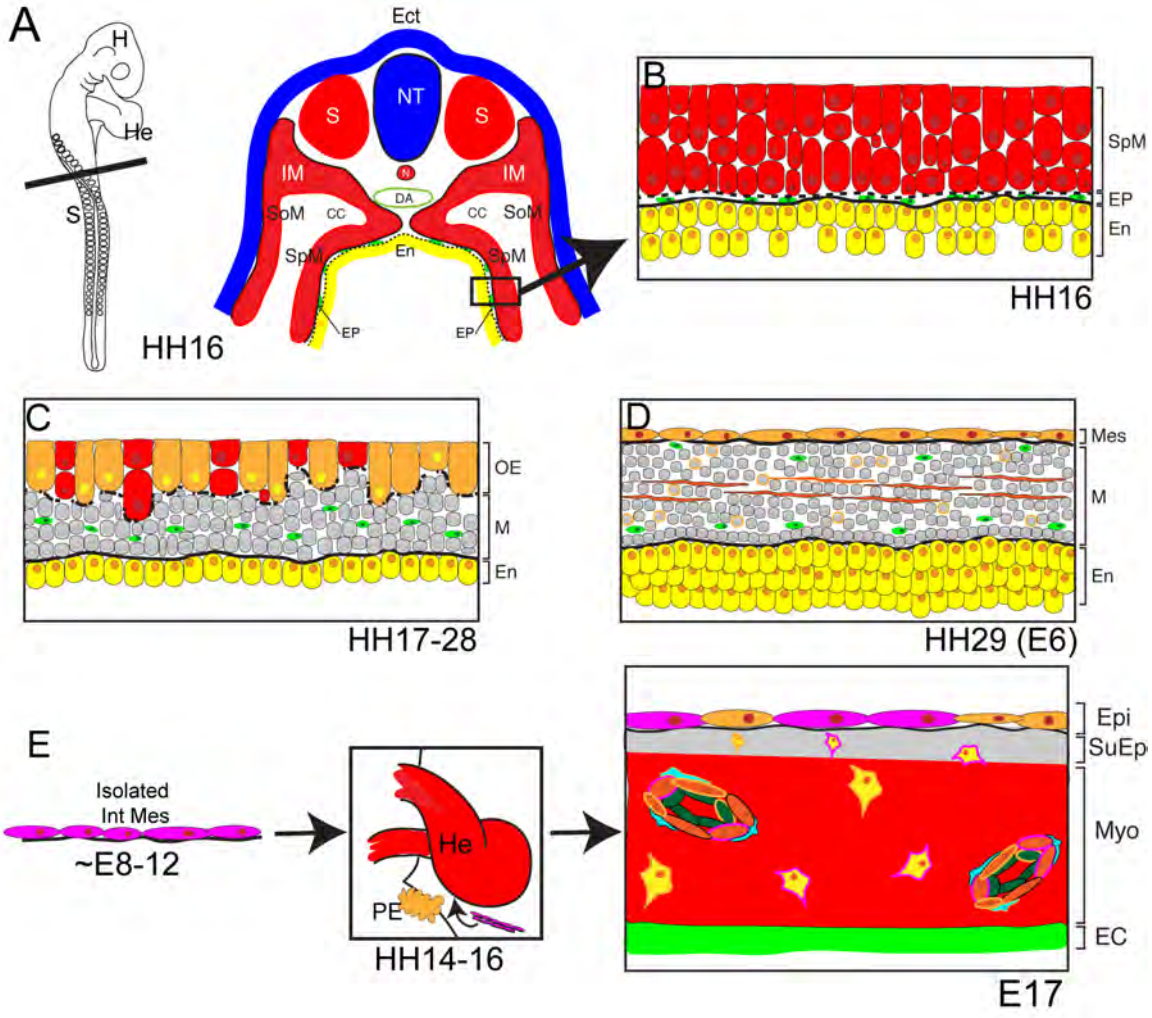
A
H
He
S
HH16
Ect
NT
S
S
IM
IM
DA
SoM
CC
CC
SoM
SpM
En
SpM
EP
EP
B
SpM
EP
En
HH16
C
OE
M
En
HH17-28
D
Mes
M
En
HH29 (E6)
E
Isolated
Int Mes
~E8-12
He
PE
HH14-16
Epi
SuEp
Myo
EC
E17

Figure 5.1 Gut mesothelial cells originate from the splanchnic mesoderm and are plastic in multiple environments. A-D: Schematics representing normal developmental processes. **A**: Schematic of avian embryo at E16, cross-section through developing gut tube region. At this stage, the gut tube is open. **B**: Cross-section through open gut tube reveals three compartments: Splanchnic mesoderm (red cells), a thin mesenchyme containing a few endothelial cells (green) and endoderm (yellow). Note two basements (black lines) are present; the endodermal basement membrane is continuous while the splanchnic mesodermal basement membrane is fragmented. **C**: As development proceeds, mesenchymal cells (gray cells) populate the mesenchymal (M) compartment. At these stages (HH17-28), splanchnic mesoderm is referred to as the outer epithelium (OE). Cells within this compartment shift towards a mesothelial phenotype (orange cells). The OE basement membrane presents dynamic phenotypes (transitioning between continuous and fragmented) as denoted by the dashed line. The endoderm is one layer of cells at this stage. **D**: Finally at HH29 (E6), a mesothelium (Mes, orange cells) is present. The mesenchyme (M) begins to organize: smooth muscle cells are present (red spindle-shaped cells), an endothelial plexus arranges into two layers (green cells), and stroma and fibroblasts (gray cells) are present throughout. Orange outlined cells represent mesothelial derivatives in the mesenchyme. The endoderm is pseudostratified. **E**: Observed contributions of intestinal mesothelium to the heart. Isolated quail gut mesothelium (pink) transplanted into the pericardial cavity of a chick host. Cross-section through the chick heart after 14 days incubation reveals contribution of chick epicardial cells (outlined in orange) to heart cell types. Gut mesothelial cells (labeled in pink) incorporate into the epicardium, contribute fibroblasts to the myocardium, and smooth muscle cells to the blood vessels (outlined in pink). CC, coelomic cavity; DA, dorsal aorta; EC, endocardium; Ec, ectoderm; En, endoderm; EP, endothelial plexus; Epi, epicardium; H, head; He, heart; IM, intermediate mesoderm; M, mesenchyme; Mes, mesothelium; Myo, myocardium; nc, notochord; NT, neural tube; OE, outer epithelium; S, somite; SoM, somatic mesoderm; SpM, splanchnic mesoderm; SuEp, subepicardium.

revealed new concepts involving shifts in the architecture of the splanchnic mesoderm and basement membrane dynamics, both histologically observed in the intestine before and upon the development of a mesothelium. The gut primordium forms as a flat sheet of layered cells, and is composed of splanchnic mesoderm, endoderm and a thin open space between containing endothelial cells (Figure 5.1 A, B, Meier, 1980). Studies have investigated basement membranes of the intestine, but mainly focused on the endodermal basement membrane (Lefebvre et al., 1999; Simon-Assmann et al., 1995). Currently, few studies provide data that explore basement membrane dynamics, closure of the coelom, and changes in the outer epithelium. Additionally, it is unclear if mesenchymal cells proliferate early in intestinal development and if most originate from the splanchnic mesoderm. While both basement membranes in the intestine are important for distinguishing what we term the “intestinal compartments,” we focused on the outer epithelial basement membrane because of the numerous breakdown and solidification events (Figure 5.1 C). Two theories to describe compartment formation arose from these observations: first, the splanchnic mesoderm may be the source of cells in the mesenchymal space (also referred to as the “space of Zijlstra”), and second, basement membrane dynamics are linked to mesothelial formation. These data suggest possible EMT or mesenchymal-to-epithelial transitions (MET) between the splanchnic mesoderm and mesenchymal space early in compartment organization. Overall, the histological evidence from our studies established detailed changes in the

splanchnic mesoderm and outer epithelium of the intestine that may be spatially and temporally correlated to the development of the mesothelium.

Generally, individual components of intestinal development are studied independently versus investigating components in a spatial and temporal context. Most studies focus on endodermal development, nervous system formation or vascular organization, for example, but may not associate one event with the other. Recent reports have started to link these developmental processes in various intestinal layers (Mao et al., 2010; Nagy et al., 2009). Murine conditional gene targeting experiments demonstrated that *Shh* and *Ihh* expression overlap in the endoderm, where they signal to mesenchymal progenitors to proliferate, thus stimulating smooth muscle differentiation (Mao et al., 2010). In another study, Nagy and colleagues showed vascular cells are intimately involved with the organization, migration, and proliferation of enteric neurons (Nagy et al., 2009). These findings are significant, but whether other developmental processes occur concurrently remains unknown. Additionally, gut mesodermal development is understudied in the field, especially in the early embryo. My data address this gap, providing the developmental timeline of mesodermal development and correlating concurrent developmental processes in the intestine at various time points in the avian embryo. Highlighting one example, at E6, a pivotal time in intestinal development, a number of interesting events emerge: the gut tube closes, a mesothelium and organized endothelial plexus are present, and visceral muscle forms (Figure 5.1 D). Whether these events are interdependent is not clear and requires further investigation. My data provide a comprehensive

approach for visualizing and integrating mesodermal development in the context of spatiotemporal studies.

These findings regarding mesodermal development in the intestine led us to investigate the origin of the mesothelium (Chapter III). Previous work suggested the gut mesothelium arrived from ‘non-resident cells’ and that gut mesothelial cells shared the same capacity to migrate over the gut, just as epicardial cells migrate over the heart (Wilm et al., 2005). However, these studies did not provide the direct lineage tracing data to corroborate these claims. Therefore, the current work utilizes direct lineage tracing techniques to establish a completely different model: gut mesothelial cells develop from a local population of cells broadly distributed in the splanchnic mesoderm (Figure 5.1 C, D). Additionally, directly labeled cells revealed the lineage of splanchnic mesoderm-derived components including vascular smooth muscle cells, stromal cells, and a few visceral smooth muscle cells. For the first time, these data demonstrate that not all mesothelial cell populations arise in the same manner, supporting the notion that organ development differs between the pericardial and peritoneal cavities.

Based on previous data in the literature, I initially hypothesized that mesothelial cell populations were developmentally compatible between the heart and intestine. Before the work presented in this dissertation, the heart and intestine mesothelium appeared similar in form and function: simple squamous cells cover coelomic organs and some cells undergo EMT to contribute vascular cells to the organs. In Chapter IV, cell potential was tested by surgically

exchanging the embryonic heart and gut mesothelium. From these experiments, I expected all mesothelial cell types to incorporate and contribute vasculogenic and stromal cells in any coelomic organ. Unexpectedly, we observed differences in the mesothelial cell potential. The gut mesothelial cells migrated and incorporated into the endogenous epicardium and myocardium, contributed smooth muscle cells to major vessels, and fibroblasts and myofibroblasts to the myocardium when transplanted in the pericardial cavity (Figure 5.1 E). In contrast, epicardium transplanted into the peritoneal cavity did not produce similar cell types in the intestine, epicardial cells migrated into the organ but never lost epithelial markers. Few, if any, cells co-stained with other cell types in the gut, and no epicardial cells incorporated into the gut mesothelium. Adding more strength to the argument that epicardial and gut mesothelial cells possess different cellular capabilities, transplanted PE cells that only migrated into the gut grouped close to the organ surface, and retained epithelial characteristics. The preservation of cell polarity in PE cells could be due in part to defects in downregulation of junctional molecules, such as cadherins. Adhesive properties of mesothelial cells, especially PE cells, should be examined more closely, with a focus on the regulation of adherens junctions.

Overall, heart mesothelial cell populations may appear similar to gut mesothelia, but when placed in an analogous coelomic cavity, heart mesothelial cells will not undergo the same differentiation processes. My findings raise questions concerning mesothelial cell specification in progenitor populations and

developed tissues. My data also suggests that organs may relay signals of attraction or repulsion to the transplanted tissue.

Collectively, data from this dissertation provide a new paradigm for mesothelial development. The major findings described in this dissertation include: 1) the developmental timing of mesoderm in the small intestine and the precise stage when a mesothelium is present, 2) intestinal mesothelial cells originate from resident cells in the splanchnic mesoderm, and 3) intestinal mesothelial cells possess plastic properties, in contrast to heart mesothelial cells which are limited in their cellular potential. We postulate that the differences between heart and gut mesothelium stem from the origin of the mesothelial tissue, even though the developed tissues appear histologically and functionally similar. In comparing the heart and gut mesothelial anlages, the PE develops exogenously to the heart, while gut mesothelium develops from the endogenous or local splanchnic mesoderm, inferring possible distinctive signaling in the induction of the two populations. If the mesothelial populations contain or respond to varying instructive cues, it is clear that the gut mesothelium possesses adaptable properties but the heart mesothelium does not. Because of the focus on the intestinal mesothelium, I anticipate these data will facilitate the innovative discovery of developmental processes and a better understanding how these cells function in the repair of adult tissues.

Future Directions

The results described in this dissertation establish the framework of spatiotemporal morphogenesis of the splanchnic mesoderm, mesenchyme, and mesothelium of the intestine during development with reference to vasculogenesis. With this foundational data in hand, future studies elucidating genetic, molecular, cellular, and mechanistic properties would be the next step to elaborate gut morphogenesis in the embryo. Based on my conclusions, major questions arise concerning mesodermal and mesothelial development: 1) which signaling molecules are involved in intestinal mesodermal and mesothelial morphogenesis? 2) What cell types do intestinal mesothelial and mesenchymal progenitors give rise to? 3) What are the genetic differences between the different mesothelial populations and ultimately progenitors? 4) Do adhesive properties play a role in mesothelial progenitor cell composition and potential? This section will outline proposed experiments to explore these questions.

The basement membranes defining the compartments of the intestine are established early in development and retained throughout adulthood. In order to better understand the dynamics, particularly of the outer epithelial basement membrane, signaling and cellular migration must be more closely investigated. The observation of basement membrane dispersal and solidification suggest a possible EMT event. To explore these dynamics in depth, expression patterns of candidate markers of EMT processes should be examined in the avian gut (i.e. *TGFβ, BMP, Notch, FGF, EGF, Wnt, Snail*) (Yang and Weinberg, 2008).

Additionally, matrix metalloprotease (MMP) activity during this process may also provide insight into EMT events, as these proteases are required prior to cellular dispersal (Duong and Erickson, 2004; Vu and Werb, 2000). Determining if common signaling factors are expressed between the splanchnic mesoderm and mesenchymal space may provide answers in addition to our data that splanchnic mesoderm contributes majority of the cells to the mesenchymal space.

Once it is determined which signaling molecules are present during basement membrane dynamics and EMT processes, it will be possible to systematically evaluate each signaling molecule involved and study its function in relation to mesothelial and mesenchyme morphogenesis in the mammalian system. Mouse models have been employed to study epicardial requirement in the embryo. In these particular mutants, disruption of *Wt1*, *VCAM-1*, or *α4-integrin* resulted in embryonic lethality, commonly due to defects in epicardial formation (Kwee et al., 1995; Moore et al., 1999) or lack of an epicardium (Yang et al., 1995). However, these reports did not assess intestine or intestinal mesothelial morphology. Since a mesothelium is present before embryonic death, analyzing the guts from these mutant animals may provide evidence of common genes involved in mesothelial development.

The cell populations of the mesenchymal space include a large variety of cell types, all required for proper intestinal function. However, the development of the early mesenchymal space in the intestinal primordial is particularly understudied. Studies investigating proliferation in the avian intestine confirmed consistent mitotically active mesenchymal cells at stages E5 and E12 throughout

the entire length of the intestine (Savin et al., 2011). This study did not investigate earlier stages, particularly the stages at which we observe modifications of the outer basement membrane. Creating a serial section library of stages before E5 up through E12 labeled with phospho-H3 antibody may easily determine if cells are proliferating more rapidly at particular stages prior to gut tube closure and mesenchymal expansion. It would be fascinating to observe levels of mitotic activity during the key time points, especially throughout transitions in the outer basement membrane and outer epithelium, to determine how or if mesenchymal expansion is associated with development of the intestinal mesothelium.

The splanchnic mesoderm is comprised of resident cells that contribute the majority of the intestinal mesothelial cells (Chapter IV). However, we remain curious about the origin of mesenchymal cells, such as the source of visceral muscle cells. Cell culture experiments would determine cell potential in a controlled environment. To explore potential cell types derived from the mesoderm, isolated splanchnic mesoderm and endoderm could be cultured individually. Based on our hypothesis that the splanchnic mesoderm contributes cells to the mesenchyme, we would expect the splanchnic mesoderm cells to differentiate into mesothelial, endothelial, possibly muscle, and stromal cells.

We have substantial evidence that the heart and gut mesothelial cells develop under different developmental programs (Chapters III and IV). Thus, it is likely that the molecular processes involved in the formation of these two organs are varied. Identifying gene candidates that are distinct between these

populations and that participate in their formation is prerequisite to advancing the field. Microarray analysis is a useful tool to reveal expression patterns and regulation of molecules. This technique can be employed to identify similarities and discrepancies between (1) PE and epicardium and, (2) splanchnic mesoderm from the gut tube and intestinal mesothelial cells. RNA would be collected from these isolates, PE, epicardium and intestinal mesoderm from E8, E10, and E12 staged embryos. These tissues would be the starting point for this analysis since we have reported discrepancies between mesothelial cellular potential *in vivo* (Chapter IV). From these data, we can compare changes in gene expression between progenitor populations and each mesothelia, thus deciphering different expression profiles between heart and intestinal mesothelia. Eventually, this information would generate a framework of mesothelial development in the intestine that would lay groundwork for mechanistic understanding. Moreover, it may be possible to assess the similar genes expressed in all tissues to determine if candidate mesothelial-specific markers exist. This would provide innovative and useful information to all mesothelial organs.

Another understudied aspect of mesothelial development is cell adhesion properties. Our data demonstrated different cell characteristics between PE, epicardium and gut mesothelium when transplanted into analogous environments. Particularly, PE cells migrated into gut tube-derived organs then remained clustered. Epicardial cells migrated and scattered through the mesenchyme of the gut, but retained epithelial markers. In contrast, intestinal mesothelial cells

spread out when transplanted into any coelomic organ. Only a few studies have focused on the adhesive properties of mesothelial cells (Bax et al., 2011; Cross et al., 2011; Osler and Bader, 2004). Thus, it would be intriguing to explore epithelial adhesion proteins in the context to how these molecules are altered when mesothelial cells are isolated. First, I would identify and compare specific epithelial junctional proteins (such as occludins, cadherins, and integrins) in mesothelial progenitor and cell populations using antibody labeling. Next, to explore the properties of cell adhesion among mesothelial populations, I would employ hanging drop co-cultures (Krieg et al., 2008; Timmins et al., 2004). Essentially, individual cells from different populations are dissociated, labeled, and aggregated, then placed in suspended drops in culture. The organization of the cells is then analyzed using antibody labeling and confocal microscopy. Based on what we observe in the transplant experiments, I predict that PE cells will only group together, while epicardial and gut mesothelial cells may assemble with each other. These studies would provide further evidence of potential similarities or disparities among mesothelial cell populations. Additionally, a better understanding of adhesion properties among precursor mesothelial cells (PE) and fully formed mesothelium (epicardium, gut mesothelium) may provide insight into potential mechanisms that are involved in maintenance of the adult structure.

From exhaustive literature searches we found that the field is disjointed, in that researchers generally tend to focus on a particular aspect of gut development. Thus, we propose creating a website that will house all

developmental gut data. From our mesodermal studies (Chapter II), we not only established a comprehensive timeline of key intestinal developmental processes, but correlations between events at specific stages began to emerge. Providing such data to the field in the format of a website would allow for creative collaboration between gut laboratories. This website would be open access and accessible for contribution from any published or unpublished data. Labs within the Vanderbilt University community have created such sites for their field of biology. One such successful example is the Beta Cell Consortium which "facilitat[es] interdisciplinary collaborations to advance our understanding of pancreatic islet development and function" via this online resource (Consortium, 2012). Designing, creating, and updating a gut development database would be a tremendous undertaking, but would ultimately provide a forum for gut researchers and provide useful information to biological, medical, and academic communities.

These future directions highlight several experiments that can be employed to understand general mesodermal development and more specifically mesothelial development. It is important to continue elucidating morphogenesis of these structures, and incorporate novel studies investigating molecular regulation in mesodermal development.

References

Bax, N. a. M., Van Oorschot, A. a. M., Maas, S., Braun, J., Van Tuyn, J., De Vries, A. a. F., Groot, A. C. G.-D. and Goumans, M. J. (2011). In vitro epithelial-to-mesenchymal transformation in human adult epicardial cells is regulated by TGFβ-signaling and WT1. *Basic Res Cardiol* **106**, 829-847.

Consortium (2012). "Beta Cell Consortium." Retrieved 3 November 2012, from http://www.betacell.org/.

Cross, E. E., Thomason, R. T., Martinez, M., Hopkins, C. R., Hong, C. C. and Bader, D. M. (2011). Application of Small Organic Molecules Reveals Cooperative TGFβ and BMP Regulation of Mesothelial Cell Behaviors. *ACS Chem Biol* **6**, 952-961.

Duong, T. D. and Erickson, C. A. (2004). MMP-2 plays an essential role in producing epithelial-mesenchymal transformations in the avian embryo. *Dev Dyn* **229**, 42-53.

Krieg, M., Arboleda-Estudillo, Y., Puech, P.-H., Käfer, J., Graner, F., Müller, D. J. and Heisenberg, C.-P. (2008). Tensile forces govern germ-layer organization in zebrafish. *Nat Cell Biol* **10**, 429-436.

Kwee, L., Baldwin, H. S., Shen, H. M., Stewart, C. L., Buck, C., Buck, C. A. and Labow, M. A. (1995). Defective development of the embryonic and extraembryonic circulatory systems in vascular cell adhesion molecule (VCAM-1) deficient mice. *Development* **121**, 489-503.

Lefebvre, O., Sorokin, L., Kedinger, M. and Simon-Assmann, P. (1999). Developmental expression and cellular origin of the laminin alpha2, alpha4, and alpha5 chains in the intestine. *Dev Biol* **210**, 135-150.

Mao, J., Kim, B.-M., Rajurkar, M., Shivdasani, R. A. and Mcmahon, A. P. (2010). Hedgehog signaling controls mesenchymal growth in the developing mammalian digestive tract. *Development* **137**, 1721-1729.

Meier, S. (1980). Development of the chick embryo mesoblast: pronephros, lateral plate, and early vasculature. *J Embryol Exp Morphol* **55**, 291-306.

Moore, A. W., Mcinnes, L., Kreidberg, J., Hastie, N. D. and Schedl, A. (1999). YAC complementation shows a requirement for Wt1 in the development of epicardium, adrenal gland and throughout nephrogenesis. *Development* **126**, 1845-1857.

Nagy, N., Mwizerwa, O., Yaniv, K., Carmel, L., Pieretti-Vanmarcke, R., Weinstein, B. M. and Goldstein, A. M. (2009). Endothelial cells promote migration and proliferation of enteric neural crest cells via beta1 integrin signaling. *Dev Biol* **330**, 263-272.

Osler, M. E. and Bader, D. M. (2004). Bves expression during avian embryogenesis. *Dev Dyn* **229**, 658-667.

Savin, T., Kurpios, N. A., Shyer, A. E., Florescu, P., Liang, H., Mahadevan, L. and Tabin, C. J. (2011). On the growth and form of the gut. *Nature* **476**, 57-62.

Simon-Assmann, P., Kedinger, M., De Arcangelis, A., Rousseau, V. and Simo, P. (1995). Extracellular matrix components in intestinal development. *Experientia* **51**, 883-900.

Timmins, N. E., Dietmair, S. and Nielsen, L. K. (2004). Hanging-drop multicellular spheroids as a model of tumour angiogenesis. *Angiogenesis* **7**, 97-103.

Vu, T. H. and Werb, Z. (2000). Matrix metalloproteinases: effectors of development and normal physiology. *Genes Dev* **14**, 2123-2133.

Wilm, B., Ipenberg, A., Hastie, N. D., Burch, J. B. E. and Bader, D. M. (2005). The serosal mesothelium is a major source of smooth muscle cells of the gut vasculature. *Development* **132**, 5317-5328.

Yang, J. and Weinberg, R. A. (2008). Epithelial-mesenchymal transition: at the crossroads of development and tumor metastasis. *Dev Cell* **14**, 818-829.

Yang, J. T., Rayburn, H. and Hynes, R. O. (1995). Cell adhesion events mediated by alpha 4 integrins are essential in placental and cardiac development. *Development* **121**, 549-560.

Zacharias, W. J., Li, X., Madison, B. B., Kretovich, K., Kao, J. Y., Merchant, J. L. and Gumucio, D. L. (2010). Hedgehog is an anti-inflammatory epithelial signal for the intestinal lamina propria. *Gastroenterology* **138**, 2368-2377-2377.e2361-2364.